CHAPTER 3 STRUCTURAL CRITERIA FOR PIERS AND WHARVES

Introduction

Piles are a common element to much of the waterfront construction and recent experience has shown them vulnerable to damage. It is very difficult to inspect and repair damage which occurs to piles underground or under water; therefore, it is desirable to design piles to limit damage under the range of possible earthquakes. For the design earthquake, Level 1, which is expected to occur one or more times during the life of the structure, the piles should be undamaged. For the upper bound earthquake, Level 2, which is a rare event, the structure must sustain limited controlled damage; under such conditions it is desirable that the seismic energy be dissipated by ductile yielding at plastic hinge regions.

General Waterfront Damage Mechanisms

Werner and Hung (1982) gives an excellent compilation of case studies mostly recounting Japanese experiences from the 1920's to 1980. They conclude that "By far the most significant source of earthquake-induced damage to port and harbor facilities has been porewater pressure buildup... which has led to excessive lateral pressures applied to quay walls and bulkheads." They cite the 1964 Niigata and 1964 Alaska earthquake where "porewater pressures buildup has resulted in complete destruction of entire port and harbor areas" They note that direct effects of earthquake induced vibrations on waterfront structures is minimal and overshadowed by liquefaction induced damage. Failure of bulkhead anchorage systems is a common significant damage inducing mechanism. Liquefaction also causes damage to piles. The Anchorage City Dock was a reinforced concrete structure supported on pipe pile with diameters from 16 to 42 inches. Some of the piles were batter piles and filled with concrete. The piles were supported on clay which consolidated and settled 4 feet. This movement resulted in deck displacements from 8 to 17 inches buckling the batter piles (Tudor/PMP, 1976) Experience from Niigata and Alaska suggests that piles deform with the soil. In the 1970 Peru earthquake, magnitude 7.8, the Sogesa Wharf suffered severe damage when the inboard piles restrained by the dike structure could not tolerate high displacements, Tudor/PMP (1976).

Table 3-1 from Werner and Hung (1982) and updated in Werner (1998) gives case studies. The first paper warns of the vulnerability of batter piles as would be observed seven years later in the Port of Oakland. Gazetas and Dakoulas (1991) evaluate numerous waterfront case histories including the performance of sheetpile bulkheads in which the major failures have resulted from large-scale liquefaction in the backfill or supporting base. Frequently the anchored bulkhead damage takes the form of excessive outward movement and tilt caused by excessive movement of the anchor. They show that Japanese code procedures were inadequate because the accelerations values are often exceeded and the vertical component is omitted, they neglect ground motion

Table 3-1
SUMMARY OF EARTHQUAKE-INDUCED DAMAGE TO PORT FACILITIES (Page 1 of 8)

Earthquake			Port		Damage	
Location	Date	Magnitude	Location	PGA (g)[1]	Description	Cause(s)[2]
Kanto, Japan	09-01-23	8.3 (M_w)	Yokohama and Yokosuka	-	Concrete Block Quay Walls: Sliding, tilting, and collapse with some bearing capacity failure of rubble foundation. Steel Bridge Pier: Buckling of pile supports.	A C, E
Kitaizu, Japan	11-26-30	6.9 (M_w)	Shimizu	-	Caisson Quay Wall (183 m long): Tilting, outward sliding (8.3 m), and settlement (1.6 m). L-Shaped Concrete Block Quay Wall (750 m long): Outward sliding (4.5 m).	A, B, C
Shizouka, Japan	07-11-35	6.2 (M_w)	Shimizu	-	Caisson Quay Wall: Outward sliding (5.5 m), settlement (0.9 m), and anchor system failure.	A, B, C
Tonoakai, Japan	12-07-44	8.1 (M_w)	Yokkaichi Nagoya Osaka	0.30-0.35	Pile-Supported Concrete Girder and Deck: Outward sliding of structure and soil (3.7 m). Sheet-Pile Bulkhead with Platform: Outward sliding (3.7 m). Steel Sheet-Pile Bulkhead: Outward bulging (3 m).	A, B, C
Nankai, Japan	12-21-46	8.3 (M_w)	Nogoya Yokkaichi Osaka Uno	0.25-0.30	Steel Sheet-Pile Bulkhead with Platform: Outward bulging (4 m). Pile-Supported Concrete Girder and Deck: Outward sliding (3.7 m). Steel Sheet-Pile Bulkhead: Outward bulging (3 m) and settlement. Gravity-type Concrete-Block and Caisson Quay Wall: Seaward sliding (0.4 m).	A, B, C

Notes: (1) PGA = Peak ground acceleration (estimated or recorded); (2) Legend for causes of earthquake damage given on Page 8 of table.

Table 3-1

SUMMARY OF EARTHQUAKE-INDUCED DAMAGE TO PORT FACILITIES (Page 2 of 8)

Earthquake			Port		Damage	
Location	Date	Magnitude	Location	PGA (g)[1]	Description	Cause(s)[2]
Olympia, Washington, USA	04-13-49	7.1 (M_s)	Seattle	-	Dock Structures: Major damage to structures and to goods awaiting shipment. Loaded tanker tied to dock reported vertical displacement of about 1 inch at a frequency of about 3 Hz. Soil Materials: Stuctures in vicinity of waterfront located on filled ground suffered significant damage. Major water spouts observed from ground fissues.	B
Tokachi-Oki, Japan	03-04-52	8.1 (M_w)	Kushiro	-	Concrete Caisson Quay Wall: Tilting, outward sliding (6 m), and settlement (1 m).	A, B, C
Chile	05-22-60	9.5 (M_w)	Puerto Montt	-	Concrete Caisson Quay Walls: Overturning and extensive tilting. Steel Sheet-Pile Sea Wall: Outward sliding (up to 1 m) and anchor failure. Gravity-Type Concrete Sea Wall: Complete overturning and sliding (1.5 m).	A, B, C
			Talcuhauno	-	Concrete-Block Quay Wall: Outward tilting.	A, B
Alaska, USA	03-27-64	9.2 (M_w)	Anchorage	-	Dock Structures: Extensive seaward tilting with bowing, buckling, and yielding of pile supports.	B, D, E
			Valdez		Entire Port: Destroyed by massive submarine landslide.	B, D, F
			Whittier		Pile-Supported Piers and Docks: Buckling, bending, and twisting of steel pile supports.	B
			Seward		Major Portion of Port: Destroyed by massive submarine landslide.	F
Niigata, Japan	06-16-64	7.6 (M_w)	Niigata	0.15-0.20	Caisson Quay Wall (183 m long): Tilting, outward sliding (8.3 m), and settlement (1.6 m). L-Shaped Block Quay Wall (750 m long): Outward sliding (4.5 m).	A, B, C

Notes: (1) PGA = Peak ground acceleration (estimated or recorded); (2) Legend for causes of earthquake damage given on Page 8 of table.

Table 3-1
SUMMARY OF EARTHQUAKE-INDUCED DAMAGE TO PORT FACILITIES (Page 3 of 8)

Earthquake			Port		Damage	
Location	Date	Magnitude.	Location	PGA (g)[1]	Description	Cause(s)[2]
Puget Sound, Washington USA	04-29-65	6.5 (M_s)	Seattle	-	General: Nearly every waterfront facility damaged to some extent. Piers 15 and 16 on Harbor Island: Structures shifted toward water by about 1 foot due to the soil losing strength or partially liquefying and pushing dock toward water Pier 5: Among the hardest hit pier areas. Bulkhead and fill behind it settled as much as 2 ft, over width of 25-40 ft. Bulkhead reported to be 6-8 in. out of line. Buildings and Utilities: At Pier 36, light fixtures were ton loose in 5-story concrete Engineers' Headquarters Building. File cabinets tipped over and most books in library fell from shelves. Damage reported to Pier 90 waterline and Pier 91 steamline.	A, B, E
Tokachi-Oki, Japan	05-16-68	8.3 (M_w)	Hachonohe	0.20-0.25	Steel Sheet-Pile Bulkheads: Outward sliding (0.9 m), tilting, and settlement, with anchor failure.	A
			Aomori	0.20-0.25	Gravity-type quay wall: Sliding and settlement (0.4 m). Gravity-type breakwater: Sliding (0.9 m) and pavement settlement (0.9 m).	A
			Hakodate	0.10-0.15	Steel sheet-pile bulkhead: Seaward tilting (0.6 m) and apron settlement (0.3 m). Quay wall: Settlement (0.6 m) and sliding (0.4 m).	A, B
Nemuro-Hanto-Oki, Japan	06-17-73	7.9 (M_w)	Hanasaki	0.25-0.30	Gravity-Type Quay Wall: Sliding (1.2 m), wall settlement (0.3 m), and apron settlement (1.2 m). Steel4-22 Sheet-Pile Bulkhead: Sliding (2 m) and anchor failure.	A, B
			Kiritappu	-	Steel Sheet-Pile Bulkhead: Relatively minor damage. Gravity-Type Quay Wall: Relatively minor damage.	

Notes: (1) PGA = Peak ground acceleration (estimated or recorded); (2) Legend for causes of earthquake damage given on Page 8 of table.

Table 3-1
SUMMARY OF EARTHQUAKE-INDUCED DAMAGE TO PORT FACILITIES (Page 4 of 8)

Earthquake			Port		Damage	
Location	Date	Magnitude.	Location	PGA (g)[1]	Description	Cause(s)[2]
Miyagiken-Oki, Japan	06-12-78	7.6 (M_w)	Shiogama	0.25-0.30	Concrete Gravity-Type Quay Wall: Outward tilting (0.6 m) and apron pavement settlement (0.4 m).	A, B
			Ishinomaki	-	Steel Sheet-Pile Bulkhead: Outward sliding (up to 1.2 m) and apron settlement (up to 1 m). Concrete-Block Retaining Wall: Sliding, tilting, and cracking with corresponding pavement settlement (0.2 m) relative to wall.	
			Yuriage	-	Concrete-Block Gravity Quay Wall and Steel Sheet-Pile Bulkhead: Horizontal displacement (1.2 m).	
			Sendai	-	Steel Sheet-Pile Bulkheads: Cracking and settlement of apron and pavements.	
					Seawall at Passenger Terminal: Lateral movement of seawall, settlement of backfill.	
Offshore Central Chile	03-03-85	7.9 (M_w)	San Antonio	-	Concrete-Block Seawall at Western Extremity of Port: Collapse of about 60 percent of seawall length, leading to significant tilting of crane structures.	A, B
			Valparaiso	-	Seawalls at Sites 6 and 7 (West Side of Port): Several inches of soil movement at top of wall, causing movement of crane rails and disruption of crane operations.	
Kalamatz, Greece	09-13-86	6.0 (M_w)	Kalamatz	0.15-0.27	Harbor Area: Soil conditions in Kalamata reportedly consist of non-uniform sandy layers intermixed with coarse sand and gravel or with varying proportions of silt and clay. No evidence of pore pressure buildup or liquefaction was observed. Very minor damage in harbor area reportedly consisted of some slope movement at wharf and along nearby coastal road, causing some pavement cracking.	C

Notes: (1) PGA = Peak ground acceleration (estimated or recorded); (2) Legend for causes of earthquake damage given on Page 8 of table.

Table 3-1
SUMMARY OF EARTHQUAKE-INDUCED DAMAGE TO PORT FACILITIES (Page 5 of 8)

Earthquake			Port		Damage	
Location	Date	Magnitude.	Location	PGA (g)[1]	Description	Cause(s)[2]
Loma Prieta, California, USA	10-17-89	6.9 (M_W)	Redwood City	0.22-0.28	Waterfront Components: Damaged batter piles, separation of concrete ramp from pier at Wharf 1. Infrastructure Components: Broken water lines, temporary disruption of power and communications. Port Operations: Not disrupted.	A, B
			Richmond	0.10-0.15	UNOCAL Terminal: Ruptured gasoline storage tank. Ford Plant east of Terminal 3: Broken water lines. Port Operations: Port fully functional two days after earthquake.	A, B
			San Francisco	0.15-0.20	Piers Supported by Fills (Rather than by Piles): Settlement. Piers Supported by Piles: Many broken batter piles. Cracked concrete decks above piers. Buildings along Waterfront: Significant structural damage (including clock tower at Ferry Building). Container Cranes: Damaged. Infrastructure Components: Many broken water lines. Pier 80 Terminal: This 1950s vintage wharf on batter-pile system was upgraded in mid-1980s to support larger 100-foot gage crane rail. New vertical pile supports for this crane rail doubled as new lateral seismic force resisting system for entire wharf. Wharf undamaged during earthquake.	A, B, E
			Oakland	0.25-0.30	Seventh Street Terminal: Sand fill dike under landside crane rail settled up to 18 in. and moved laterally about 6 in. Settlement of crane rail, broken batter piles, separation of piles from deck. South perimeter dike had one location where settlements exceeded 3 ft. and lateral spread displacements were about 2-4 ft. Extended closure of terminal. Matson Terminal: Separation between piles and deck slabs. Cracking of piles. Yard settlements of up to 2 ft. Terminal stayed in operation but with limited live loads during crane operations. Middle Harbor Terminal: 0.5 to 2 ft. of subsidence in yard areas. Howard Terminal: Some lateral movement of landslide crane rail (the crane remained operational). Good performance of vertical piles designed as ductile moment frame system. Marine Operations Building located just behind dike settled about 12 in., with no damage other than utility connections. This was small two-story building on flat slab that floated on liquefied soils. Liquefaction: In yards of each of above terminals.	A, B, C

Notes: (1) PGA = Peak ground acceleration (estimated or recorded); (2) Legend for causes of earthquake damage given on Page 8 of table.

Table 3-1
SUMMARY OF EARTHQUAKE-INDUCED DAMAGE TO PORT FACILITIES (Page 6 of 8)

Earthquake			Port		Damage	
Location	Date	Magnitude	Location	PGA (g)[1]	Description	Cause(s)[2]
Philippine Islands	07-16-90	7.7 (M_w)	San Fernando	-	Government Pier No. 1: Significant cracking, buckling, and deformation of reinforced concrete pile-supported pier. Extensive cracking of concrete piles, and particularly severe damage to batter piles. Sever cracking of adjacent concrete sea wall. Operations suspended. , Coal Pier: Large lateral movement caused concrete slab between pier and sea wall to fall off its seat. Dry Bulk Handling Equipment: Collapsed.	A, B, C
Costa Rica	04-22-91	7.4 (M_w)	Limon	-	Soil Conditions: Founded on fill beyond natural shoreline and an old breakwater. North Dock Area: Severe liquefaction, with settlement and lateral spreading of concrete slabs, abutments, and retaining walls. Displacements of up to ½ meter. Intense east-west shaking caused major damage to large 2-story warehouse, including failure of second floor and collapse of middle one-third of building (resulting in serious injuries to five people). Permanent deformations at dock expansion joints hampered post-earthquake crane operations.	A, B, E
			Moin	-	Soil Conditions: Relatively stable soils, with no obvious signs of liquefaction-induced settlement. Port Operations: Normal operations restored soon after earthquake. Coastal uplift (of up to 1 meter) caused fire pump suction lines mounted on pier to terminate about 0.1 meter above water level..	
			Almirante (Panama)		Railroad Trestle: Concrete piled bents severely damaged, closing trestle to rail traffic.	
				-	Concrete Pier: Severe damage, resulting in significant reduction of ship-loading capacity.	B, E
Hokkaido Nansei-Oki, Japan	07-12-93	7.8 (M_w)	Adane, Esashi	-	Widespread damage due to tsumami damage and scour. Structural damage to buildings due to differential ground settlement.	B, F
			Hakodate and Setana	-	Quay walls displaced or tilted by up to 1 meter. Damage to paved aprons due to ground settlement.	B
			Okushiri-Cho	-	Fuel lines damaged by ground settlement and permanent lateral ground displacement. Ferry building damaged by tsunami impact and ground settlement. Portions of concrete breakwater toppled by tsunami and lateral spreading of foundation soils. Fuel tank buckled due to landslide.	B B, C, F

Notes: (1) PGA = Peak ground acceleration (estimated or recorded); (2) Legend for causes of earthquake damage given on Page 8 of table.

Table 3-1
SUMMARY OF EARTHQUAKE-INDUCED DAMAGE TO PORT FACILITIES (Page 7 of 8)

Earthquake			Port		Damage	
Location	Date	Magnitude	Location	PGA (g)[1]	Description	Cause(s)[2]
Guam	08-08-93	7.7 (M_w)	Apra Harbor	0.20-0.30	Navy Facilities: Damage to piers founded in dredged backfill. Sheet-pile bulkheads and anchor systems moved as much as 3 ft. Damage to batter piles near pile caps. Commercial Facilities: Lateral spreading in container-handling portion of port.	A, B
Northridge, California, USA	01-17-94	6.7 (M_w)	Los Angeles	0.15-0.20	Berths 121-126 of American President Lines Terminal: Seaward movement of berths (0.5 ft.) and settlement and liquefaction of backland fill areas. Dikes settled. Damage to 171-lb crane rail. Several days of down time before full operations restored. Newer portion of wharfs (with vertical piles designed as ductile moment frame and with 86 ft. rock dike) performed well. Some damage to vertical and batter piles at older portions of Berth 126. Other Terminals. Settlement, lateral spreading, liquefaction of fills. Some older facilities damaged. Infrastructure Components. Ruptured water lines, loss of power to some cranes (which interrupted crane operations), and interruption of telephone service (for up to several hours).	A, B
			Long Beach	0.10-0.15	No damage reported.	
Hyogoken Nanbu, Japan	01-17-95	6.8 (M_s)	Kobe	0.20-0.70	International Shipping: Virtually all container terminals on Port Island and Rokko Island severely damaged and inoperable, due to liquefaction of fills along waterfront areas. Seaward movement of caisson quay walls (up to 25 ft.) and associated vertical settlement (up to 10 ft.) of fills behind quay walls. Large lateral deformations extended into backland areas over distances of 250-350 ft. Cranes suffered, de-railing, overturning, and buckling of legs. Domestic Shipping: Major damage to ferry terminals and to main trunk line for domestic commodity distribution. Quay walls on piles performed much better than caisson quay walls (although damage to lightly reinforced concrete piles and buckling of steel pipe piles was observed). Infrastructure. Good performance of symmetrical shear wall buildings. Poor performance of buildings with soft stories or other lateral load resistance deficiencies. . Reduced port access due to damage to highway transportation system. Extensive damage to water lines.	A, B, E
			Osaka	0.20-0.27	General: Good overall seismic performance, due to such factors as the use of clayey fill thorughout the port, and densification of sandy trench fill beneath caissons at North Port.	

Notes: (1) PGA = Peak ground acceleration (estimated or recorded); (2) Legend for causes of earthquake damage given on Page 8 of table.

Table 3-1

SUMMARY OF EARTHQUAKE-INDUCED DAMAGE TO PORT FACILITIES (Page 8 of 8)

Earthquake			Port		Damage	
Location	Date	Magnitude	Location	PGA (g)[1]	Description	Cause(s)[2]
Antofagasta, Chile	07-30-95	7.8 (M_s)	Antofagasta	-	Port of Antofagasta is forth largest port in Chile, and is most important port for copper exports in northern section of country. Settlements of up to 0.6 meter resulted in reduction of cargo handling capability of port to only 20 percent of its pre-earthquake capability. Almost all cranes in port suffered operational damage. Almost no damage to warehoused founded on piles.	B
Manzanillo, Mexico	10-09-95	7.9 (M_s)	Manzanillo	0.40	Some liquefaction with considerable differential settlement in areas of this industrial port located on dredged fill overlying reclaimed estuary wetlands. Significant lateral spreading of dredged fills where not contained by rock dikes. Two large gantry cranes at new container facility for off-loading container ships had both crane rails located on pile-supported wharf, and were not damaged during earthquake. However, crane runway rail shifted laterally causing offsets at rail splice. For container cranes to gantry entire length of wharf, sections of these rails had to be readjusted. Moderate damage to longitudinal and transverse batter piles, and concrete spalling of about 10% of underside of deck. About 80 batter piles either completely severed or suffered extensive damage. Port buildings that were either not pile-supported or only partially pile-supported in areas with differential settlement suffered architectural and structural damage. Buildings supported totally on piles performed well. Some water and sewage lines ruptured.	B,C
Gulf of Aqaba, Egypt, Jordan, and Israel	11-22-95	7.2 (M_s)	Eilat, Israel Nuweiba, Egypt	0.08-0.11 0.16-0.25	General: Relatively light damage. Some liquefaction and sand boils in port area. Ground fracture and cracking of road surfaces. Some cracking of infill walls and at building expansion joints. Waterfront Facilities: Two out of four berths were severely damaged, due to liquefaction of fill materials. Significant seaward rotation of quay walls, leading to separation between capping beam and backfill. Excessive settlement of apron slabs. Other Port Facilities: Collapse of stone walls, and architectural masonry walls of arrival hall. At desalination plant, sliding of unanchored steel tank and buckling of tank shell. Sliding of transformer at electrical substation damaged conduits and caused loss of power supply.	B A, B

Notes: (1) PGA = Peak ground acceleration (estimated or recorded).
(2) Legend for causes of earthquake damage is as follows:
A: Large lateral pressure from backfills. B: Liquefaction. C: Localized ground movement
D: Massive submarine sliding. E: Structural vibrations. F: Tsunami.

amplification, and they do not take into account lateral soil spreading caused by a loss of stiffness. They note limitations in traditional pseudostatic sheetpile procedures to properly define the location of the active sliding surface. They develop an empirical seismic design chart based on the observed case histories. Other works of significance include Swanson (1996) which summarizes observed damage in the Kobe earthquake, Harn and Malick (1992) which gives design guidance, and Erickson and Fotinos (1995) which summarizes various code requirements.

The 1978 magnitude 7.4 earthquake Miyagi-Ken-Oki earthquake caused severe damage to gravity quay walls, piers and sheet pile bulkheads. The Sendai Port area has a soil profile composed of a sand layer 3 to 20 meters thick underlain by layers of medium coarse sand and silty loam. Dense sand and bedrock underlie the silty loam layer. Two nearby bulkheads serve as a comparison study, Figure 3-1. A seismic lateral coefficient of 0.1 g was used in the design. Bulkhead No. 4 was anchored with vertical H-beam. The area behind this bulkhead experienced cracking and settlement.. Bulkhead No. 5 was constructed in a similar manner except that it used batter piles to restrain the anchor. This bulkhead withstood the earthquake without damage. Note as shown in Figure 3-1 the near surface soil behind Bulkhead No. 4 had lower blowcounts which when combined with reduced anchorage could have caused the increased lateral spread and associated damage.

Damage To Waterfront Structures Having Piles

The 1989 Loma Prieta Earthquake caused major port damage to the Port Of Oakland, Table 3-1. Soil liquefaction caused damage to the terminal facilities much of which is filled land composed of loose dumped or hydraulically placed sand underlain by soft normally consolidated Bay Mud. There were four areas damaged: the 7th Street Terminal, the Matson Terminal, the APL Terminal and the Howard Terminal. All of these terminals had pile supported wharves typically represented by Figure 3-2. The piles extended through the rock dike which served as containment for the fill composed of fine dredged sands and silty sands. The most severe damage occurred at the 7th Street Terminal where liquefaction of the fill resulted in settlements and lateral soil spreading, cracking the pavement over a wide area. Maximum settlements of the paved yard area were up to 12 inches. The inboard crane rail was supported on the fill directly which settled; the outboard crane rail was supported on the wharf piles and did not settle. As a result of this differential movement the cranes were inoperable. Damage occurred to the tops of the batter piles, Figure 3-2, through shear, compression, and tension. The vertical piles were largely undamaged with a few exceptions. The stiff batter piles absorbed much of the loading among the other more flexible elements. Seed et al. (1990) suggests “the mode of failure was predominantly tensile failure driven by outward thrust of the fill, suggesting that liquefaction and associated spreading were important factors”. As a result of this damage the port of Oakland is replacing all the 7th Street Terminal batter piles with vertical piles designed to resist lateral forces. The pile-wharf deck is being extended inboard to provide support for the crane rails. The Howard Terminal and the APL Terminal which had vertical or near vertical piles instead of batter piles did not sustain

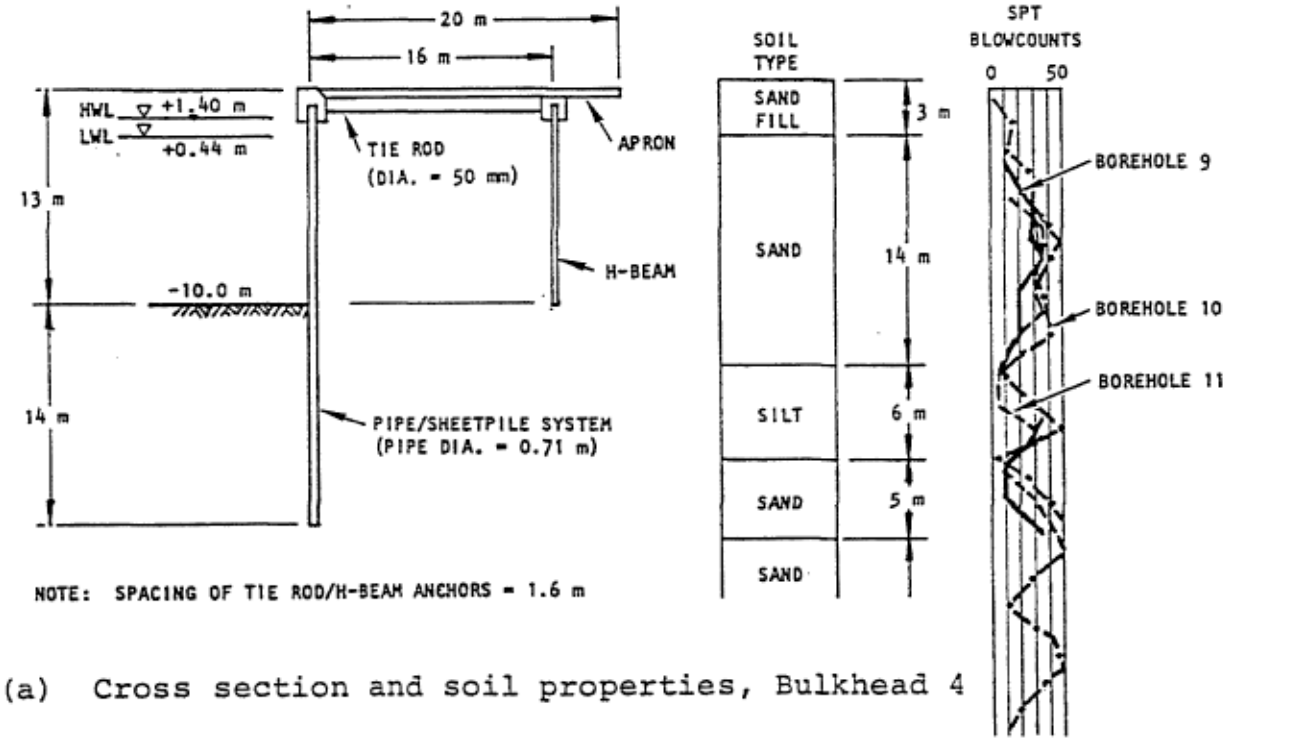

(a) Cross section and soil properties, Bulkhead 4

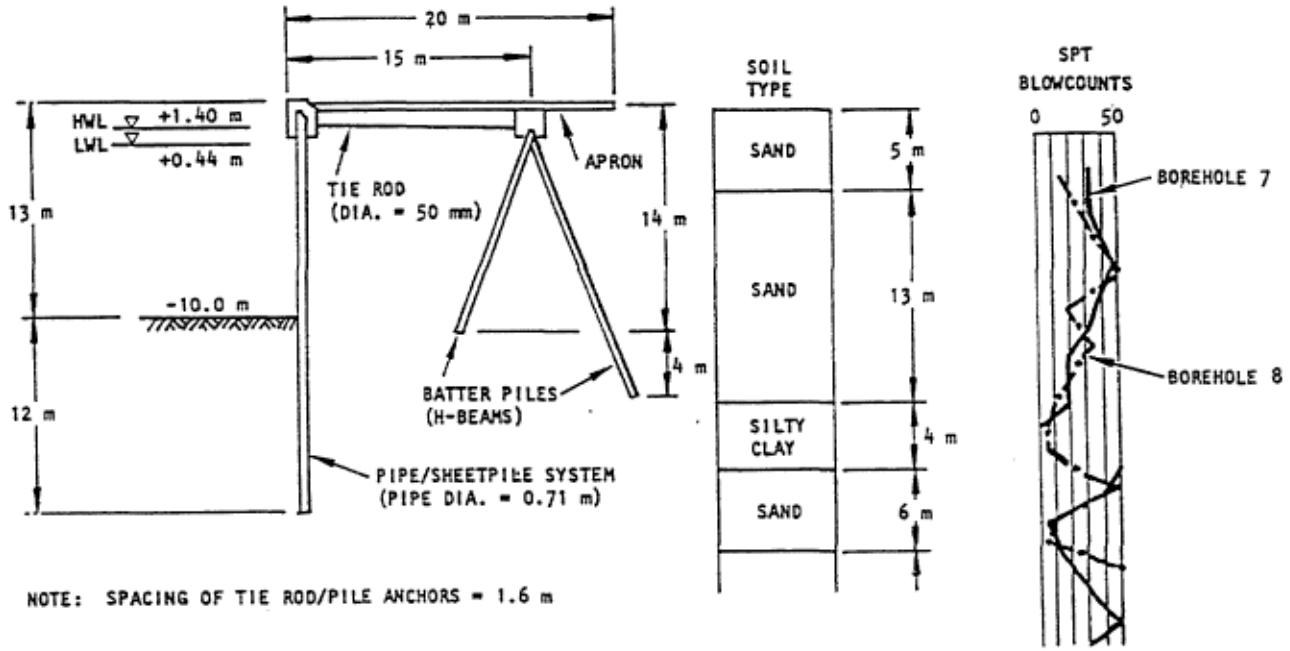

(b) Cross section and soil properties, Bulkhead 5

Figure 3-1. Bulkheads 4 and 5 at Nakano wharf, Sendai Port.

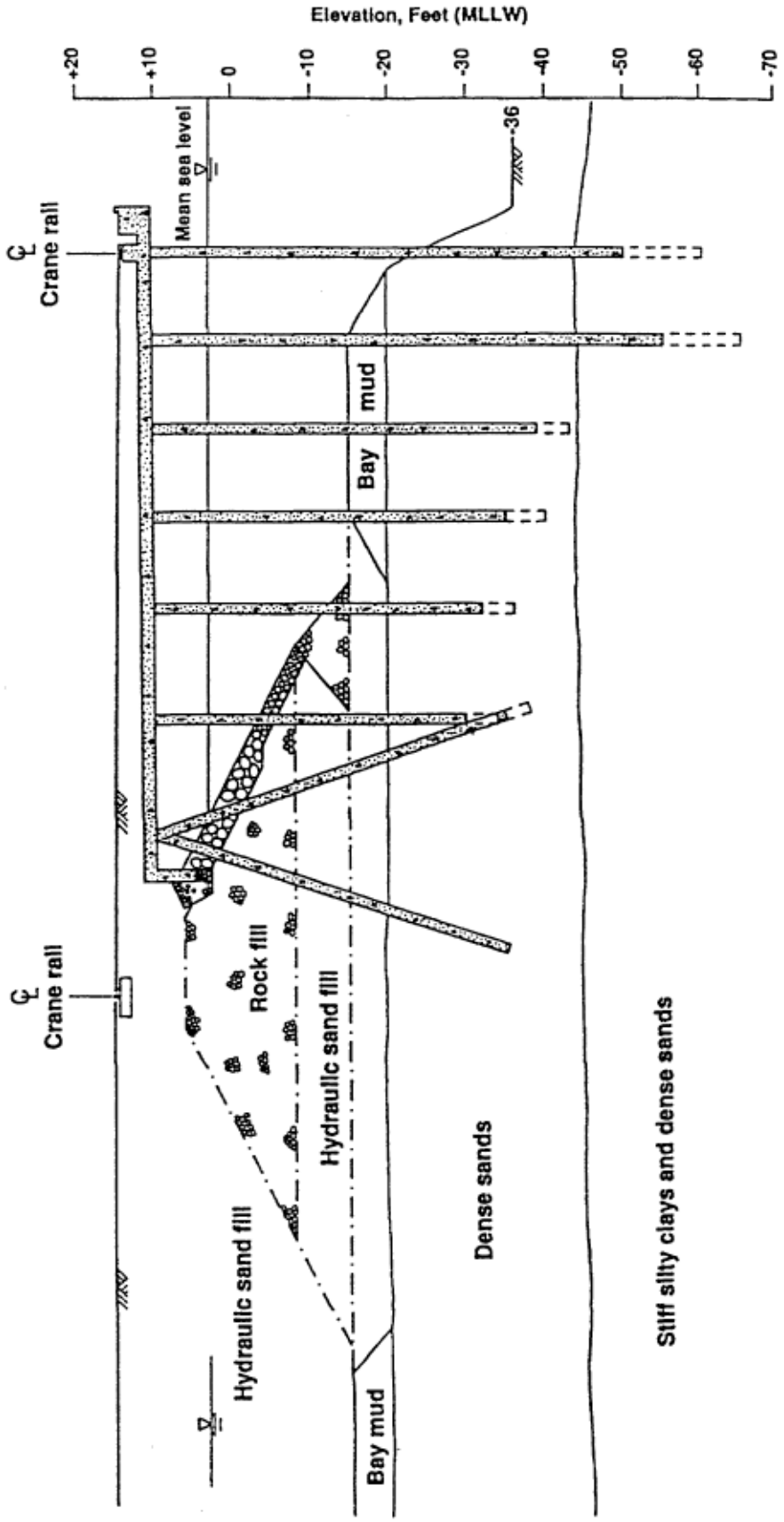

Figure 3-2. Cross-section 7th St Terminal, Port of Oakland.

pile damage although liquefaction caused comparable settlements in the filled areas. Both crane rails were also pile supported.

On August 8, 1993 a magnitude 8.1 earthquake occurred offshore 50 miles from Guam and caused over $125 million in damages to Naval facilities on Guam, Table 3-1. Nearly all of Guam is firm soil or rock except for the region containing the Navy port which had soft soil composed of natural alluvium and artificial fill. It is estimated the peak horizontal ground accelerations were about 0.25g. Liquefaction was a major problem and lateral spreading of 1 to 2 feet was observed at wharf areas. It also resulted in settlements, backfill collapse and bulkhead movements. Buried water and power lines were fractured. Sheet piles failed in shear and deadman anchors pulled out. Batter piles failed in shear at the pile cap. Other Navy damage consisted of fuel tank leaks, sloughing of a dam, damage to masonry housing units and major damage to the power plant which supplied 20 percent of the island's power capacity.

In January 1995, the Hyogo-ken Nambu (Great Hanshin Kobe) earthquake, Japanese magnitude 7.2 (about 6.9 moment magnitude), occurred in Kobe Japan. This event produced major damage to Japan's second busiest port. Liquefaction was a major contributor to the extent of the damage producing typical subsidence of a half meter. Piles were used extensively in this area. They were designed to account for the negative skin friction and additional ground improvement was also performed. Structures on such piles performed well even though major subsidence occurred in surrounding areas. Other structures not on piles suffered differential settlement and tilting and significant damage. Liquefaction caused up to 3 meters of lateral spread displacement, sunk quay walls, broke utility lines, and shut down 179 out of 186 berths at the port. It was responsible for major damage to crane foundations. Hydraulic fill behind concrete caisson perimeter walls fill liquefied causing the caissons to move outward rotating up to 3 degrees and settling from 0.7 to 3.0 meters. The caissons were designed for a lateral coefficient of 0.1g. A seismic coefficient of 0.2g was normally specified for dockside cranes. Peak accelerations of 0.8g in the NS direction, 0.6g in the EW direction and 0.3g vertical were noted from accelerograph recordings. The event had a duration of about 20 seconds. The outboard crane rails which were supported on the caisson also spread outward, Figure 3-3. The middle crane rails which were supported on piles did not move. The inboard crane rails settled between 1 and 2 meters. The increase in distance between crane rails resulting from lateral spreading was from 1 to 5 meters. Both old and new caisson construction faired equally poorly. The resulting deformation disabled all the dockside container cranes collapsing one and shutting down all port operations. Damage is attributed to liquefaction since structures supported on pile suffered much less damage, Liftech (1995). It should be noted that caissons designed for 0.25g sustained lower levels of damage.

Pile designs must be checked for the location of the maximum moment, generally at the pile cap. The second highest point is within the support soil. Damage below the soil line cannot be seen and easily repaired; thus, consideration of this must be included in the design. POLA provides for decreased ductility for wharf pile sections below the soil line. It is important to note that the pile curvatures are influenced by the stiffness of the supporting soil. Soil movement may be concentrated at interfaces between stiff and soft

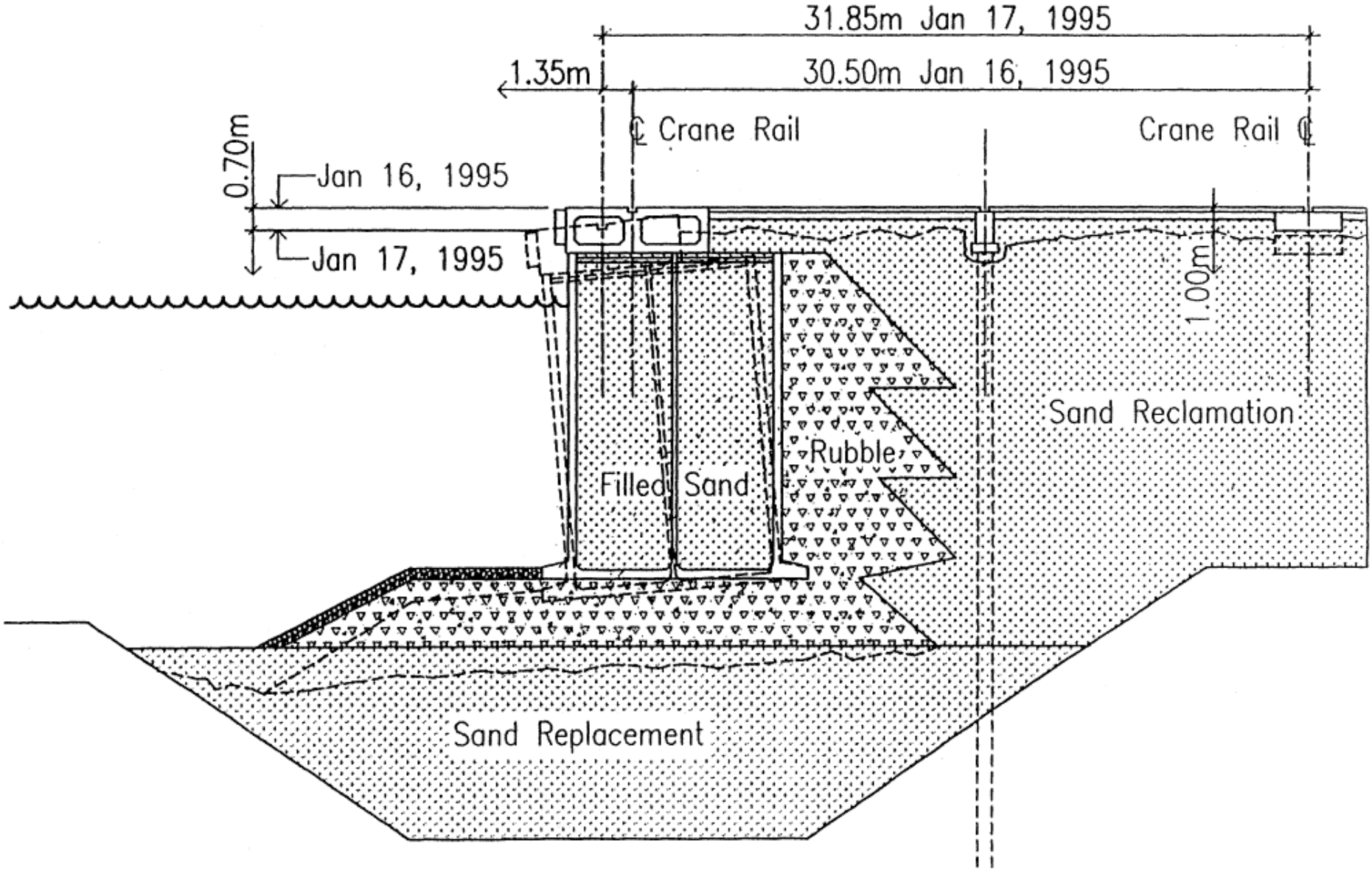

Figure 3-3. Typical wharf, Kobe Japan.

soils causing local increases in curvature, overstressing the pile. Soil layers and their associated stiffness must be accurately modeled in a pile analysis.

During the 1995 earthquake in Kobe Japan damage occurred to precast concrete piles on Port Island, Matso, K. (1995). Typically the failure mode consisted of anchor reinforcing bars pulling out of the pile caps producing separation between the piles and the pile cap. The Hanshin Expressway which collapsed was an elevated roadway supported on a series of single concrete pier. The failure of the pier was associated with failure of the transverse shear reinforcement and premature termination of longitudinal reinforcement. This reinforcement consisted of perimeter ties lapped at the ends and was spaced 30 cm on center. The inadequate shear reinforcement resulted in non-ductile behavior. Additionally gas-pressure weld splices of reinforcing bars failed.

Most pile failures are associated with liquefaction of soil which can result in buckling of the pile, loss of pile friction capacity, or development of pile cracking and hinging. Hinging may be at the cap location or at an interface between soil layers of differing lateral stiffness, Figure 3-4. Damage to piles in the soil may also occur about 1 – 3 pile diameters below grade in non-liquefying soils due to vibrational response of the wharf, Priestley et al (1998). Meyerson et al. (1992) present a state-of-the-art approach for evaluating pile buckling capacity for conditions of liquefaction of a soil layer and also determining allowable lateral deformation capacity. Most buckling occurs when the zone of liquefaction extends to the surface with the water table at the surface producing a large unsupported length. An axial transition load exists such that at less than that load the pile will not buckle.. Typically the transition load is at one-fourth to one-third of the ultimate bearing capacity. Flexible piles will tend to try to conform to soil movement and will have large curvatures at the interface between liquefied and non-liquefied material. Meyerson et al. present dimensionless curves relating pile lateral displacement capacity before formation of a hinge as a function of pile characteristic length. Yoshida and Hamada report on 2 case studies of piles beneath buildings which were damaged by liquefaction during the 1964 Niigata Earthquake. The first building, Building A, was a three-story reinforced concrete building and is shown in Figure 3-5. The piles in this case were end-bearing piles. The piles exhibited tensile cracks and concrete crushing. Pile number 2 exhibited a total disintegration of concrete probably from a lack of adequate confining steel. The second building designated as Building S is also a three-story reinforced concrete building and is shown in Figure 3-6. The piles in this case were friction piles. All piles in both buildings were damaged by the lateral deformation associated with the liquefaction. Generally pier piles will develop hinges first at the pile cap; however this may not be the case for wharves having piles with much shorter freestanding lengths.

Priestley et al. (1996) contains an extensive report on the causes of bridge damage much of which is relevant to piers. In discussing damage to existing older bridges they note " All deficiencies tend to be a natural consequence of the elastic design philosophy almost uniformly adopted for seismic design of bridges prior to 1970, and still used in some countries notably Japan." Seismic deflections were underestimated in part by use of gross rather than cracked member stiffness. Seismic design forces were low and the ratio

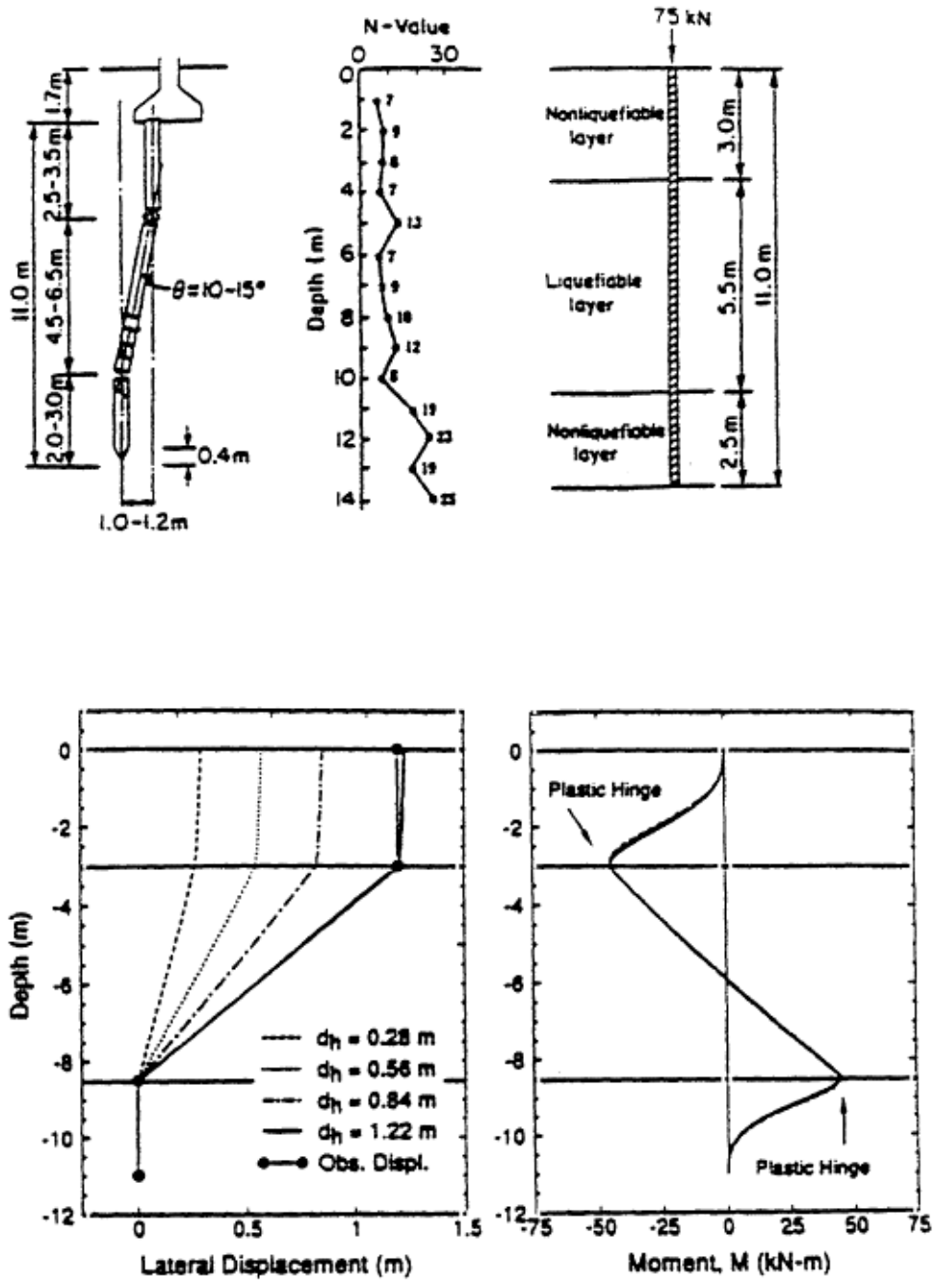

Figure 3-4. Typical pile damage in liquefaction zone.

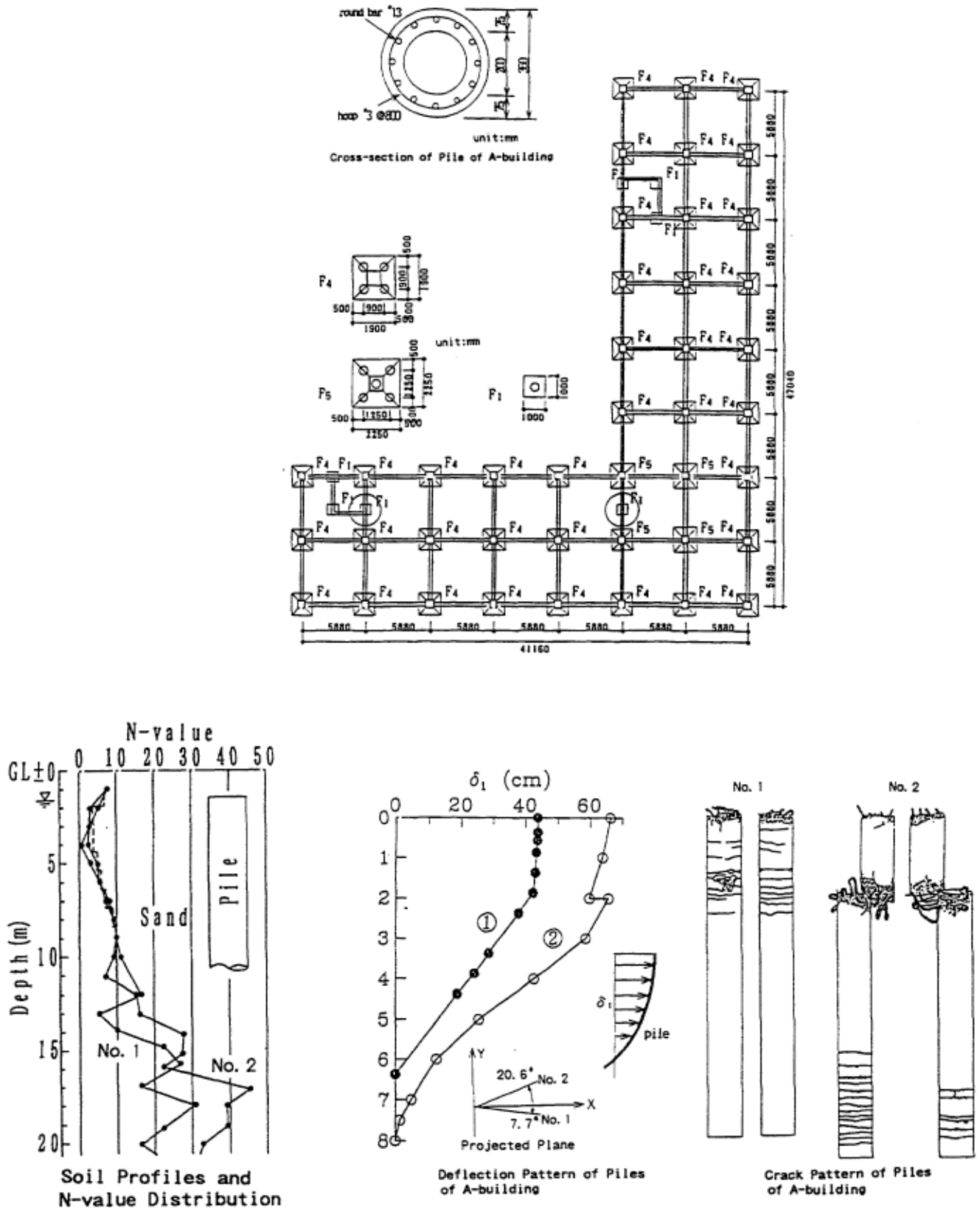

Figure 3-5. Building A pile damage, Niigata Earthquake.

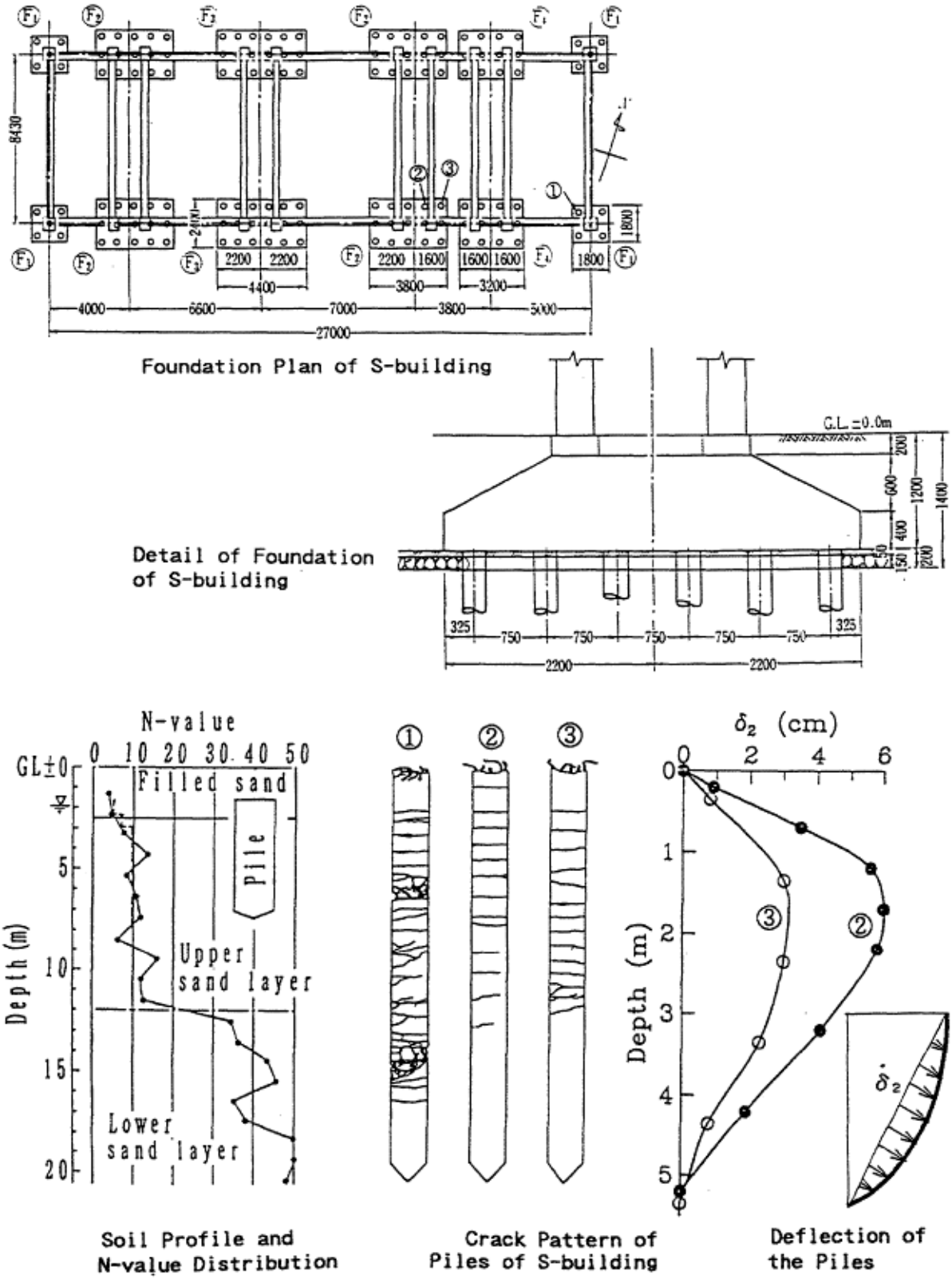

Figure 3-6. Building S pile damage, Niigata Earthquake

of seismic to static loads was incorrect resulting in erroneous moment patterns. Points of contraflexure were mislocated resulting in premature termination of reinforcement. Adjacent frames of bridges experienced out-of-phase-motion, with displacements often exceeding member supports. Soft soils amplified motion and liquefaction caused loss of pile support. Pounding of bridge members can impart high impact forces. Column longitudinal reinforcement was often lap-spliced immediately above the foundation with an inadequate development length of 20 bar diameters. " Displacement ductility factors as high as μ = 6 to 8 may be needed in some cases. At ductility levels of 2-3, concrete compression strains in the plastic hinge regions exceed the unconfined strain capacity and spalling of the cover concrete occurs. Unless the core concrete is well confined by closely spaced transverse hoops or spirals, the crushing rapidly extends into the core, the longitudinal reinforcement buckles, and rapid strength degradation occurs.." Cap beam failures were attributed to low shear capacity, early cutoff of negative top beam reinforcement, and insufficient anchorage of large diameter cap reinforcement in the column. Development lengths of 3 to 5 feet for # 18 bars was shown to be inadequate in the Loma Prieta earthquake resulting in large flexural cap beam cracks. Rupture of # 18 bars bent on a 18-inch radius. "Problems can be expected for columns with longitudinal reinforcement anchorage provided by 90 degree hooks bent away from the column axis, creating an unfavorable tension field in the joint region.. ... Current analysis indicates that considerable amount of vertical and horizontal shear reinforcement is required in the joint region, but are commonly omitted in older designs.

Priestley and Seible (1997) discuss aspects of analysis and design of piles for bridge structures, much of which is directly relevant to wharves and piers. Japanese research, Kubo, 1969 and Hayashi, 1974 reports that piles move with the soil during elastic portions of motion. Locations of potential failure occur at the point of sharpest curvature in the pile top, at just below the mud line, and at a depth in the soil profile at high curvature. Piles tend to move with the soil such that the region of maximum displacement slope variation in the soil field controls the pile response. The extent of this action depends on the soil stiffness and the pile stiffness. Batter piles exert large reactions on the pier structure which may have detrimental effect on the pile cap. The pier should be structurally separated from the abutment to provide isolation.

Characterization Of Soil Forces Acting On Piles

Novak (1991) gives a state-of the-art paper on pile dynamics in which he discusses causes of damage to piles such as liquefaction and earth movement. He discusses theoretical studies which develop dynamic soil-pile interaction; he shows that there is a cylindrical boundary zone around a pile which undergoes nonlinear behavior. Pile soil separation is possible under lateral load, Figure 3-7. The length of the pile separation, $L_{s,}$ is a function of the lateral deformation:

$$L_s / d = 260\ \Delta/d \qquad (3\text{-}1)$$

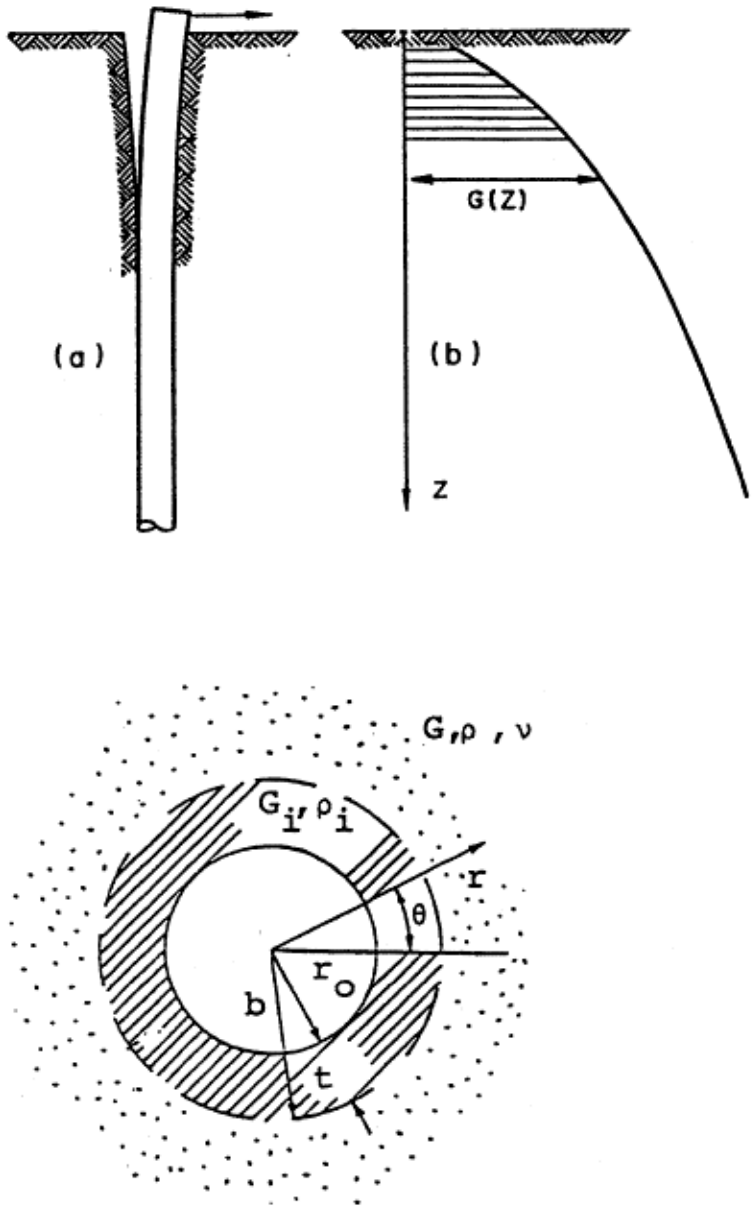

Figure 3-7. Pile separation and zone of plastic behavior.

where

the amount of lateral deformation , $0.001 \leq \Delta/d \quad 0.005$

d Pile diameter

Wolf and Weber (1986) show the difference in horizontal stiffness and damping for alternative modeling assumptions. Figure 3-8a shows a linear model with soil tension. Figure 3-8b allows soil separation which is seen to reduce damping. Figure 3-8c allows soil separation and slipping of the pile in the soil which reduces both horizontal stiffness and damping. Large displacements require nonlinear representation of the soil around the pile. To account for gapping, slippage and friction lumped mass finite element models evolved as the most often used approach. Soil resistance deflection relationships known as p-y curves were developed. Figure 3-9 is a typical p-y curve. To account for pile separation the soil reaction displacement curve shown in Figure 3-10 has been used. Figure 3-11 shows cyclic loading p-y curves for sand and clay.

Yoshida and Hamada (1991) report on the Japanese Highway Bridge Code which establishes the subgrade modulus reaction k for use with piles:

$$k = 0.2 * 28N * D^{-0.35} \quad (kgf/cm^3) \qquad (3\text{-}2)$$

where

D the diameter of the pile in cm

N Japanese penetration test N value of blowcounts

The spring constant is found by multiplying the diameter of the pile times k times the pile length between springs.

Martin and Lam (1995) present a recent state-of-the-art summary of the design of pile foundations. They show that a nonlinear soil model is required to capture the lateral behavior of a pile. A Winkler Spring Beam-Column representation with nonlinear springs is shown to be an acceptable method for computing pile behavior to lateral loads. They have reviewed procedures for computing the required soil load-deformation relationship to characterize the spring properties and found the American Petroleum Institute (1994) procedure to be the accepted common practice. This procedure is found in a recent recommended practice and is approved by the American National Standards Institute.

The origin of the API equation for sand evolved from work by Reese, Cox, and Koop (1974) who established a set of equations based on the forces associated deformation of a soil wedge and the lateral deformation of a rigid cylinder into soil. They established the early shape of the soil load deflection p-y curve based on the soil subgrade modulus. The procedure was modified by Bogard and Matlock (1980) principally as a simplification by consolidation of terms. The shape of the p-y curve was finally based on work by Parker and Reese (1970). O'Niell and Murtcheson (1983) wrote an excellent summary of the development of the procedure for constructing p-y curves and performed

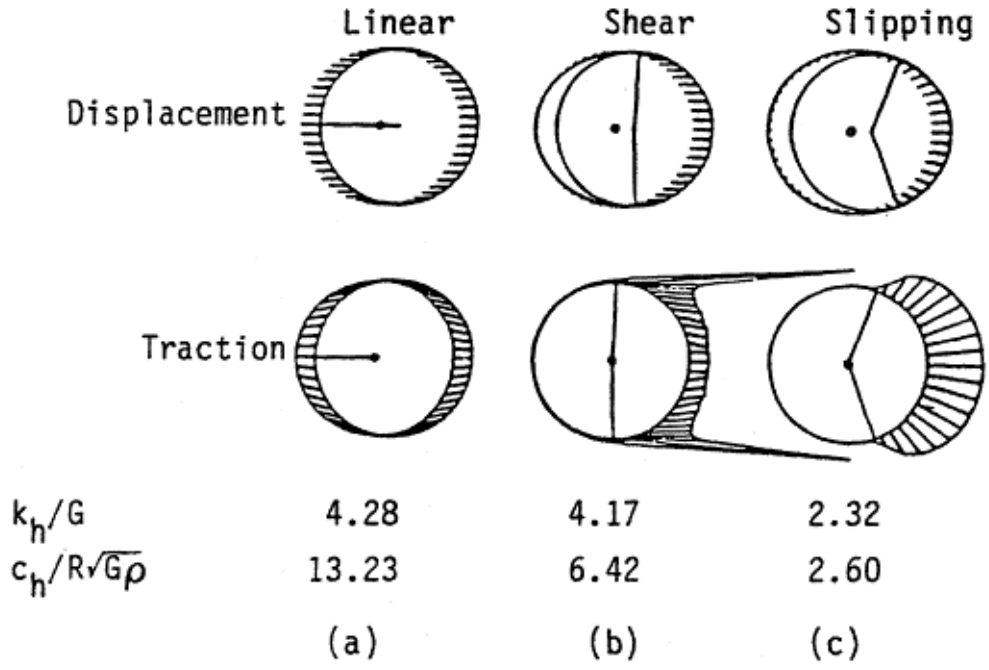

Figure 3-8. Influence of model on behavior.

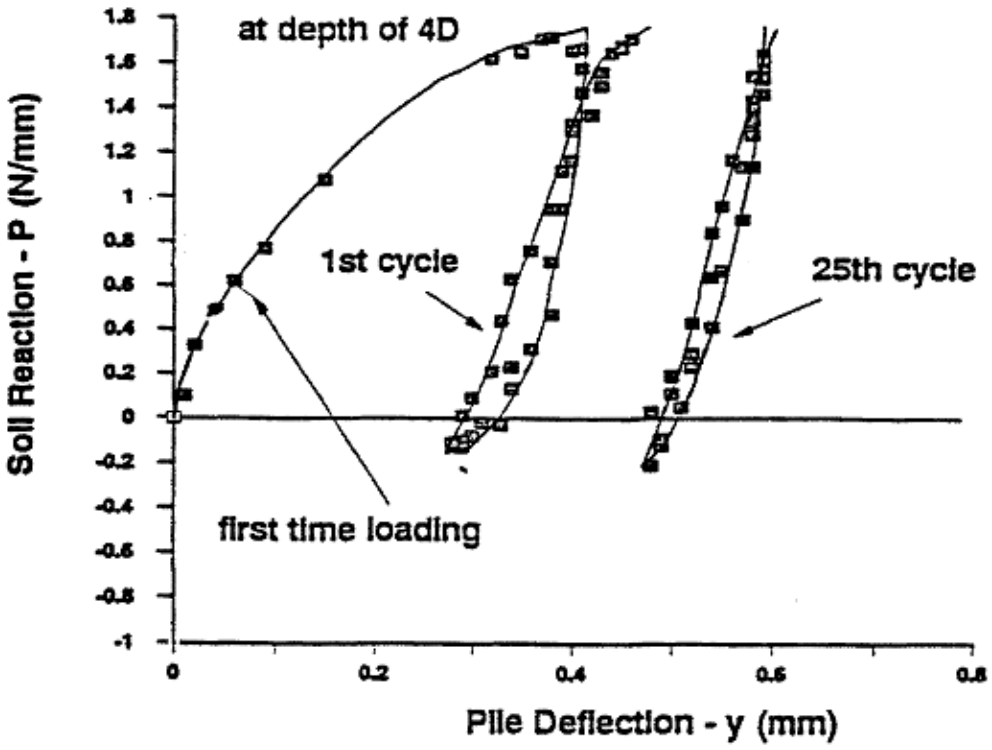

Figure 3-9. Typical p-y curve.

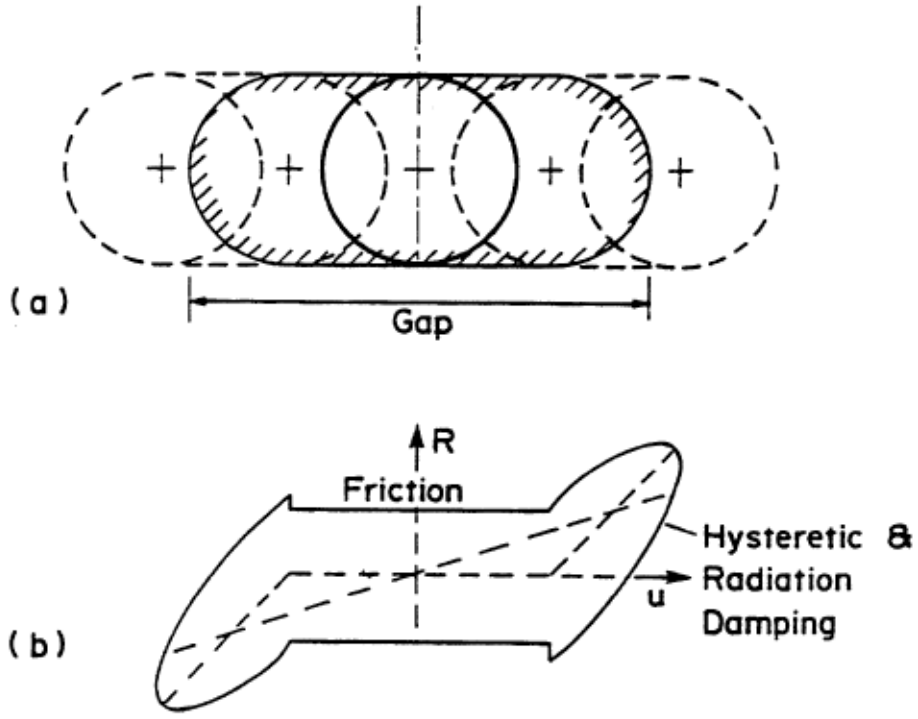

Figure 3-10. Gapping and hysteretic behavior.

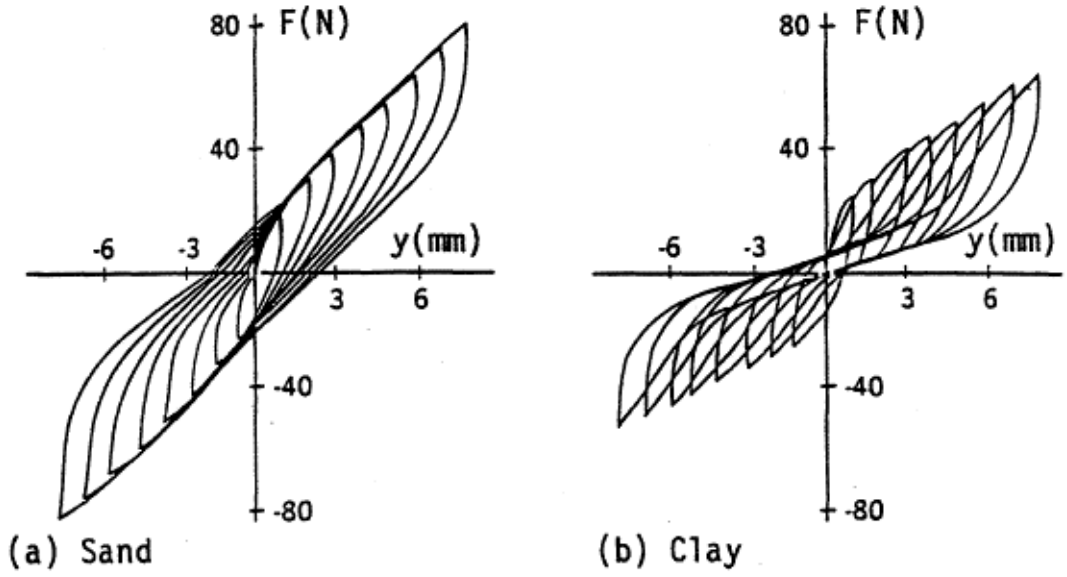

Figure 3-11. Cyclic behavior for sand and clay.

a comparison study showing the API equation as having least cumulative error in comparison with experimental data from full scale pile tests, although one must consider that this is still a very approximate procedure.

The American Petroleum Institute (1994) recommended practice for offshore platforms gives guidance in determining p-y curves. That information is reported verbatim in the following sections:

> **Lateral Bearing Capacity for Soft Clay.** For static lateral loads the ultimate unit lateral bearing capacity of soft clay p_u has been found to vary between 8c and 12c except at shallow depths where failure occurs in a different mode due to minimum overburden pressure. Cyclic loads cause deterioration of lateral bearing capacity below that for static loads. In the absence of more definitive criteria, the following is recommended. The value of p_u increases from 3c to 9c as X increases from 0 to X_R according to:
>
> $$p_u = 3c + \gamma' X + J c X / D \qquad (3\text{-}3)$$
>
> and
>
> $$p_u = 9 c \text{ for } X \geq X_R \qquad (3\text{-}4)$$
>
> where:
>
> p_u ultimate resistance, in stress units
> c undrained shear strength of undisturbed clay soil samples, in stress units
> D pile diameter
> γ' buoyant unit weight of soil, in weight density units
> J dimensionless empirical constant with values ranging from 0.25 to 0.5 having been determined by field testing. A value of 0.5 is appropriate for Gulf of Mexico clays.
> X depth below soil surface
> X_R depth below soil surface to bottom of reduced resistance zone. For a condition of constant strength with depth, Equations 3-3 and 3-4 are solved simultaneously to give:
>
> $$X_R = 6D / ((\gamma' D / c) + J) \qquad (3\text{-}5)$$
>
> Where the strength varies with depth, Equations 3-3 and 3-4 may be solved by plotting the two equations, i.e., p_u vs. depth. The point of first intersection of two equations is taken to be X_R. These empirical relationships may not apply where strength variations are erratic. In general, minimum values of X_R should be about 2.5 pile diameters.
>
> Lateral soil resistance-deflection relationships for piles in soft clay are generally nonlinear, Figure 3-12. The p-y curves for the short-term static load case may be generated from the following table:

p/p_u	y/y_c

0.00	0.0
0.50	1.0
0.72	3.0
1.00	8.0
1.00	

where:

p actual lateral resistance, in stress units
y actual lateral deflection
y_c $2.5\ _c D$
$_c$ strain which occurs at one-half the maximum stress on laboratory undrained compression tests of undisturbed soil samples

For the case where equilibrium has been reached under cyclic loading, the p-y curves may be generated from the following table:

$X > X_R$		$X \ X_R$	
p/p_u	y/y_c	$p/\ p_u$	y/y_c
0.5	1.0	0.5	1.0
0.72	3.0	0.72	3.0
0.72		$0.72X/X_R$	15.0
		$0.72X/X_R$	

Lateral Bearing Capacity for Stiff Clay. For static lateral loads, the ultimate bearing capacity, p_u, of stiff clay (c > 96 kPa or 1 Tsf) as for soft clay would vary between 8c and 12c. Due to rapid deterioration under cyclic loadings, the ultimate static resistance should be reduced for cyclic design considerations. While stiff clays also have nonlinear stress-strain relationships, they are generally more brittle than soft clays. In developing stress-strain curves and subsequent p-y curves for cyclic loads, consideration should be given to the possible rapid deterioration of load capacity at large deflections for stiff clays.

Lateral Bearing Capacity for Sand. The ultimate lateral bearing capacity for sand has been found to vary from a value at shallow depths determined by Equation 3-6 to a value at deep depths determined by Equation 3-7. At a given depth the equation giving the smallest value of Pu should be used as the ultimate bearing capacity.

$$P_{us} = (C_1X + C_2D)\ \gamma'X \qquad (3\text{-}6)$$

$$P_{ud} = C_3\,D\ \ \gamma'\ X \qquad (3\text{-}7)$$

where

Pu ultimate resistance (force/unit length) (s=shallow, d=deep)
γ' buoyant soil weight, in weight density units
X depth
γ' angle of internal friction in sand
Cl Coefficient determined from Figure 3-13 as a function of ϕ'

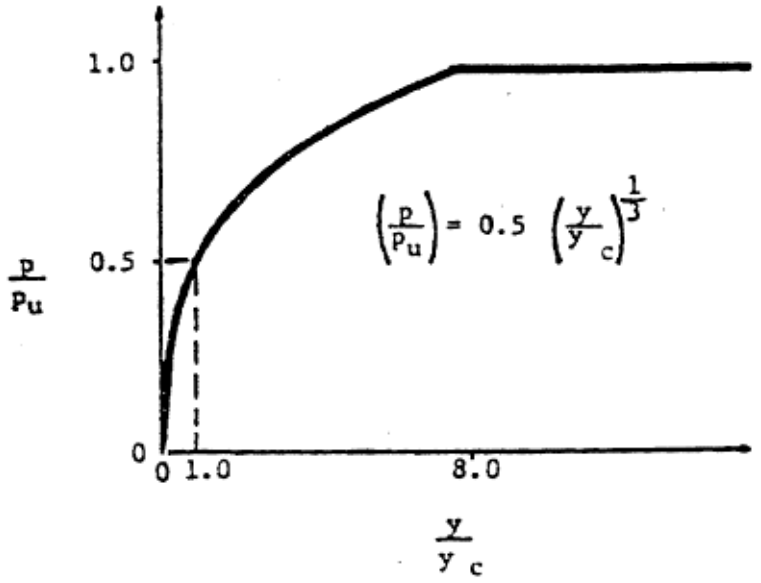

a. Static loading

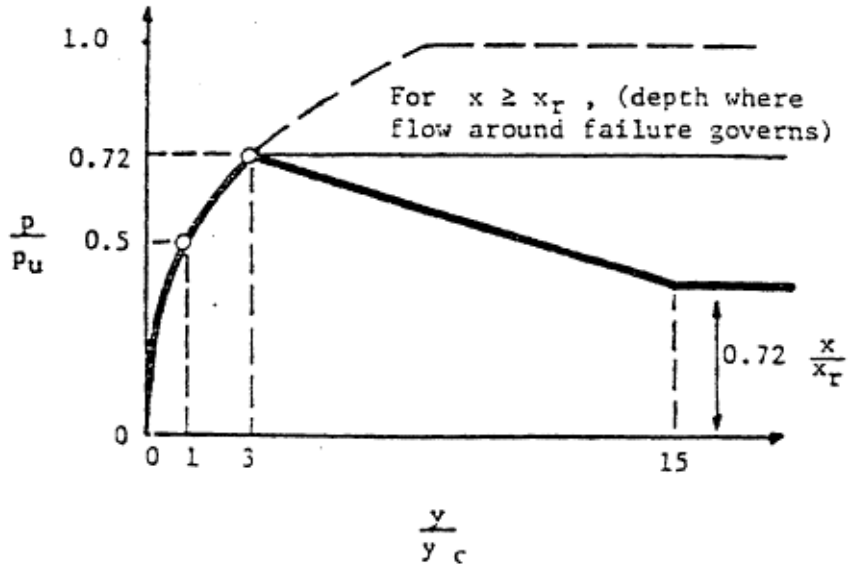

b. Cyclic loading

Figure 3-12. Shape of p-y curves for soft clay

C2 Coefficient determined from Figure 3-13 as a function of ϕ'
C3 Coefficient determined from Figure 3-13 as a function of ϕ'
D average pile diameter from surface to depth

The lateral soil resistance-deflection (p-y) relationship for sand is also nonlinear and in the absence of more definitive information may be approximated at any specific depth X, by the following expression.

$$P = A\, p_u \tanh [\ (k\ X\ y\ )/(A\, p_u)] \qquad (3\text{-}8)$$

where

A factor to account for cyclic or static loading continued.

A = 0.9 for cyclic loading.

$A = (3.0 - 0.8X/D) \geq 0.9$ for static loading.

p_u ultimate bearing capacity at depth X in units of force per unit length
k initial modulus of subgrade reaction in force per volume units. Determine from Figure 3-14 function of angle of internal friction.
y lateral deflection
X depth

Pile group. Consideration should be given to the effects of closely spaced adjacent piles on the load and deflection characteristics of the pile group. Generally, for pile spacing less than eight diameters, group effects may have to be evaluated.

For piles embedded in clays. the group capacity may be less than a single isolated pile capacity multiplied by the number of piles in the group; conversely, for piles embedded in sands, the group capacity may be higher than the sum of the capacities of the isolated piles. The group settlement in either clay or sand would normally be larger than that of a single pile subjected to the average pile load of the pile group.

For piles with the same pile head fixity conditions and embedded in either cohesive or cohesionless soils, the pile group would normally experience greater lateral deflection than that of a single pile under the average pile load of the corresponding group. The major factors influencing the group deflections and load distribution among the piles are the pile spacing, the ratio of pile penetration to the diameter, the pile flexibility relative to the soil, the dimensions of the group, and the variations in the shear strength and stiffness modulus of the soil with depth.

It has been noted that piles spaced 5 pile diameters apart do not exhibit a significant group effect.

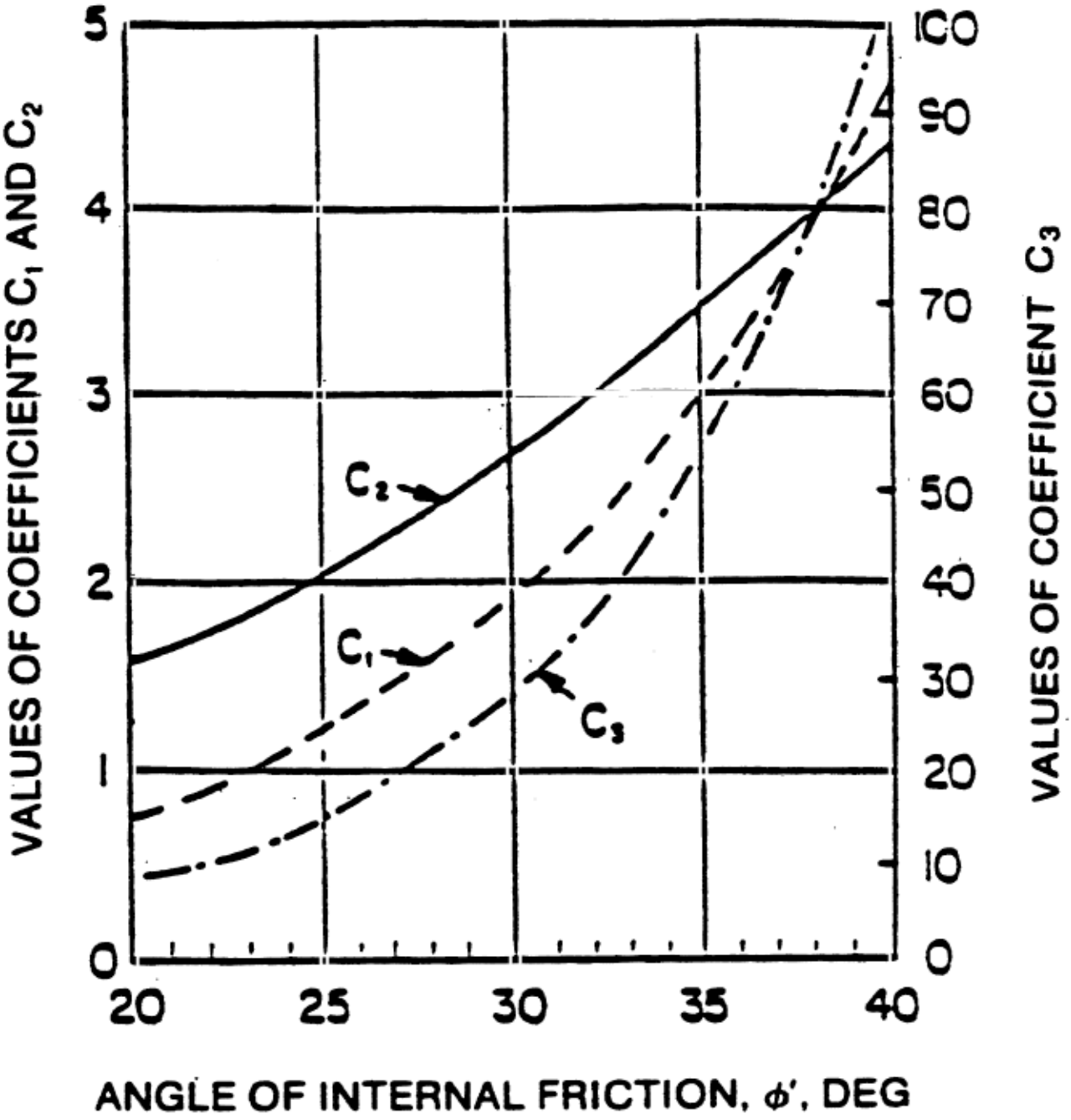

Figure 3-13. API Coefficients for sand.

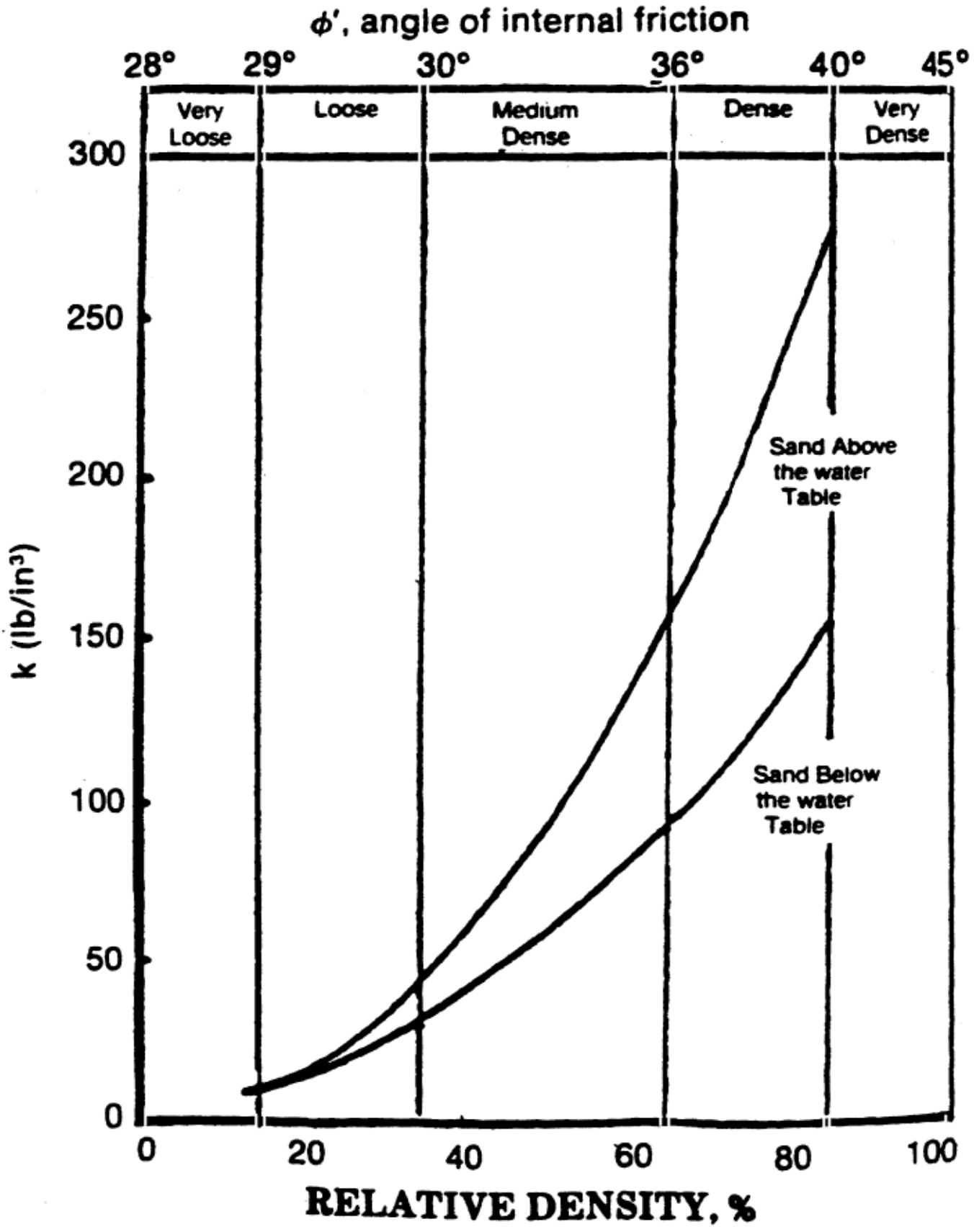

Figure 3-14. API initial modulus of subgrade reaction.

Soil Properties

The soil properties which influence the pile lateral deflection and are required for definition of a spring model are as follows:

Cohesionless Soils

γ' buoyant soil weight, in weight density units

ϕ' angle of internal friction in sand

Cohesive Soils

ε_c strain which occurs at one-half the maximum stress on laboratory undrained compression tests of undisturbed soil samples

γ' buoyant unit weight of soil, in weight density units

c undrained shear strength of undisturbed clay soil samples, in stress units

J dimensionless empirical constant with values ranging from 0.25 to 0.5 having been determined by field testing. A value of 0.5 is appropriate for Gulf of Mexico clays.

The following soil properties are taken from the NCEL Handbook for Marine Geotechnical Engineering (1985).

Properties for Cohesionless Soil

Type	Standard Penetration Blow Count, N	ϕ (Degrees)	Relative Density, D_r (%)	Effective Unit Weight, γ_b (lb/cu ft)
Very Loose to loose	<10	28-30	0-35	45-55
Medium Dense	10-30	30-36	35-65	55-65
Dense	30-50	35-42	65-85	60-70
Very Dense	50 +	40-45	85-100	60-70

Properties of Cohesive Soils

Type	Undrained Shear Strength, (Lb/sq in)	Strain at 50% maximum stress ε_c	Effective Unit Weight, γ_b (lb/cu ft)
Unconsolidated clays	0.35-1.0	2	20-25
Normally consolidated soils at depth z , inches.	1.0 + 0.0033z	2-1	25-50
Overconsolidated soils based on consistency:			
medium stiff	3.5-7	1.0	50-65
stiff	7-14	0.7	50-65
very stiff	14-28	0.5	50-65
hard	over 28	0.4	50-65

Values of ε_c can be estimated from the following table when other data is not available:

Shear Strength lb/sq ft	ε_c %
250-500	2.0
500-1000	1.0
1000-2000	0.7
2000-4000	0.5
4000-8000	0.4

Pier Analysis

A typical pier was studied, Ferritto (1997). The pier was 80 feet across and a typical bent is illustrated in Figure 3-15. The 9 piles are 24-inch octagonal prestressed piles discussed in the previous section. The pier was modeled by a 2-dimensional analysis. A static lateral force push over analysis was applied in conjunction with the standard vertical dead and live loads. It was found that the pier resisted 261 kips applied horizontally before collapse began. Yielding of the piles at the deck level with the formation of the first hinge; a second hinge developed at the mud line depth which produced a collapse mechanism. The structure underwent large gradual deformation near failure. The structure was analyzed using the El Centro earthquake record as a dynamic lateral load function. The structure was able to undergo large deflection without the occurrence of a computational instability indicating collapse. As a practical limit, a 10-inch displacement was set as an effective limit. This occurred at a lateral load of about 0.75g.

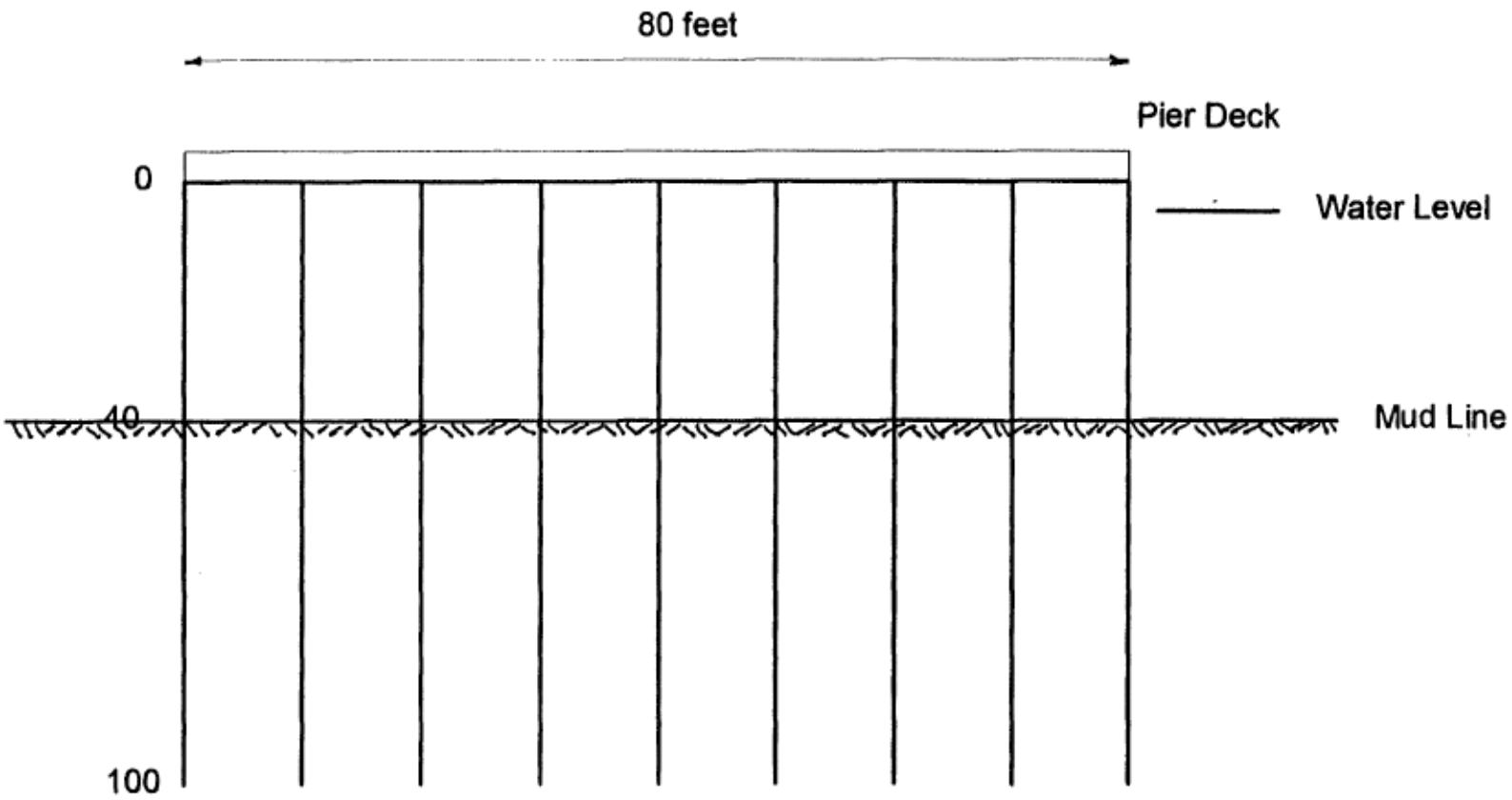

Figure 3-15. Typical pier used in 2-dimensional analysis.

The pier was modified by the inclusion of two 24-inch octagonal prestressed concrete batter piles as shown in Figure 3-16. The extent of restraint provided by the batter piles is a function of soil restraining the piles. Modeling of batter piles involves not only the horizontal py soil resistance but also the tz vertical soil resistance and the amount of q-w end-bearing. These will be discussed in the next section. For this case, the batter piles had a significant stiffening effect on the structure. A static lateral force push over analysis was performed and a lateral force of 648 kips was found to cause. As loading increased the batter pile in tension reached its failure capacity first. When this pile failed load was transferred to the remaining batter pile which failed causing failure of all the remaining piles. The structure performed in a brittle manner such that collapse occurred immediately after the first pile failed. This structure was also analyzed using the El Centro earthquake record as a dynamic lateral load function. Collapse occurred at a peak horizontal acceleration of about 0.9g. The structure had substantially reduced lateral displacements compared to the pier without batter piles. Again the onset of batter pile failure resulted in the rapid collapse of the structure and was initiated by exceeding pile tensile limits.

Batter Piles

Previous sections focused on the lateral resistance of vertical; to fully understand the behavior of a batter pile it is necessary to review the axial pile soil skin friction (tz component) and the pile end bearing (qw component). For a vertical pile the axial and end bearing components are also vertical. Figure 3-17 shows the force components acting on a vertical pile. The spring elements are intended as visual aids to represent the forces acting along the entire length of the pile. Ultimate capacity of a vertical pile is given by:

$$Q = f A_s + qA_p \qquad (3\text{-}9)$$

where

f	Unit skin friction, tz
A_s	Area side surface of pile
q	Unit end bearing capacity, qw
A_p	Area of end of pile

For cohesive soils the skin friction is

$$f = a\,c \qquad (3\text{-}10)$$

where

$$a = 0.5^{-0.5} \quad 1.0$$
$$a = 0.5^{-0.25} > 1.0 \qquad (3\text{-}11)$$

and

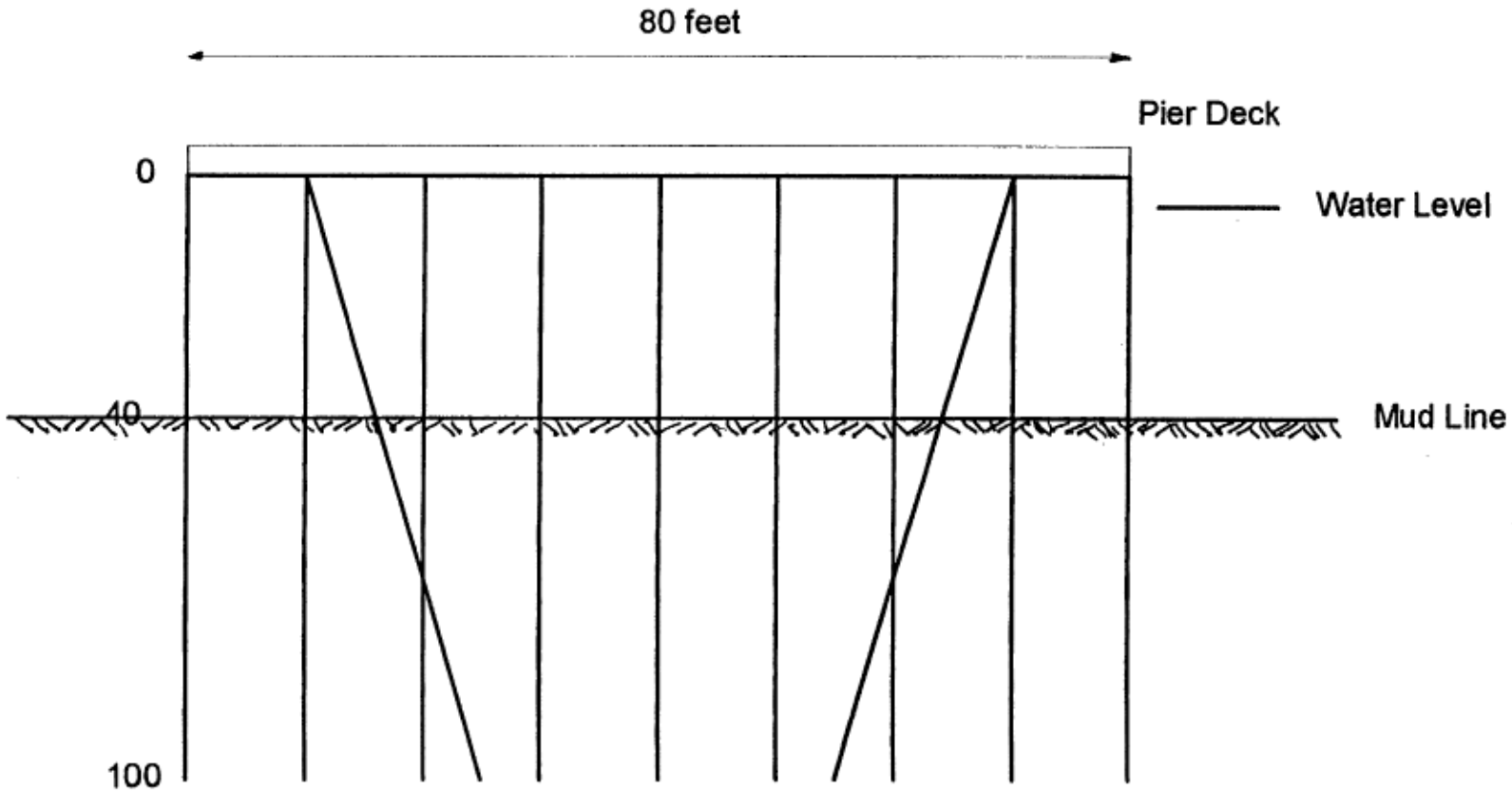

Figure 3-16. Typical pier with batter piles used in 2-dimensional analysis.

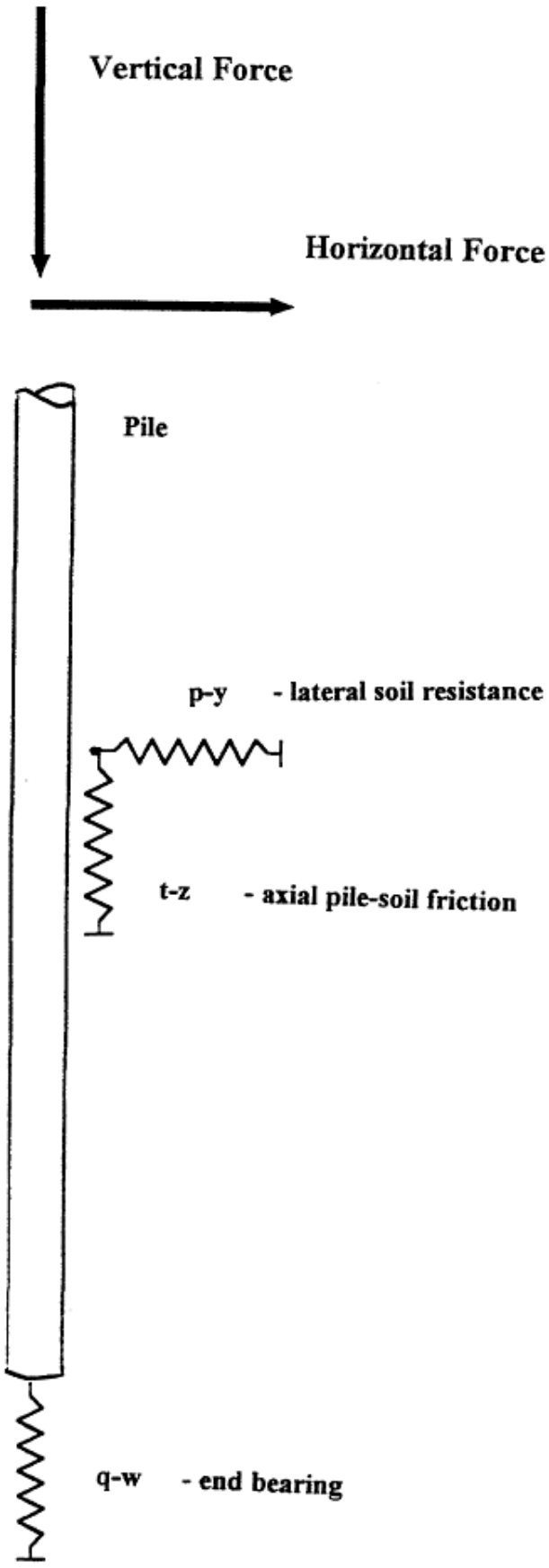

Figure 3-17. Vertical pile in soil showing restraints.

c	Undrained shear strength
ψ	c/p_o'
p_o'	Effective overburden at point in question

For cohesive soils the end bearing unit stress of piles is:

$$q = 9\ c \qquad (3\text{-}12)$$

For cohesionless soils the unit skin friction is:

$$f = K\ p_o'\ \tan\ \delta \qquad (3\text{-}13)$$

where

K	dimensionless coefficient of lateral earth pressure, usually = 1
δ	friction angle between the soil and pile

For cohesionless soils the unit end bearing stress is:

$$q = p_o'N_q \qquad (3\text{-}14)$$

API (1994) gives procedures for computing tz axial force-deflection curves and qw end bearing-deflection curves which define the soil resistance pictured in Figure 3-17. For comparison consider the following for cohesionless soils:

Lateral	Vertical
$pu/D = (c1\ X + C2\ D)\ \gamma'\ X/D$	$f = K\ p_o'\tan\ \delta\ D$

for a depth of 10 feet, 18-inch pile diameter

pu/D (14) γ' X	f (.7) γ' X

For cohesive soils

Lateral	Vertical
$pu \cong 10\ c$	$q \cong 1\ c$

From the above it may be seen that the py lateral resistance is much greater than the tz axial skin friction. For this reason it is logical that most of the lateral resistance of a pile is mobilized in the near surface region of a pile to a depth of 5 to 10 pile diameters. To resist vertical loads without end bearing requires long pile development lengths. End bearing is a significant component in pile capacity. The magnitude of the end bearing resistance is on the same order as the lateral resistance. The capacity of a pile in tension is less than in compression and less than in lateral resistance. The above are general

observations and the ratio of lateral capacity to tension or compression capacity depends on a number of factors:

- Length of the pile
- Flexural and shear strength of the pile
- Vertical distribution of soil strength
- Acceptable lateral displacement limits.

Having reviewed the fundamentals of vertical pile behavior, it is now possible to discuss batter piles.

Figure 3-18 illustrates a batter pile based rotation of a vertical pile. For simplicity the forces are kept normal and axial to the pile. Consider as the tz axial resistance of the soil goes to zero the pile would tend to slip out of the ground with minimal axial loading in tension. The modeling of a pile by finite element representation must accurately capture this interaction. In a finite element model, it is possible to use spring/truss elements to model the soil resistance. Use of horizontal and vertical springs to model the components of py and tz resistance would introduce a major problem of how to combine these elements. The axial tz acts independent of the normal py and must allow pile slippage. End bearing is an axial component. After a number of trial iterations of various models, it was found that the most accurate and easiest to use is one with spring elements axial and normal to the batter pile. Additionally the end bearing must be an axial spring. All py, tz and qw load deflection curves are based on the depth of the element below the ground surface.

An analysis was performed on a batter pile with a 1 horizontal to 2 vertical slope driven to a depth of 50 feet and loaded laterally at a height of 3 feet above the ground. The pile was a 24-inch circular pipe pile in medium sand. The soil py and tz curves were calculated at intervals of 1 foot using the equations in API (1994). Normal and axial soil springs were spaced at 1-foot intervals for the first 20 feet and then at 2-foot intervals. The soil springs utilized bilinear material properties. A vertical load of 20 kips was used. The lateral capacity of the batter pile when pulled horizontally in a direction away from the batter was 12 kips compared to 36 kips when pulled horizontally in the direction of the batter. The lateral capacity of an equivalent vertical pile was 20 kips.

From a series of studies of a batter pile it is concluded that the lateral load capacity of the batter pile is dependent upon the vertical load of the pile. When the lateral load acts horizontally opposite to the direction of the batter, a component of this load acts on the pile axially in tension. The vertical load offsets this effect and can increase pile capacity up to a limit. This is generally the direction of lower pile capacity. When the lateral load acts horizontally toward the direction of the batter the vertical load resists the moment caused by the lateral load and reduces deflection.

The vertical distribution of pile soil reaction is a function of pile length. The longer the pile the greater the friction along the pile and the less in end bearing. Since

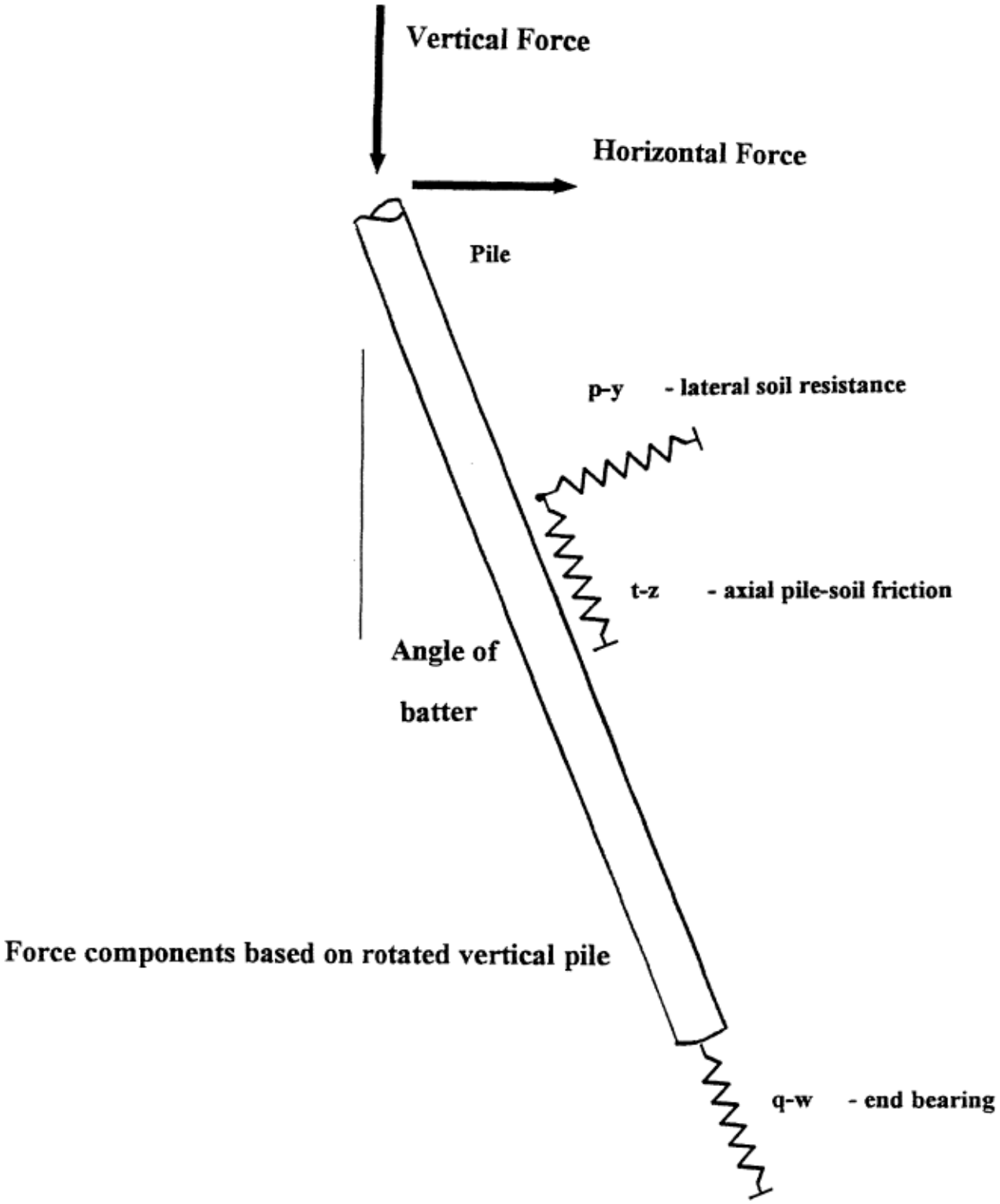

Figure 3-18. Batter pile in soil showing restraints.

stiffness increases with depth more force is transferred into the soil at deeper depths (assuming pile compression is not significant).

It should be noted that connections to adjacent piles in group should be capable of developing the calculated tension including earthquake forces, but not less than a tension equal to one-half the compression load less the dead weight in the pile. Unless special provisions are made for the difficulties of installation and the effects of diminution of the hammer blow on the capacity, keep the slope of the batter piles to one horizontal to two vertical or steeper (preferably 1 horizontal to 2.5 vertical).

P - Delta Effect

One element of structural analysis should be noted- that of the P - delta effect associated with columns in frames. This is usually thought of as a secondary effect composed of the additional moment which is imposed on a column by the axial load acting on a moment arm caused by the lateral deflection of the top of the column. For piers and bridge structures this can be significant. Duan and Cooper, 1995 discuss this extensively and conclude that the effect should be included in seismic analysis. Note that the peak lateral resisting force is reduced.

Use of Elastic Response Spectra Techniques

The above sections have illustrated the need for nonlinear representation of the soil-pile interface and the p- effects. Use of linear response spectra and force reduction factors in building codes has been common practice. The use of linear techniques should be applied rationally. In pier design, such linear techniques should be used when appropriate and avoided where there is significant nonlinear yielding such as where soft soils are present. The engineer has a variety of tools which are tailored to the complexity of the problem.

Design Performance And Earthquake Levels

Performance Goal

The goal of this criteria is to standardize the seismic design of piers and wharves providing an acceptable uniform level of seismic safety for all waterfront locations. This criteria is intended to produce a level of design in piers and wharves such that there is a high probability the structures will perform at satisfactory levels throughout their design life. Waterfront structures have been classified as essential structures. Although the criteria focus on the regions where seismicity is highest such as on the West Coast, it is applicable to other areas as well. Structures located in areas of high seismicity shall be designed:

To resist earthquakes of moderate size which can be expected to occur one or more times during the life of the structure without structural damage of significance. This represents a condition of expected repeated loading.

To resist major earthquakes which are considered as infrequent events maintaining environmental protection and life safety, precluding total collapse but allowing a measure of controlled inelastic behavior which will require repair. . This represents a condition of expected loading to occur at least once during the design life of the structure. In reality most structures end up being used well beyond their design life.

To preclude major spills of hazardous and polluting materials for very rare earthquakes The intention is to prevent spills on fuel piers. This may be accomplished by installation of cutoff valves, and containment to limit the size of the spill and prevent its spread. It may also be accomplished by increased strengthening of components.

To utilize economic/risk analysis where necessary. This is intended to allow the designer freedom to consider economic analysis of alternative load conditions in the infrequent case where a local fault dominates a site and is capable of very high ground motions. Such a condition requires specialized extensive evaluation of the site hazard.

To consider liquefaction as a major waterfront problem. The designer shall consider liquefaction factors of safety in design of remedial measures of backfill. Rigid adherence to developing fixed factors of safety may not be economically achievable. The intent is to place more credence in the expected deformations and consequences of liquefaction which will occur rather than the simple factor of safety. Assurance of limited deformations shall be given precedence over a factor of safety. The designer shall have the option of using current technology to demonstrate that settlements and lateral deformations are sufficiently limited to insure structural performance and factors of safety lower than limit values may be used. The term *current technology* refers to the use of procedures for the computation of vertical and lateral deformations.

In general all waterfront construction which supports fuel transfer operations (excluding piers and wharves) falls within the category of essential construction. The policy is to minimize downtime for these facilities. Determination of essential construction shall be determined by the user in conjunction with the California State Lands Commission, Marine Facilities Division. Piers and wharves shall be considered essential construction. Emphasis shall be placed on minimizing downtime and interruption to essential functions.

Limit States

Level 1 Earthquake; Serviceability Limit State Two levels of design earthquake are considered. Level 1, has a high probability of occurrence during the life of the pier or wharf. Under this level of excitation the structure should satisfy the serviceability criterion of continued functionality immediately after the Level 1 earthquake. Any repairs required should be essentially cosmetic. Structural damage requiring repair is not permitted. Note that this does not imply a requirement for elastic response, which would limit concrete strains to about 0.001, and steel strains to yield strain. Concrete structures may be considered serviceable, without any significant decrement to structural integrity, provided concrete strains reached during maximum seismic response to the Level 1 earthquake do not cause incipient spalling of concrete cover, and if residual crack widths after the earthquake has ceased are sufficiently small to negate the need for special corrosion protection measures, such as crack grouting. Note that this latter requirement implies that significantly larger crack widths might momentarily exist during seismic response, since these have no effect on corrosion potential.

Thus the performance of potential plastic hinges should be checked under Level 1 earthquake to ensure that maximum material strains do not exceed the limits defined for Structural Performance Limit States.

Note that this check will normally only be required at the pile/deck interface, since curvatures will be higher there than in any potential in-ground hinges. Also, confinement of the cover concrete of potential in-ground plastic hinges by the lateral pressure developed in the soil increases the concrete strain at which spalling initiates, Budek et al (1997), increasing the corresponding serviceability curvatures, particularly for prestressed piles, where steel strains are unlikely to be critical.

Level 2 Earthquake; Damage-control Limit State Level 2 earthquake represents an earthquake with a low probability of occurring during the design life of the structure. Repairable damage to structure and/or foundation, and limited permanent deformation are acceptable under this level of earthquake

Since the design philosophy (discussed subsequently) is to restrict inelastic action to careful defined and detailed plastic hinges in piles, strain limits may again be used to

define acceptable response. Distinction needs to be made between the pile/deck hinge and the in-ground hinge locations, since access to the latter will frequently be impractical after an earthquake. **As a consequence the in-ground hinge should satisfy serviceability criteria even under Level 2 earthquake. Thus the steel strain should not exceed 0.01.** However, as noted above, passive confinement by the soil increases the spalling strain, and a concrete strain of 0.008 may be adopted. The pile/deck connection hinge will have allowable concrete strains dependent on the amount of transverse reinforcement provided. As a consequence of these actions, the maximum strains calculated under a Level 2 earthquake must not exceed the strain capacities defined below under *Structural Criteria For Piers and Wharves.*

Level 4 Earthquake; Prevent Major Spill Wharves and piers on which hazardous materials are stored or used shall be capable of resisting a Level 4 earthquake without release of a major spill of hazardous materials.

Load Combinations

Two load combinations are to be considered.

$$(1 + k)(D + rL) + E \qquad (3\text{-}15)$$

$$(1 - k) D + E \qquad (3\text{-}16)$$

where D = Dead Load
L = Design Live Load
r = Live Load reduction factor(depends on expected L present in actual case typically 0.2 but could be higher)
E= Level 1 or Level 2 earthquake, as appropriate.
k= 0.5 * (PGA), where PGA is the effective peak horizontal ground acceleration.

The first equation, Equation 3-15, includes maximum gravity load effects and incorporates a realistic assessment of probable live load, while the second, Equation 3-16, includes minimum gravity loads. Influences of vertical acceleration are considered through the factor **k** which increases gravity load effects in Equation 3-15, but reduces the effects of gravity in Equation 3-16. The value of **k** is taken as 0.5 times the effective peak horizontal ground acceleration. This is based on the observation that peak vertical accelerations are generally less than peak horizontal accelerations. A typical value of 67% is often assumed. Further, peak vertical response is likely to be of very short duration and unlikely to coincide with peak horizontal response. The simplified approach suggested has been proposed for bridge design, Priestley et al (1996), and will be adequately conservative in most cases. An exception may occur when a large proportion of the seismic risk at the site comes from a fault closer than 10km from the site. In this case special studies should be undertaken to determine the peak vertical acceleration, and a value of 75% of effective peak vertical acceleration adopted for **k**. Alternatively

inelastic analysis incorporating simultaneous excitation by vertical and horizontal acceleration records may be carried out.

Note that the main influence of the combination of gravity and seismic effects will be on the design of deck members, where the combined forces (moment, shear, etc.) from gravity and seismic effects must remain below the dependable strength, in accordance with capacity design principles. For the primary seismic resisting elements, which are typically the wharf or pier piles, gravity effects have comparatively little influence. Even at the serviceability limit state, the deformations corresponding to gravity loads will be small compared with those due to the Level 1 earthquake. Also, the variation in gravity axial load on piles implied by the difference between Equations 3-15 and 3-16 will not generally result in significant differences in lateral displacement capacity. As discussed in the section on pier and wharf response, seismic performance is judged primarily in terms of displacement capacity and demand, with force levels being of only secondary significance.

Note further that earlier seismic design procedures, where seismic forces calculated by elastic analysis procedures were reduced by a force reduction factor R, and were then added to the corresponding forces resulting from gravity effects, are fundamentally in error, since they grossly exaggerate the importance of the gravity effect, Priestley et al. (1996).

Combination of Orthogonal Effects

The traditional 100% X + 30%Y; 30% X + 100% Y combinations of orthogonal effects is retained. In this context the principal actions referred to are the displacements in the horizontal plane. This is clarified in Figure 3-19, where a plane view of a wharf is analyzed under both X and Y direction actions, resulting in the deflected shapes of Figure 3-19(a) and 3-19(b) respectively. Considering only the corner pile 1, the design displacements Δ_d corresponding to Equations 3-17 and 3-18 are given by:

$$\Delta_X = \Delta_{XX} + 0.3\Delta_{XY}$$

$$\Delta_Y = \Delta_{YX} + 0.3\Delta_{YY} \qquad (3\text{-}17)$$

$$\Delta_d = \sqrt{\Delta_X^2 + \Delta_Y^2}$$

$$\Delta_X = 0.3\Delta_{XX} + \Delta_{XY}$$

$$\Delta_Y = 0.3\Delta_{YX} + \Delta_{YY} \qquad (3\text{-}18)$$

$$\Delta_d = \sqrt{\Delta_X^2 + \Delta_Y^2}$$

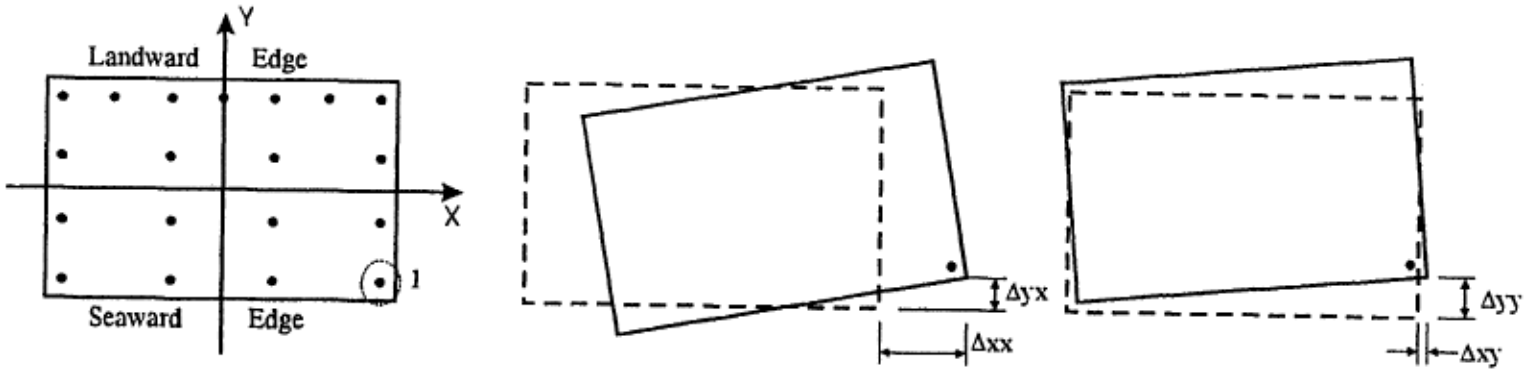

Figure 3-19 Plan view of wharf segment under X and Y seismic excitations.

The displacements Δ_d corresponding to Equations 3-17 and 3-18 are then compared with the displacement capacities at the relevant performance limit state.

Methods Of Analysis For Seismic Response

In comparison with many other structures such as multistory buildings, or multispan bridges, wharves and piers are frequently structurally rather simple. As such, analyses to determine seismic response can often utilize comparatively simple analysis procedures, as discussed below, without significant loss of accuracy. Complexity tends to come more from the high significance of soil-structure interaction, from significant torsional response resulting from the typical increase in effective pile lengths from landward to seaward sides (or ends) of the wharf (or pier), and from interaction between adjacent wharf or pier segments separated by movement joints with shear keys, rather than from structural configuration.

Analytical effort must be placed into the best possible modeling of these effects, and of the influence of cracking on member stiffness in the elastic range of response. Effort placed into the accurate modeling of member stiffness and soil-structure interaction effects will have a greater significance on the accurate prediction of peak response than will the choice of analytical procedure (e.g. Methods A, B, or D below). Indeed there is no point in carrying out a sophisticated time-history analysis unless detailed and accurate simulation of member stiffness and strength has preceded the analysis.

Modeling Aspects

Soil-Structure Interaction

Figure 3-20(a) represents a typical transverse section through a wharf supported on a soil foundation comprised of different materials (insitu sand and gravel, perhaps with clay lenses; rip-rap and other foundation improvement materials etc.). The most precise modeling of this situation would involve inelastic finite element modeling of the foundation material to a sufficient depth below, and to a sufficient distance on each side, such that strains in the foundation material at the boundaries would not be influenced by the response of the wharf structure. The foundation would be connected to the piles by inelastic Winkler springs at sufficiently close spacing so that adequate representation of the pile deformation relative to the foundation material, and precise definition of the in-ground plastic hinging would be provided. Close to the ground surface, where soil spring stiffness has the greatest influence on structural response, the springs should have different stiffnesses and strengths in the seaward, landward, and longitudinal (parallel to shore) directions, as a consequence of the dyke slope.

The pile elements would be represented by inelastic properties based on moment-curvature analyses. Since the key properties of piles (namely strength and stiffness)

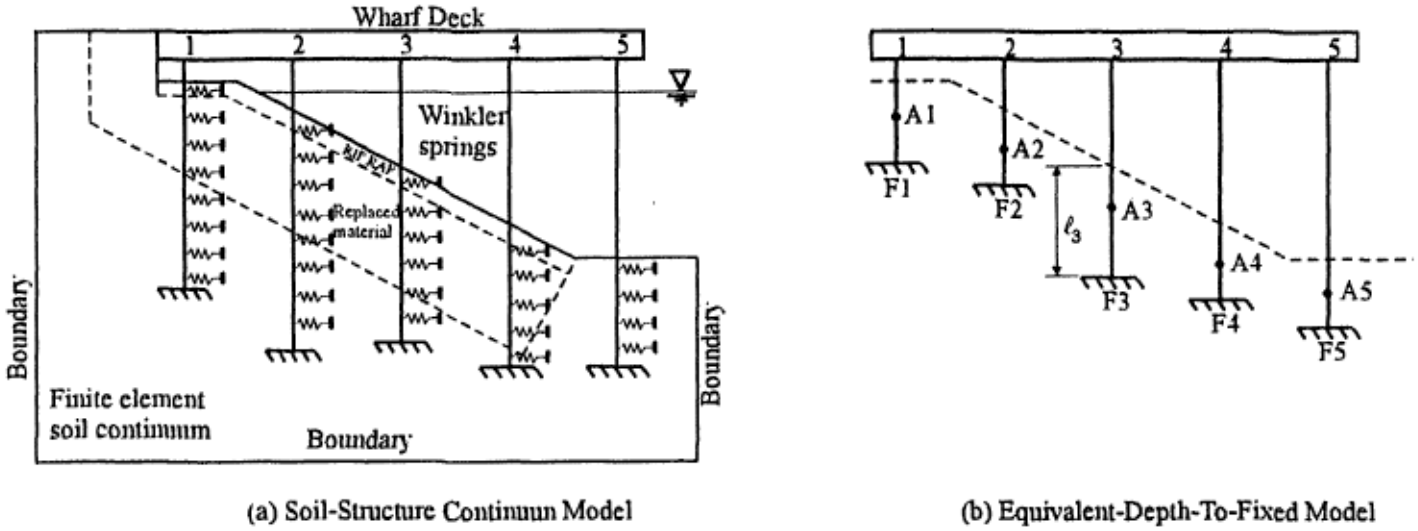

(a) Soil-Structure Continuun Model

(b) Equivalent-Depth-To-Fixed Model

Figure 3-20. Modeling soil-structure interaction for a wharf.

depend on the axial load level, which varies during seismic response, sophisticated interaction modeling would be necessary.

It is apparent that structural modeling of the accuracy and detail suggested above, though possible, is at the upper limit of engineering practice, and may be incompatible with the very considerable uncertainty associated with the seismic input. In many cases it is thus appropriate to adopt simplified modeling techniques. Two possibilities are illustrated in Figure 3-20. In Figure 3-20(a), the complexity may be reduced by assuming that the piles are fixed at their bases with the seismic input applied simultaneously and coherently to each pile base. The soil springs also connect the piles to the rigid boundary. Thus the assumption is made that the deformations within the soil are small compared with those of the wharf or pier.

In Figure 3-20(b), the complexity is further reduced by replacing the soil spring systems by shortening the piles to "equivalent fixity" piles, where the soil is not explicitly modeled, and the piles are considered to be fixed at a depth which results in the correct overall stiffness and displacement for the wharf or pier. Where different soil stiffnesses are appropriate for opposite directions of response, average values will be used, or two analyses carried out, based on the two different stiffnesses respectively. It should be noted that though this modeling can correctly predict stiffness, displacements and elastic periods, it will over-predict maximum pile in-ground moments. The model will also require adjustment for inelastic analyses, since in-ground hinges will form higher in the pile than the depth of equivalent fixity for displacements.

Geotechnical guidance will be needed to determine the appropriate depth to fixity (e.g. l_3 in Figure 3-20(b)), but an approximate value may be determined from the dimensionless charts of Figure 3-21. A typical value of $l_3 = 5D_p$ where D_p is the pile diameter, may be used as a starting point for design

Movement Joints

Long wharf structures, and less commonly piers, may be divided into segments by movement joints to facilitate thermal, creep and shrinkage movements. Typically the joints allow free longitudinal opening, but restrain transverse displacement by the incorporation of shear keys. Modeling these posses problems, particularly when elastic analysis methods are used. Under relative longitudinal displacement, the segments can open freely, but under closing displacements, high axial stiffness between the segments develops after the initial gap is closed. Relative transverse rotations are initially unrestrained, but after rotations are sufficient to close one side of the joint, further rotation implies relative axial displacement, resulting in axial compression between the segments. The behavior can be modeled with a central shear spring allowing longitudinal displacement but restraining transverse displacements, and two axial springs, one at each end of the joint, as suggested in Figure 3-22. These two springs have zero stiffness under relative opening displacement, but have a very high compression stiffness after the initial gap $_g$ is closed.

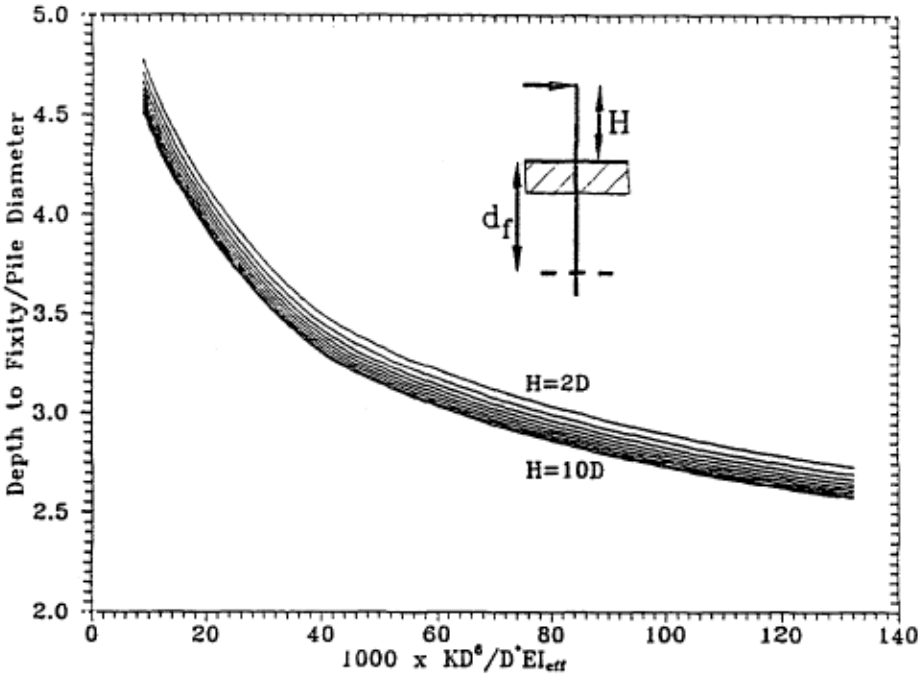

(a) Free-head pile

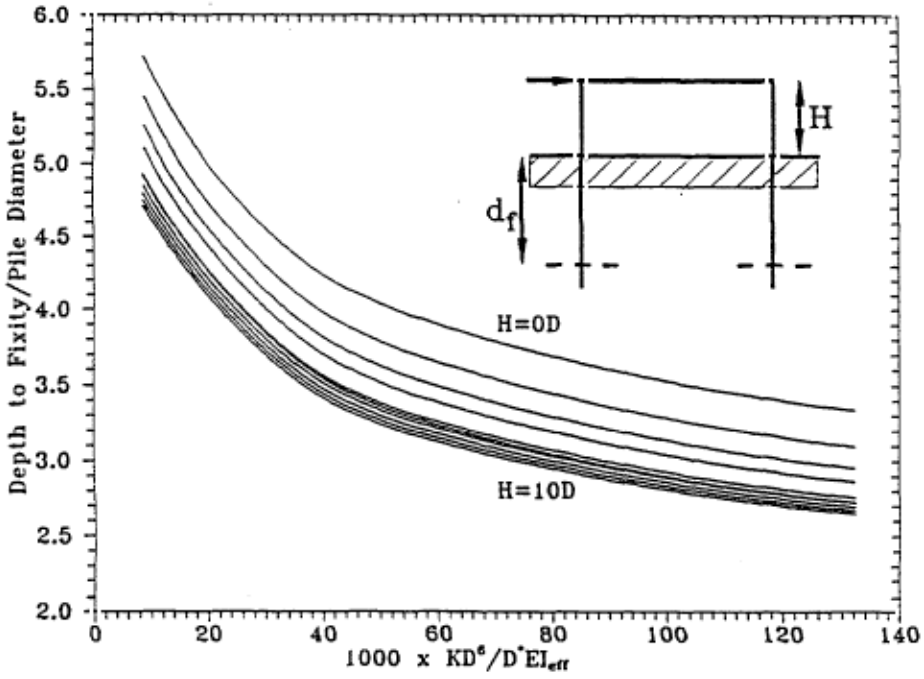

(b) Fixed-head pile

Figure 3-21. Equivalent depth to fixity for CLDH piles.

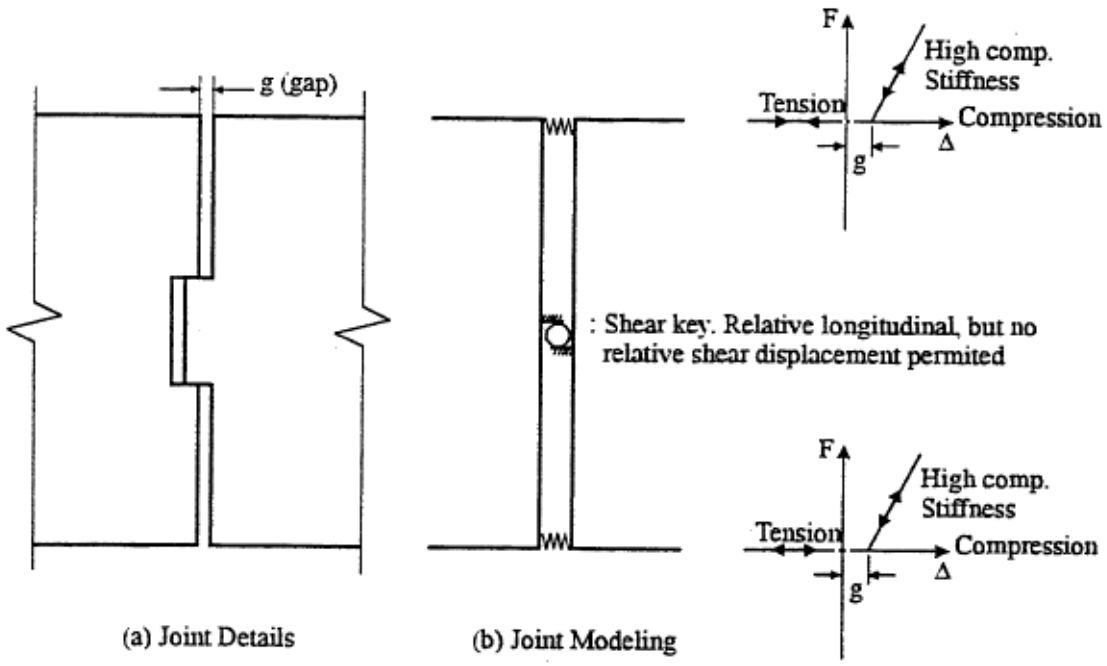

Figure 3-22. Modeling of movement joints.

Clearly it is not feasible to represent this nonlinear response in an elastic modal analysis. Even in an inelastic analysis accurate modeling is difficult because of the need to consider different possible initial gaps, and difficulty in modeling energy dissipation by plastic impact as the joint closes.

Method A: Equivalent Single Mode Analysis

Long wharves on regular ground tend to behave as simple one-degree-of-freedom structures under transverse response. The main complexity arises from torsional displacements under longitudinal response, and from interaction across shear keys between adjacent segments, as discussed above. An individual segment, particularly, will respond with significant torsional component when excited by motion parallel to the shore, or length of the wharf. Dynamic analyses, Priestley (1999) indicate that the torsional response is reduced when segments are connected by shear keys, and with multiple-segment wharves, the torsional response of the inner segments is negligible. It is thus conservative to estimate the displacement response based on the behavior of a single wharf segment between movement joints, except when calculating shear key forces.

Extensive inelastic time-history analyses of single and multi-segment wharves have indicated that an approximate upper bound on displacement response of the piles could be established by multiplying the displacement response calculated under pure transverse (perpendicular to the shore) excitation by a factor taking into account the orthogonal load combinations of Equations 3-17 and 3-18, including torsional components of response. For the critical shorter landward line of piles

$$\Delta_{max} = \Delta_t \sqrt{1 + (0.3(1 + 20\ e/L_L))^2} \qquad (3\text{-}19)$$

where

Δ_t = displacement under pure translational response,
e = eccentricity between center of mass and center of rigidity
L_L = longitudinal length of the wharf segment.

Note that the corner piles of the line of piles at the sea edge of the wharf will be subjected to slightly higher than given by Equation 3-19, but these piles will not be critical because of their greatly increased flexibility and hence increased displacement capacity, compared with the landward piles.

The shear force across shear keys connecting adjacent wharf segments cannot be directly estimated from a Method A analysis. However, time-history analysis of multiple wharf segments indicates that the highest shear forces will occur across movement joints in two-segment wharves, and that these forces decrease, relative to segment weight approximately in inverse proportion to wharf segment aspect ratio L_L/L_T where L_L and L_T where the longitudinal and transverse plan dimensions of the wharf segment pile

group. The following expression may be used as an approximate upper bound to the shear key force V_{sk}:

$$V_{sk} = 1.5\ (e/L_L)\ V_{\Delta T} \qquad (3\text{-}20)$$

Where $V_{\Delta T}$ is the total segment lateral force found from a pushover analysis at the level of displacement Δ_T calculated for pure translational response at the appropriate limit state, L_L is the segment length, and e is the eccentricity between the center of stiffness and the center of mass.

Method A is of adequate accuracy for design of many simple structures when supplemented by a Method C pushover analysis, and is particularly useful for the preliminary stages of design, even of relatively important and complex structures. Final design verification may be made by one of the more sophisticated analysis methods.

The approximate lateral stiffness of a wharf structure analyzed using Method A should be determined from a pushover analysis, as discussed below in relation to Method C.

Method B Multi-Mode Spectral Analysis

Spectral modal analysis will be the most common method used for estimating maximum displacement levels, particularly when deck flexibility is significant. However, as noted above, when multiple segments of long wharves are connected by movement joints with shear keys, it is difficult to model the interactions occurring at the movement joints adequately, because of their non-linear nature.

It is thus doubtful if it is worth modeling the joint, particularly if conditions are relatively uniform along the wharf. It should also be recognized that it is unlikely that there will be coherency of input motion for different segments of a long wharf. Longitudinal motion of the wharf is likely to be reduced as a consequence of impact across joints, and restriction of resonant build-up.

It is thus reasonable, for regular wharf conditions to consider an analysis of single wharf segments between movement joints as “stand alone” elements. It will also be reasonable in most cases to lump several piles together along a given line parallel to the shore an provide an analytical “super pile” with the composite properties of the tributary piles, to reduce the number of structural elements, which can be excessive, in a multi-mode analysis. Since the modal analysis will be used in conjunction with a Pushover Analysis, it will be worth considering adopting further reduction in the number of structural elements by representing the composite stiffness of a transverse line of piles, found from the Pushover analysis, by a single pile, and using a damping level appropriate to the expected displacement, is discussed in more detail in the following section.

In most stand-alone analyses of single wharf or pier segments, there will be only three highly significant modes; two translational and one torsional. These will generally be closely coupled. As a consequence it will not generally be difficult to satisfy the 95% participating mass requirement, which is larger than commonly specified in design codes. Note that to correctly model the torsional response it is essential to model the torsional inertia of the deck mass. This can either be done by distributing the deck mass to a sufficiently large number of uniformly distributed mass locations, (with a minimum of 4 located at the radius of gyration of the deck area) or by use of a single mass point with rotational inertia directly specified. Deck mass should include a contribution for the mass of the piles. Typically adding 33% of the pile mass from deck level to point of equivalent foundation fixity is appropriate.

Because of the typical close coupling of the key modes of vibration, the modal responses should be combined using the Complete Quadratic Combination (CQC) rule, Wilson et al (1981).

Method C: Pushover Analysis

Typically, as a result of large variations in effective depth to fixity of different piles, in a given wharf or pier, the onset of inelastic response will occur at greatly differing displacements for different piles. This is illustrated in Figure 3-23, representing the response of a 20-foot. segment of a typical wharf loaded in the transverse (perpendicular to shoreline) direction. There are a number of important consequences to this sequential hinging:

It is difficult to adequately represent response by an elasto-plastic approximation, which is the basis of the common force-reduction factor approach to design.
The appropriate elastic stiffness to be used in analysis is not obvious.
Different piles will have greatly different levels of ductility demand, with the shortest piles being the most critical for design or assessment.
The center of stiffness will move from a position close to the landward line of piles to a position closer to the center of mass as inelasticity starts to develop first in the landward piles.

As a consequence it is not directly feasible to carry out an elastic analysis based on the typically assumed 5% equivalent viscous damping, and then determine member forces by reducing elastic force levels by a force-reduction factor. Amongst other failings, this will grossly underestimate the design forces for the longer piles. It is thus strongly recommended that a key aspect of the design or analysis process be a series of inelastic pushover analyses, in both transverse and longitudinal directions, where 2-D sections of the wharf or pier are subjected to incremental increases in displacement, allowing the inelastic force-displacement response (e.g. Figure 3-23(b)), the sequence of hinge formation, and the magnitude of inelastic rotation $_p$ developing in each hinge to be determined. The results of such analyses can be used to

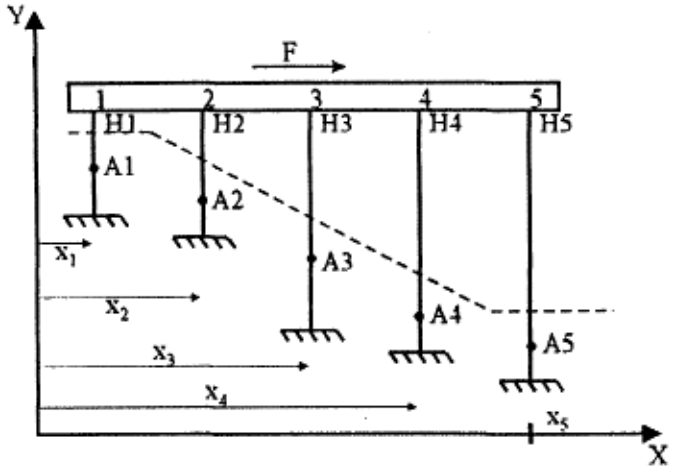

(a) Transverse section for analysis

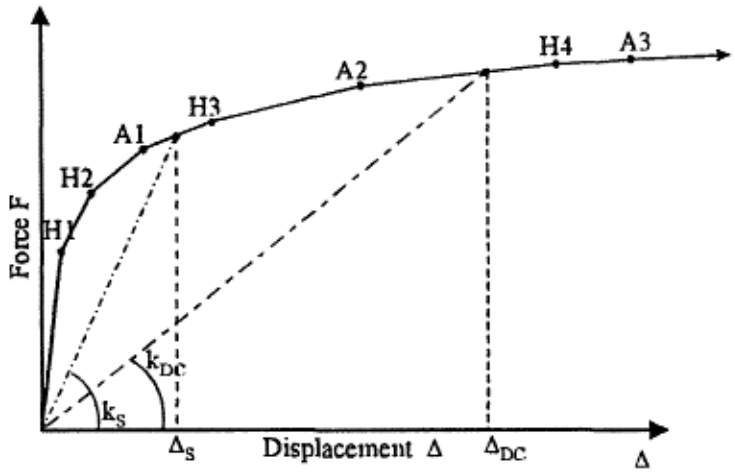

(b) Force-Displacement Response and hinge sequence for Transverse Excitation.

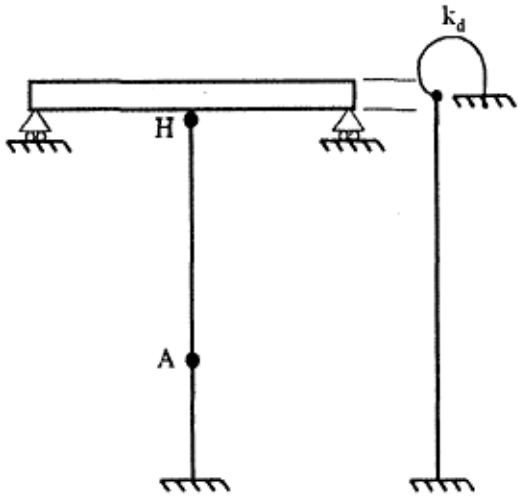

(c) Pile Model for Longitudinal Analysis

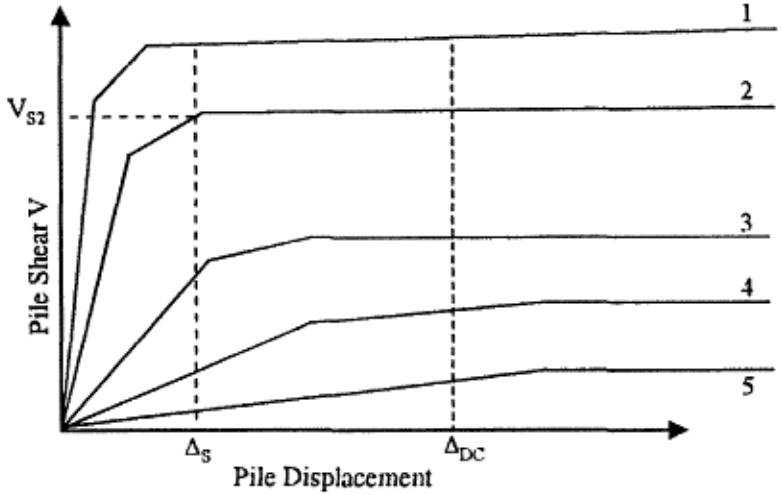

(d) Individual Pile longitudinal Force-Displacement response

Figure 3-23. Pushover analysis of a wharf segment.

Determine an appropriate stiffness for a Method A or B analysis,
Determine appropriate damping levels for elastic analyses, and
Determine peak plastic rotations of critical hinges at the maximum displacements predicted by the Method A or B analyses.

These aspects are discussed in more detail in the following sections.

Elastic Stiffness from Pushover Analysis

It is recommended that elastic analyses used for Method A or B analyses be based on the substitute structure analysis approach, Gulkan and Sozen (1974), where the elastic characteristics are based on the effective stiffness to maximum displacement response anticipated for the given limit state, and a corresponding level of equivalent viscous damping, based on the hysteretic characteristics of the force displacement response (e.g. Figure 3-23(b). Thus for the transverse response, the stiffness for a 20ft. tributary length of wharf would be $\mathbf{k_S}$ or $\mathbf{k_{DC}}$ for the Serviceability and Damage Control limit states respectively, based on the expected limit states displacements Δ_S and Δ_{DC} respectively. Since these displacements will not be known prior to a Method A or B analysis, some iteration will be required to determine the appropriate stiffnesses.

For a Method A analysis, the transverse period can then be directly calculated from the stiffnesses and tributary mass, in the usual manner. For a Method B analysis, using a reduced number of piles as suggested above, longitudinal push analyses will be required on characteristic sections of wharf or pile. As suggested in Figure 3-23(c), the characteristic element for a wharf may be taken as a pile plus deck section extending midway to adjacent piles on either side. A set of pushover analyses for each of the characteristic piles A, B,..E, can then be carried out and plotted as shown in Figure 3-23(d). Again, based on the expected limit states displacements, the total stiffness of the tributary length of wharf considered can be calculated as

$$\mathbf{K_L} = \sum n_i V_i / \Delta_{ls} \qquad (3\text{-}21)$$

Where n_i is the number of piles in row i in the tributary width considered, and V_i is the pile shear force at the limit state deflection Δ_{ls}.

The center of rigidity, measured relative to the arbitrary datum shown in Figure 3-23(a) is given by

$$x_r = \frac{\sum (n_i V_i x_i)}{\sum (n_i V_i)} \qquad (3\text{-}22)$$

Thus, for a Method B analysis, the complete longitudinal and transverse stiffness of a given length of wharf may be represented by a single "super pile" located at the longitudinal center of the length modeled by the pile, and located transversely at the

position defined by Equation 3-22, with stiffness values as defined above. Note that different stiffnesses and centers of rigidity will normally apply for the serviceability and damage control limit states.

Damping

The substitute structure approach models the inelastic characteristics of structures by elastic stiffness and damping levels appropriate for the maximum response displacements, rather than using the initial elastic parameters. The advantage is a more realistic representation of peak response, and an elimination of the need to invoke force-reduction factors to bring member force levels down from unrealistically high elastic values to realistic levels. The damping level is found from the shape of the complete hysteresis loop for a single cycle of displacement at maximum response as illustrated in Figure 3-24. In this, the skeleton force-displacement curve for both directions of response is calculated by a pushover analysis, as illustrated in Figure 3-23(b). The unloading curve is based on a modified Takeda approach where the unloading stiffness k_u is related to the structure ductility , defined in Figure 3-24, and the initial stiffness k_I by

$$k_u = k_I \ \mu^{-1/2} \qquad (3\text{-}23)$$

The residual displacement Δ_r is thus given by

$$\Delta_r = (\Delta_{ls} - F_m/k_u) \qquad (3\text{-}24)$$

The remainder of the stabilized hysteresis loop is constructed as shown in Figure 3-24. The equivalent viscous damping, as a percentage of critical damping, is then given by

$$\eta = A_h /(2\pi.F_m\Delta_{ls}) \ 100\% \qquad (3\text{-}25)$$

where A_h is the area of the stabilized loop, shown shaded in Figure 3-24.

For initial analyses of wharves or piers supported on reinforced or prestressed concrete piles, damping values of 10% and 20% at the serviceability and damage control limit states will generally be appropriate.

Capacity Design Checks

When the pushover analyses are based on the dependable material propertied for the wharf or pier elements, the member forces resulting from the analyses represent lower bound estimates of the forces developed at the appropriate limit state. Although this may be appropriate for determining required strength of plastic hinge regions, and for ensuring that calculated limit state displacements are not exceeded, the results will

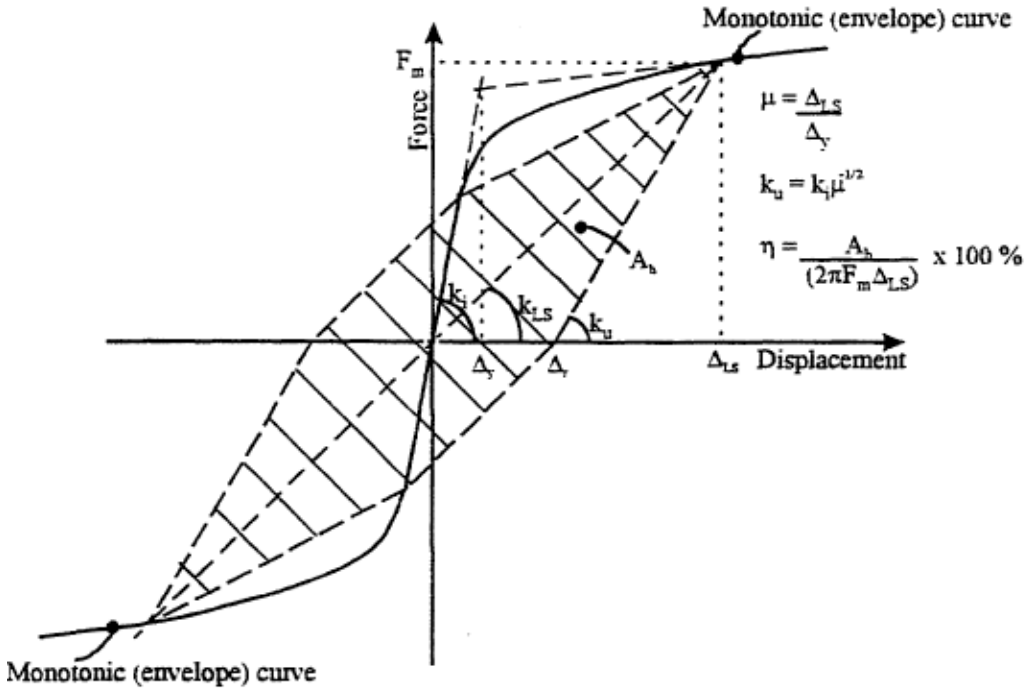

Figure 3-24. Equivalent viscous damping for substitute-structure analysis.

not be appropriate for determining the required strength of members whose force levels must not exceed there dependable capacities during seismic response. It is clear that if material strengths exceed the specified strength, then the flexural strength of plastic hinges may significantly exceed the dependable strength, and as a consequence, the shear forces in piles and deck members may be as much as 20-30% higher than predicted by the pushover analysis.

In order to ensure that a conservative upper limit on the possible strength of members or actions which are to be protected against inelastic response is achieved, a second set of pushover analyses should be carried out, where the material strengths adopted represent probable upper bounds. This approach, based on Capacity Design Principles, is discussed in detail in Priestley et al. (1996).

Iteration Considerations

When checking a completed design, iteration will be needed to ensure compatibility between the Method A or B elastic analysis used to determine response displacements, and the stiffness and damping values determined from the pushover analysis. Typically the necessary adjustments to the substitute structure characteristics take very few cycles to converge with adequate accuracy.

In the design process, the limit state displacements will generally be known before the design strength is established, provided the type and diameter of pile is known. This is discussed further under structural response. In this case the iteration required will be centered on determining the correct number and location of piles to limit the response displacements to the structural limit state displacements.

Method D : Inelastic Time-History Analysis

Inelastic time-history analysis is potentially the most accurate method for estimating the full seismic response of a wharf or pier. It has the capability of determining the maximum displacements, and the inelastic rotations in plastic hinges, from a single analysis. However, to do this, it is necessary to model each pile individually, and to simulate the pile/soil interaction by a series of Winkler springs as discussed above. This can result in unacceptable matrix sizes for analysis of wharves or piers with very large numbers of piles. An alternative is to combine the analysis with inelastic push analyses, and represent groups of piles by equivalent “super piles” as discussed above for modal analysis. Although this somewhat reduces the attraction of the time-history analysis, it makes the analysis more tractable, and still enables several advantages of the method, not available with Methods A or B, to be retained.

A disadvantage of the method is that considerable variation in response can be obtained between two different spectrum-compatible acceleration records. As a consequence it is essential to run an adequately large number of simulations using

different acceleration records, and to average the results. A minimum of five spectrum-compatible records is recommended.

The following points need to be considered before undertaking a time-history analysis:

1. A full simulation of the wharf or pier will require use of a computer program capable of modeling 3-D response. There are comparatively few 3D inelastic time-history programs available at present (March 1999), and experience with them outside of research applications is rather limited. Frequently approximations must be made relating to hysteresis rules and strength interactions in orthogonal directions which make the added sophistication of time-history analysis of reduced utility.
2. If the deck has sufficient rigidity to justify its approximation as a rigid element both in-plane and out-of-plane, a 2-D plan simulation may provide adequate accuracy. However, special multi-direction spring elements with realistic hysteresis rules are required for such a simulation.
3. Time-history analysis enables different stiffnesses to be used for different directions of response. Thus, provided the necessary hysteresis rules are available, it will generally be possible to model the higher stiffness for movement into the shore than for movement away from the shore, and to have a separate stiffness for longitudinal response.
4. It is comparatively straightforward to model the interactions across shear keys, using inelastic time-history analysis.
5. When modeling reinforced or prestressed concrete members, degrading stiffness models such as the Modified Takeda rule should be adopted. There is little point in carrying out time history analyses if simplified rules, such as elasto-plastic, or even bilinear stiffness rules are adopted.
6. Care needs to be exercised into how elastic damping is handled. It is common to specify 5% elastic initial stiffness related damping. This can greatly overestimate the damping at high ductilities. In fact, since the hysteretic rules available in the literature have generally been calibrated to experimental results, the justification for adding elastic damping, which should be apparent in the experimental hysteresis loops, is of doubtful validity. There is thus a case for ignoring elastic damping, if levels of inelastic response are high. However, at low levels of displacement response, the simplifications inherent in the hysteresis rules generally mean that the damping is underestimated for “elastic” or near-elastic response.
7. Results from a time-history analysis should always be compared with results from a simplified approach (e.g. a Method A or B analysis) to ensure that reasonable results are being obtained.

Method E: Gross Foundation Deformation Analysis

As discussed above, the assumption will normally be made that the foundation material is competent when carrying out any of the analyses described above. However, examination of the performance of wharves and piers in past earthquakes reveals that liquefaction and foundation sliding or slumping are common. Analysis techniques to

estimate the sensitivity of the foundation to such failures, and the extent of deformation to be expected, are dealt with elsewhere in this document. Where geotechnical analyses indicate that moderate permanent deformations are to be expected, the structure should be analyzed under the deformed soil profile to estimate the influence on the structure. This will generally require at least a 2-D analysis incorporating discrete modeling of piles and soil springs, with foundation deformations applied at the boundary ends of the springs, as appropriate.

Structural deformations resulting from dynamic vibratory response, and estimated by any of methods A to D will generally occur much earlier in the response to an earthquake than will gross soil deformations. Indeed, liquefaction failure may well occur some minutes after the ground motion has ceased. Consequently it is not necessary to combine the results from a method E analysis with the results of a method A to D analysis. It will be sufficient to confirm that response of each type is individually satisfactory.

Structural Criteria For Piers And Wharves

Deformation Capacity Of Pile Plastic Hinges

The ability of wharves and piers to respond inelastically to seismic excitation depends on the displacement capacity of pile plastic hinges. This displacement capacity will depend on what type of piles are used in the structure, their length, cross-section dimensions, axial load, and material properties. A brief discussion of the deformation capacities of different pile types is included below. This is based on an examination of their moment-curvature characteristics.

Until recently, piles were designed neglecting the confinement effects of the reinforcing on the concrete. Work by Joen and Park (1990a) shows the significant increase in moment capacity by considering the effect of spiral confinement on the concrete. This work uses the Mander et al (1988) concrete model for confined and unconfined concrete. Typically the ultimate compressive concrete strain of unconfined concrete is about 0.003 for use in computing flexural strength as reported by Priestley et al. (1992). For confined concrete the following may be used, Priestley et al. (1992),

$$\varepsilon_{cu} = 0.004 + (1.4\,\rho_s\, f_{yh}\, \varepsilon_{sm})/ f'_{cc} \quad 0.005 \qquad (3\text{-}26)$$

where

ρ_s	effective volume ratio of confining steel
f_{yh}	yield stress of confining steel
ε_{sm}	Strain at peak stress of confining reinforcement, 0.15 for grade 40 and 0.12 for grade 60
f'_{cc}	Confined strength of concrete approximated by 1.5 f_c'

Moment-Curvature Characteristics of Piles.

The key tool for investigating the deformation characteristics of piles is moment-curvature analysis. The analysis adopted must be capable on modeling the full stress strain curves of reinforcement and concrete realistically. For the concrete, this entails discrimination between the behavior of unconfined cover concrete, if present, and that of the confined core, which will have enhanced strength, and particularly enhanced deformation capacity. Elastic, yield plateau, and strain-hardening sections of the steel stress-strain curve should be modeled separately; a simple elasto-plastic or bi-linear representation will be inadequate for mild steel reinforcement, but may be adequate for prestressing steel. The computer code used should provide output of moment and curvature at regular intervals of a sequential analysis to failure, and should identify the peak values of extreme fiber concrete strain, and maximum reinforcement and/or prestressing strain at each increment of the analysis, so that curvatures corresponding to the serviceability and damage-control limit state can be identified.

A sample moment-curvature response, appropriate for a reinforcing steel dowel connection between a prestressed pile and a reinforced concrete deck is shown in Figure 3-25. For structural analysis, it will often be adequate to represent the response by a bi-linear approximation, as shown. The initial elastic portion passes through the first yield point (defined by mild steel yield strain, or an extreme fiber concrete compression strain of 0.002, whichever occurs first), and is extrapolated to the nominal flexural strength. This defines the nominal yield curvature, $_y$. The second slope of the bi-linear approximation joins the yield curvature and the point on the curve corresponding to the damage-control limit-state strains. As defined in the document, these are taken to be:

Concrete extreme fiber compression strain:

Pile/deck hinge:	Value given by Equation 3-26, but <0.025
In-ground hinge:	Value given by Equation 3-26, but <0.008
Reinforcing steel tension strain:	0.05
Structural Steel (pile and concrete filled pipe):	0.035
Prestressing strand:	
Pile/deck hinge:	0.04
In-ground hinge:	0.015
Hollow steel pipe pile	0.025

Equation 3-26 defines a safe lower bound estimate of the ultimate compression strain of concrete confined by hoops or spirals, Priestley et al. (1996). Actual compression failure, initiated by fracture of spiral or hoop confinement will typically not

occur until strains are on average 50% larger than the value given by Equation 3-26, providing an adequate margin for uncertainty of input.

Curvatures at the serviceability limit state are based on strain limits sufficiently low so that spalling of cover concrete will not occur under the Level 1 earthquake, and any residual cracks will be fine enough so that remedial grouting will not be needed. As defined in the document, these are taken to be:

Concrete extreme fiber compression strain:	0.004
Reinforcing steel tension strain:	0.010
Prestressing strand incremental strain:	0.005
Structural steel (pile and concrete-filled pipe):	0.008
Hollow steel pipe pile:	0.008

The specified incremental strain for prestressing strand is less than for reinforcing steel to ensure that no significant loss of effective prestress force occurs at the serviceability limit state. For steel shell piles, either hollow or concrete filled, it is recommended that the maximum tension strain in the shell be also limited to 0.01 to ensure that residual displacements are negligible. Note that if the steel shell pile is connected to the deck by a dowel reinforcing bar detail, the connection is essentially a reinforced concrete connection confined by the steel shell. As such the limit strains for reinforced concrete apply.

Figure 3-26 shows examples of theoretical moment-curvature curves for different types of piles, each with an outside diameter of 610mm, and each subjected to different levels of axial load. Comparison of the curves for the two reinforced concrete doweled connections of Figures 3-26(a) and 3-26(b), show the significant influence of the concrete cover on the moment-curvature characteristics. Flexural strength is significantly higher with the reduced concrete cover of Figure 3-26(b). Sections with high cover (102mm) show significant reductions in moment capacity when spalling initiates, for all levels of axial load, while piles with 63.5mm cover exhibit much more satisfactory response. Similar behavior is apparent for circular or octagonal prestressed piles, as shown for two different values for concrete cover in Figures. 3-26(c) and 3-26(d). Moment-curvature curves for hollow and concrete-filled steel shell piles are shown in Figures 3-26(e) and 3-26(f). For the hollow steel shell pile, the influence of axial load is rather limited, with axial compression tending to reduce the flexural strength. The influence of internal concrete is to increase the moment capacity significantly, particularly when axial load is high. Another advantage of the concrete infill is that it reduced the sensitivity of the steel shell to local buckling.

Rectangular section reinforced or prestressed concrete piles confined by square spirals and a rectangular distribution of longitudinal reinforcing bars or prestressing

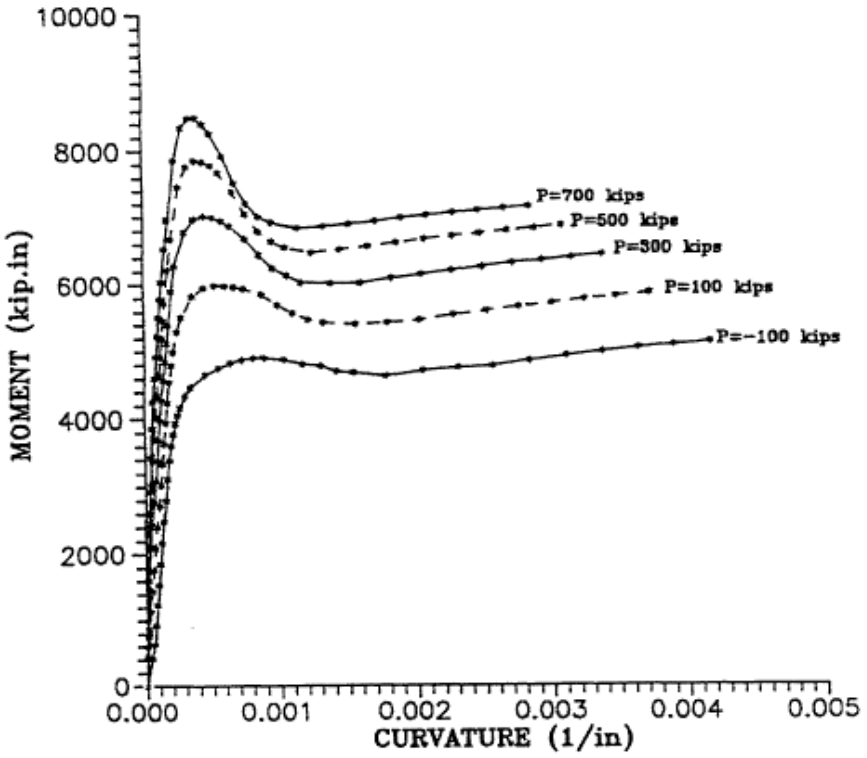

a) cover = 4 inches (102mm) RC dowel connection 8#10 bars

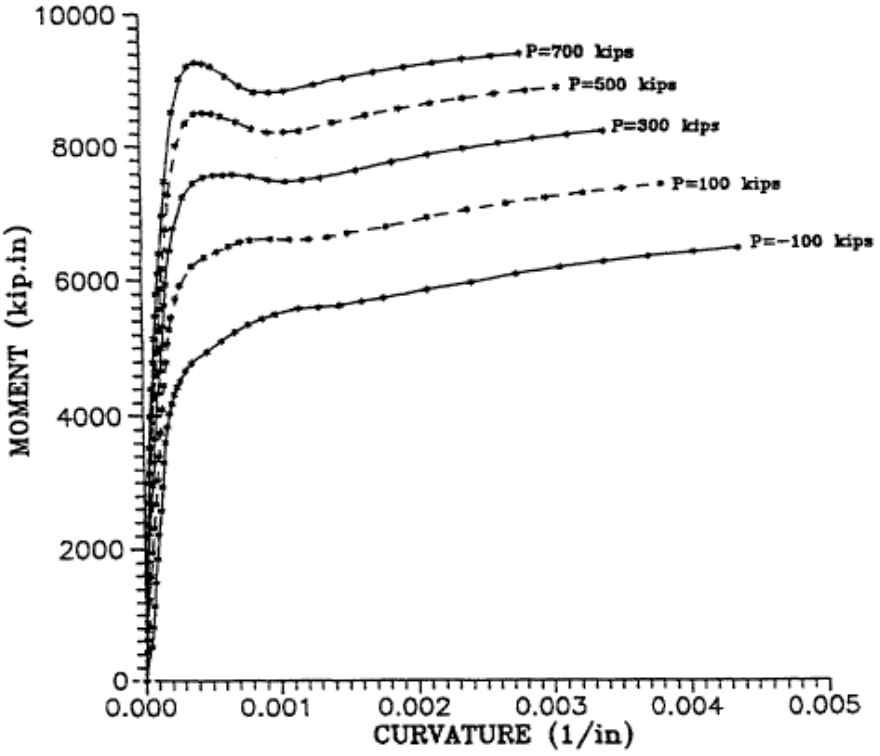

b) cover = 2.5 inches (64mm) RC dowel connection 8#10 bars

Figure 3-26. Moment-curvature curves for 610 mm diameter piles.

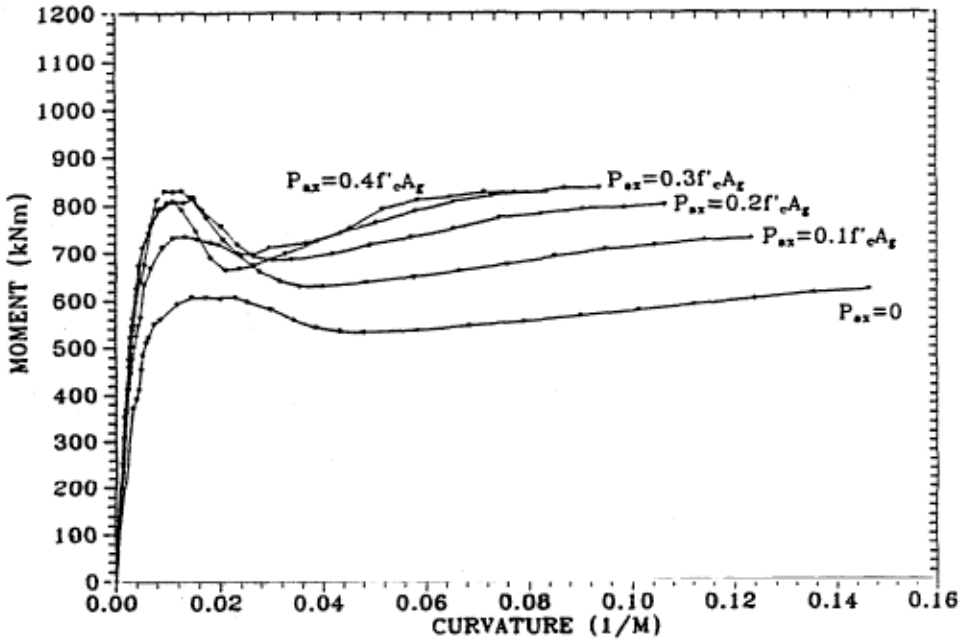

c) prestressed pile, F/A = 6.4 Mpa, cover = 76mm

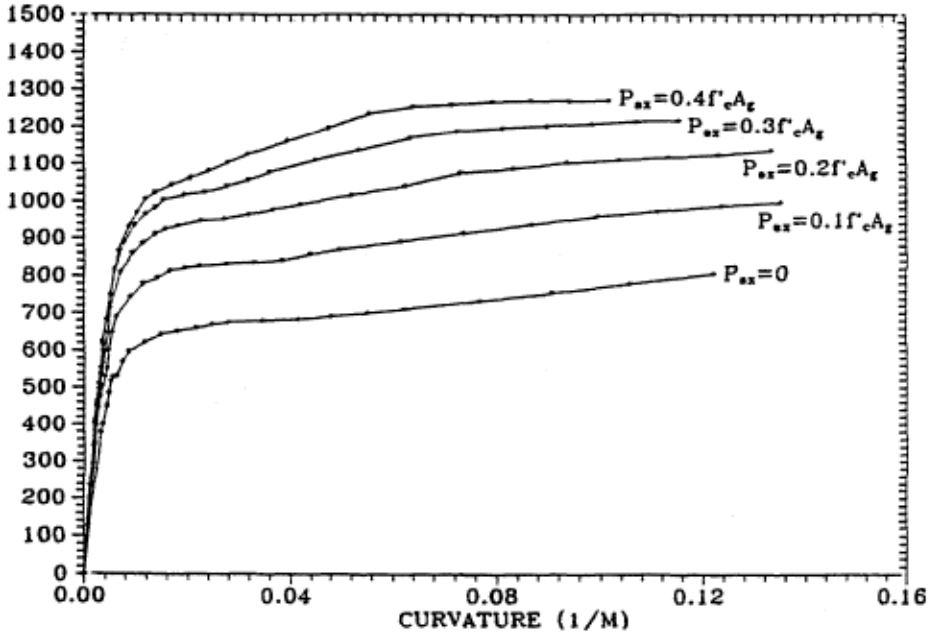

d) prestressed pile, F/A = 6.4 Mpa, cover = 25mm

Figure 3-26. Continued.

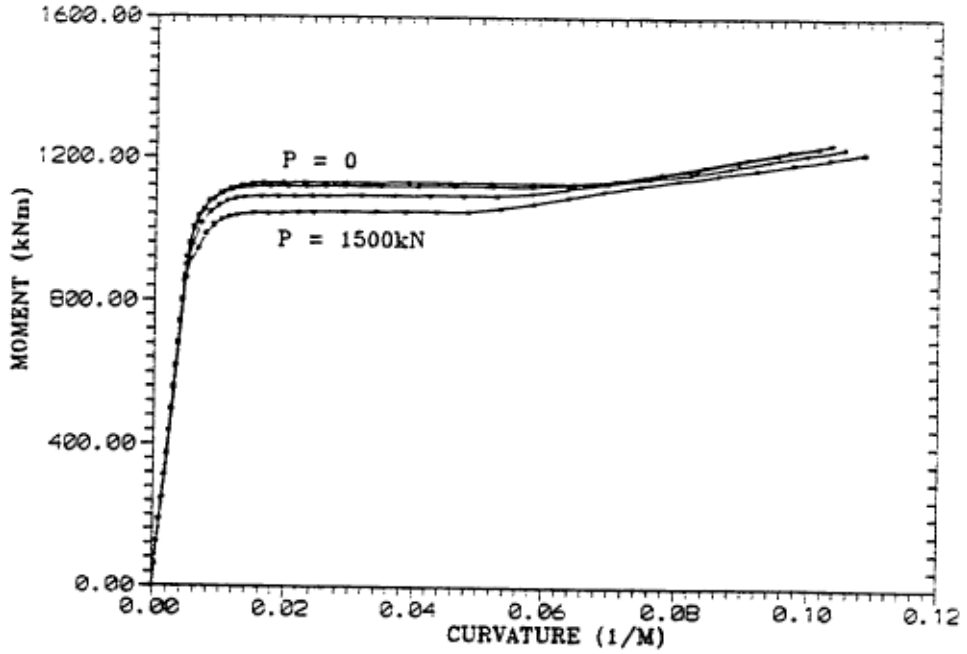

e) Steel shell pile, t = 12mm

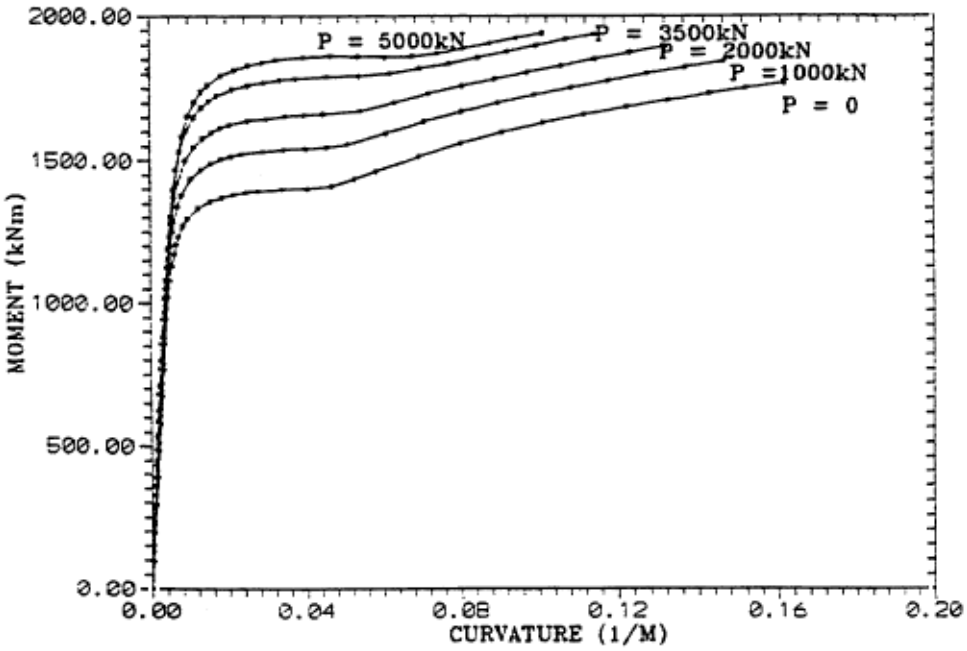

f) Concrete filled steel shell pile, t = 12mm

Figure 26. Continued.

strand should not be used for new construction, since the confinement provided to the core concrete by the rectangular spirals is of very low efficiency. For assessment of existing structures, the concrete core maximum strain corresponding to the damage-control limit state should not be taken larger than 0.007 at the pile/deck hinge. Higher maximum concrete strains , as given by Equation 3-26, are appropriate if the core of the rectangular pile is confined by a circular spiral, and the longitudinal reinforcement or prestressing is also circularly disposed. However, such sections typically have low ratios of concrete core area to gross section area, resulting in flexural strength of the confined core being less than that of the unconfined gross section.

Hollow prestressed piles are sometimes used for marine structures. These, however, have a tendency to implode when longitudinal compression strains at the inside surface exceed 0.005. Consequently the damage control limit state should have an additional requirement to the strain limits defined in the document, that inside surface compression strains must not exceed 0.005. Note that to check for this condition, the moment-curvature analysis must be able to model spalling of the outside cover concrete when strains exceed about 0.004 or 0.005. The outside spalling can cause a sudden shift of the neutral axis towards the center of the section, resulting in strains on the inside surface reaching the critical level soon after initiation of outside surface spalling. More information on piles is available in Priestley and Seible (1997).

Elastic Stiffness

The effective elastic stiffness may be calculated from the slope of the "elastic" portion of the bi-linear approximation to the moment-curvature curve (e.g. Figure 3-25), as

$$EI_{eff} = M_N / \phi_y \qquad (3\text{-}27)$$

The value of the yield curvature, ϕ_y , for a reinforced concrete pile, or pile/deck connection is rather insensitive to axial load level or longitudinal reinforcement ratio. Results of analyses of a large number of cases indicate that Equation 3-27 may be approximately expressed as a fraction of the gross section stiffness as

$$EI_{eff} / EI_{gross} = 0.3 + N / (f'_c . A_{gross}) \qquad (3\text{-}28)$$

Where N is the axial load level, and A_{gross} is the uncracked section area.

For prestressed piles the effective stiffness is higher than for reinforced concrete piles, and values in the range $0.6 < EI_{eff} / EI_{gross} < 0.75$are appropriate. For prestressed piles with reinforced dowel connections to the deck, the effective stiffness should be an average of that for a reinforced and a prestressed connection, or a short length, approximately $2D_p$ long of reduced stiffness appropriate for reinforced pile should be located at the top of the prestressed pile.

Plastic rotation

The plastic rotation capacity of a plastic hinge at a given limit state depends on the yield curvature, ϕ_y, the limit-state curvature,(ϕ_S or ϕ_{LS}) and the plastic hinge length L_p, and is given by

$$\Theta_p = \phi_p L_p = ((\phi_S \text{ or } \phi_{LS}) - \phi_y) L_p \qquad (3\text{-}29)$$

Plastic Hinge Length

The plastic hinge length for piles depends on whether the hinge is located at the pile/deck interface, or is an in-ground hinge. Because of the reduced moment gradient in the vicinity of the in-ground hinge, the plastic hinge length is significantly longer there. For pile/deck hinge locations with reinforced concrete details, the plastic hinge length can be approximated by

SI units $L_P = 0.08\ L + 0.022 f_y d_b > 0.044 f_y d_b$ (Mpa, mm) (3-30a)

US units $L_P = 0.08\ L + 0.15 f_y d_b > 0.30 f_y d_b$ (ksi, in.) (3-30b)

where f_y is the yield strength of the dowel reinforcement, of diameter d_b, and L is the distance from the pile/deck intersection to the point of contraflexure in the pile.

For prestressed piles where the solid pile is embedded in the deck (an unusual detail in the USA), the plastic hinge length at the pile/deck interface can be taken as

$$L_p = 0.5 D_p \qquad (3\text{-}31)$$

For in-ground hinges, the plastic hinge length depends on the relative stiffness of the pile and the foundation material. The curves of Figure 3-27 relate the plastic hinge length of the in-ground hinge to the pile diameter, D_p, a reference diameter D* = 1.82m, and the dimensionless soil lateral subgrade coefficient, k (N/m^3).

For structural steel sections, and for hollow or concrete-filled steel pipe piles, the plastic hinge length depends on the section shape, and the slope of the moment diagram in the vicinity of the plastic hinge, and should be calibrated by integration of the section moment-curvature curve. For plastic hinges forming in steel piles at the deck/pile interface, and where the hinge forms in the steel section rather than in a special connection detail (such as a reinforced concrete dowel connection), allowance should be made for strain penetration into the pile cap. In the absence of experimental data, the increase in plastic hinge length due to strain penetration may be taken as 0.25 D_p, where D_p is the pile diameter or pile depth in the direction of the applied shear force.

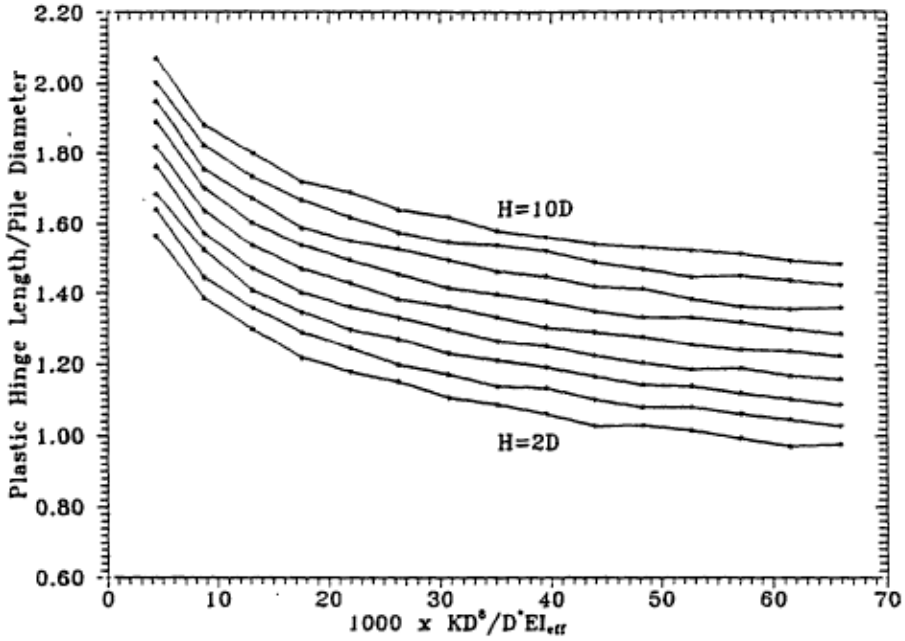

Figure 3-27. In-ground plastic hinge length
(H = height of contraflexure point above ground, D = pile diameter)

In-Ground Hinge Location

The location of the in-ground plastic hinge for a pile may be found directly from an analyses where the pile is modeled as a series of inelastic beam elements, and the soil is modeled by inelastic Winkler springs. When the pile/soil interaction is modeled by equivalent-depth-to-fixity piles, the location of the in-ground hinge is significantly higher than the depth to effective fixity, as illustrated in Figure 3-28 by the difference between points A, at the effective fixity location, and B, the location of maximum moment. Note that when significant inelastic rotation is expected at the in-ground hinge, the location of B tends to migrate upwards to a point somewhat higher than predicted by a purely elastic analysis. It is thus important that its location, which is typically about 1- 2 pile diameters below grade, should be determined by inelastic analysis. An alternative is to determine the depth of B using the dimensionless curves of Figure 3-29, which uses the same dimensionless parameters as Figure 3-27.

Pile Force-Displacement Response

The information provided in the previous few section enables an inelastic force displacement response to be developed individually for each pile. This may be directly carried out on a full 2-D section through the wharf, involving many piles, as part of a push-over analysis, or it may be on a pile-by-pile basis, with the push-over analysis assembled from the combined response of the individual piles. With respect to the equivalent-depth-to-fixity model of Figure 3-28, the pile is initially represented by an elastic member, length L, with stiffness EI_{eff} given by Equation 3-27 or 3-28, as appropriate, and the deck stiffness represented by a spring k_d as shown. Often it will be sufficiently accurate to assume the deck to be flexurally rigid, particularly with longer piles.

The deflection and force corresponding to development of nominal strength M_n at the pile/deck hinge can then be calculated. Note that for elastic deformation calculations the interface between the deck and pile should not be considered rigid. The effective top of the pile should be located a distance $0.022 f_y d_b$ into the deck, to account for strain penetration. This is particularly important for short piles. This additional length applies only to displacements – maximum moment should still be considered to develop at the soffit of the deck.

The elastic calculations above result in a pile displacement profile marked 1 in Figure 3-28(b), and the corresponding point on the force displacement curve of Figure 3-28(c). For the next step in the pile pushover analysis, an additional spring k_{pt} must be added at A, the deck/pile interface (i.e. the deck soffit) to represent the inelastic stiffness of the top plastic hinge. This stiffness can be determined from Figure 3-25 as

$$k_p = \frac{(M_u - M_N)}{(\phi_{LS} - \phi_y)L_p} \qquad (3\text{-}32)$$

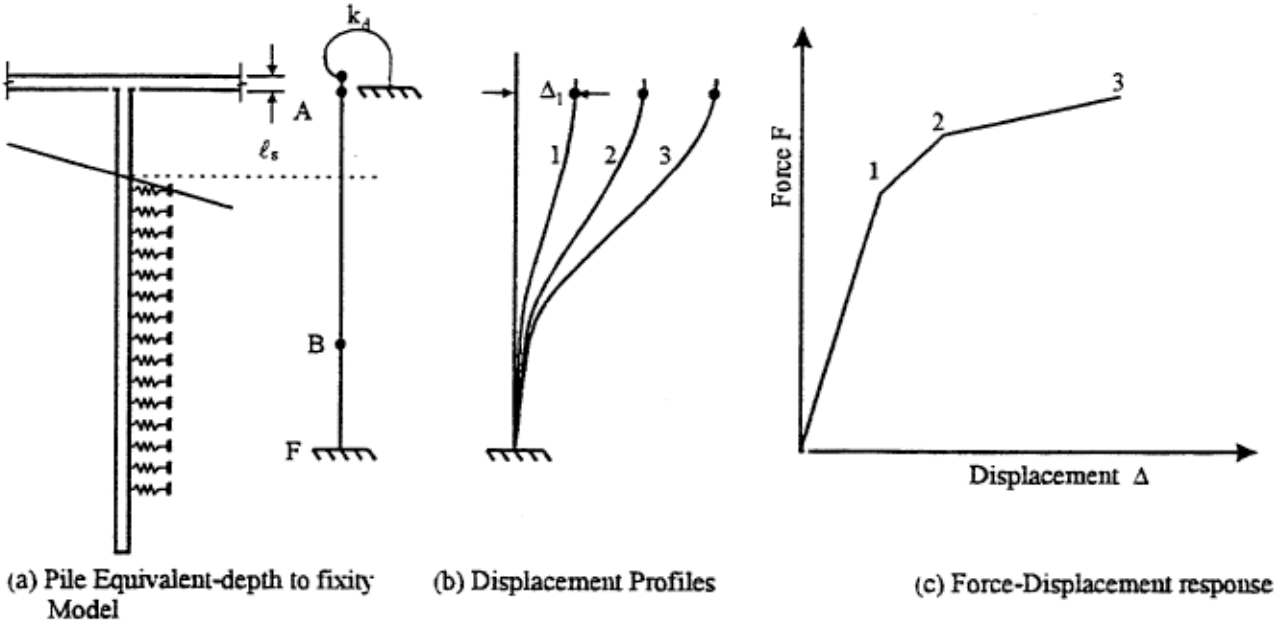

Figure 3-28. Force - displacement response of an isolated pile.

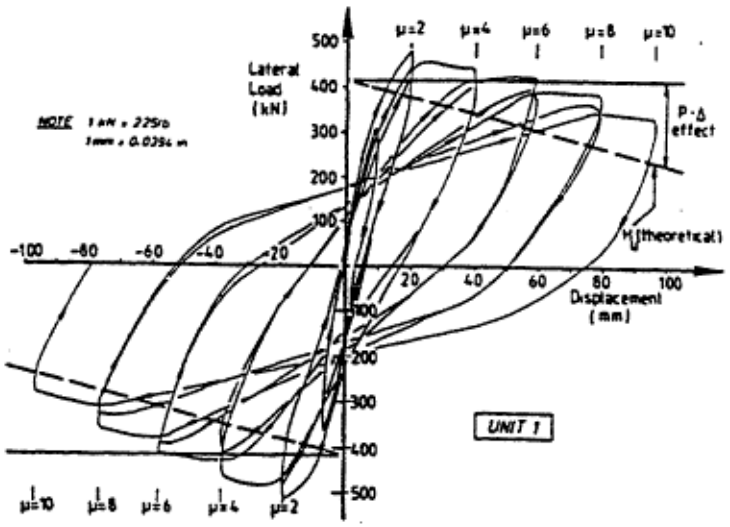

(a) Fully confined pile with additional longitudinal mild steel reinforcement.

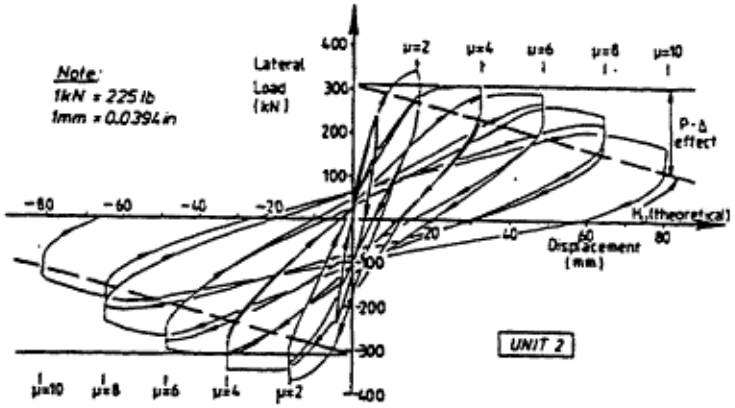

(b) Fully confined pile without additional longitudinal mild steel reinforcement.

Figure 3-29. Load - displacement hysteresis loops for prestressed piles tested by Falconer and Park.

Essentially this spring is in series with the deck spring. Additional force can be applied to the modified structure until the incremental moment at B is sufficient to develop the nominal moment capacity at the in-ground hinge. The deflection profiles and force-displacement points marked 2 in Figures. 3-28 (b) and (c) refer to the status at the end of this increment. Finally the modified structure with plastic hinges at the deck/pile interface, and B is subjected to additional displacement until the limit state curvature ϕ_{LS} is developed at the critical hinge, which will normally be the deck/pile hinge. Note that the inelastic spring stiffnesses at the two hinge locations will normally be different, due to differences in the structural details between the in-ground and hinge locations, and due to the different plastic hinge lengths.

The procedure outlined above is sufficiently simple to be carried out by spreadsheet operations, and has the advantage that the post yield moment-rotation stiffness of the hinges can be accurately modeled. This function is not available in all push-over codes.

Material Properties for Plastic Hinges

For both design of new structures, and the assessment of existing structures, it is recommended that the moment-curvature characteristics of piles be determined based on probable lower bound estimates of constituent material strengths. This is because strength is less important to successful seismic resistance than is displacement capacity. For the same reason, there is little value in incorporating flexural strength reduction factors in the estimation of the strength of plastic hinges. Flexural strength reduction factors were developed for gravity load design, where it is essential to maintain a margin of strength over loads to avoid catastrophic failure. Inelastic seismic response, however, requires that the flexural strength be developed in the design level earthquake. Incorporation of a strength reduction factor will not change this, and at best may slightly reduce the ductility demand. In fact, it has been shown, Priestley (1997) that even this is doubtful, and the provision of extra strength, resulting from the incorporation of strength reduction factors in the design of plastic hinges, may reduce the ductility capacity slightly, compensating for any benefits accruing from additional strength.

On the other hand, the use of nominal material strengths and strength reduction factors in design or assessment will place a demand for corresponding increases in the required strength of capacity protected actions, such as shear strength. This is because the maximum feasible flexural strength of plastic hinges, which dictates the required dependable shear strength will be increased when design is based on conservatively low estimates of material strength. This will have an adverse economic impact on the design of new structures, and may result in an unwarranted negative assessment of existing structures.

As a consequence, the following recommendations Priestley et al. (1996) are made for the determination of moment-curvature characteristics of piles.

Concrete compression strength	$f'_{ce} = 1.3f'_c$
Reinforcement Yield strength	$f_{ye} = 1.1f_y$
Prestress strand ultimate strength	$f_{pue} = 1.0f_{pu}$

Where f'_c is the specified 28 day compression strength for the concrete, and f_y and f_{pu} are the nominal yield and ultimate strength of the mild steel reinforcement and prestressing strand respectively. For assessment of existing structures, higher concrete compression strength will often be appropriate due to natural aging, but should be confirmed by in-situ testing.

In both new design and assessment of existing structures, the flexural strength reduction factor for pile plastic hinges should be taken as unity.

Confinement of Pile Plastic Hinges

Research by Budek et al (1997) has shown that lateral soil pressure at the in-ground plastic hinge location helps to confine both core and cover concrete. This research found that as a consequence of this confinement, for both reinforced and prestressed circular piles, the plastic rotation capacity of the in-ground hinge was essentially independent of the volumetric ratio of confinement provided. As a consequence of this, and also as a result of the low material strains permitted in the in-ground hinge at the damage-control limit state, much lower confinement ratios are possible than those frequently provided for piles. It is recommended that, unless higher confinement ratios are required for pile-driving, the confinement ratio for the in-ground portion of the pile need not exceed

$$\rho_s = \frac{4A_{sp}}{(D_p - 2c_o)s} = 0.008 \qquad (3\text{-}33)$$

where A_{sp} = area of the spiral or hoop bar,
D_p = pile diameter
c_o = concrete cover to center of hoop or spiral bar
s = spacing of spiral or hoop along the pile axis.

In the vicinity of the potential plastic hinge at the top of the pile, the amount of spiral or hoop reinforcement can be adjusted to ensure that the ultimate compression strain given by Equation 3-26 is adequate to provide the required displacements at the damage-control limit state. Thus the designer has some ability to optimize the design of pile confinement, dependent on the displacement requirement predicted under the lateral response analysis. The calculated value should be supplied for at least 2 D_p from the critical section. Because of uncertainties associated with final position of the tip of a driven pile prior to driving, a longer region of pile should have the increased confinement determined from the above approach. In many cases the full pile length

will conservatively be confined with the volumetric ratio required at the deck/pile hinge location.

As an alternative to the approach outlined above, a prescriptive requirement, modified from bridge design, and defined by Equation 3-34 may be adopted:

$$\rho_s = 0.16\frac{f'_{ce}}{f_{ye}}(0.5+\frac{1.25(N_u+F_p)}{f'_{ce}\,A_{gross}})+0.13(\rho_l-0.01) \qquad (3\text{-}34)$$

where N_u= axial compression load on pile, including seismic load,
F_p = axial prestress force in pile
ρ_l = longitudinal reinforcement ratio, including prestressing steel.

The volumetric ratio of transverse reinforcement given by Equation 3-34 may be used as a starting point, but the adequacy of the amount provided must always be checked by comparing displacement demand with capacity.

The pitch of spiral reinforcement provided for confinement should not exceed $6d_b$ nor $D_p/5$, where d_b is the diameter of the dowel reinforcement. For in-ground hinges in prestressed piles, the pitch should not exceed $3.5d_p$ where d_p is the nominal diameter of the prestressing strand.

Addition of Mild Steel Reinforcement to Prestressed Piles

The use of mild steel dowels to provide moment-resisting connections between piles and decks is common. It is also common to provide additional mild steel reinforcement throughout the length of the pile in the belief that this will enhance the performance of the in-ground hinge. Tests by Falconer and Park have shown this additional reinforcement to be unnecessary. Provided adequate confinement is provided at a pitch not greater than 3.5 times the prestress strand nominal diameter, dependable ductile response can be assured. Figure 3-29 compares lateral force-displacement hysteresis loops of prestressed piles with and without additional longitudinal mild steel reinforcement, and subjected to high axial load levels. Both piles were able to sustain displacement ductility levels of 10 without failure. The pile with additional mild steel reinforcement was, as expected stronger than the pile without additional reinforcement, and the loops indicated somewhat enhanced energy dissipation. However, in-ground hinges will normally only be subjected to moderate levels of ductility demand, for which the added damping provided by the mild steel reinforcement will be of only minor benefit.

It is thus recommended that additional longitudinal mild steel reinforcement be provided in piles only when there is a need to increase the flexural strength.

Capacity Protection of Elastic Actions and Members.

The essence of modern seismic design is the precise determination of where and how inelastic actions may occur (i.e. by inelastic flexural rotations in specified plastic hinge locations), and the protection of other locations (e.g. the deck) and other actions (e.g. shear) to ensure these remain elastic. This is termed Capacity Design, Priestley et al (1996) and is done by ensuring that the dependable strengths of the protected locations and actions exceeds the maximum feasible demand based on high estimates of the flexural strength of plastic hinges. Since development of flexural plastic hinge strength is certain at the design seismic input, the consequence of material strengths significantly exceeding design values will be that corresponding increases will develop in the forces of capacity protected members.

The most consistent method for determination of the required strength of capacity protected actions and members is to carry out a second series of pushover analyses, or dynamic time-history analyses, where the moment curvature characteristics of the pile plastic hinges are based on realistic upper bound estimate of material strengths. The following values are recommended:

Concrete compression strength	$f'_{cm} = 1.7\, f'_c$
Reinforcement yield strength	$f_{ym} = 1.3\, f_y$
Prestress strand ultimate strength	$f_{pum} = 1.1 f_{pu}$

The design required strength for the capacity protected members and actions should then be determined from the pushover analyses at displacements corresponding to the damage control limit state. Since these force levels will be higher than those corresponding to the serviceability limit state, there is no need to check capacity protection at the serviceability limit state.

A simpler, conservative approach to the use of a second “upper bound” pushover analyses is to multiply the force levels determined for capacity protected actions from the initial design analysis by a constant factor, representing the maximum feasible ratio of required strength based on upper bound and lower bound material strengths in plastic hinges. This ratio should be taken as 1.4, Priestley et al. (1996).

Shear Strength of Piles

The requirement for capacity protection is that the dependable strength exceeds the maximum feasible demand. Hence shear strength should be based on nominal material strengths, and shear strength reduction factors should be employed.

Most existing code equations for shear strength of compression members, including the ACI 318 equations which are widely used in the USA, tend to be unreasonably conservative, but do not adequately represent the influence of reduction of

the strength of concrete shear resisting mechanisms. An alternative approach, Kowalski et al (1998), which has been widely calibrated against experimental data and shown to provide good agreement over a wide range of parameter variations is recommended for assessing the strength of piles. This approach is based on a three parameter model, with separate contributions to shear strength from concrete (V_c), transverse reinforcement (V_s), and axial load (V_p):

$$V_N = V_c + V_s + V_p \qquad (3\text{-}35)$$

A shear strength reduction factor of 0.85 should be applied to Equation 3-35 to determine the dependable shear strength.

Concrete Mechanism Strength: The strength of the concrete shear resisting mechanisms, which include the effects of compression shear transfer, aggregate interlock, and dowel action, is given by:

$$V_c = k\sqrt{f'_c}.A_e \qquad (3\text{-}36)$$

Where k = factor dependent on the curvature ductility within the plastic hinge region, given by Figure 3-30,

$f'_{c=}$ concrete compression strength in MPa,
A_e=0.8A_{gross} is the effective shear area.

The reduction in k with increasing curvature ductility $\mu_\phi = \phi / \phi_y$ occurs as a result of reduced aggregate interlock effectiveness as wide cracks develop in the plastic hinge region. For regions further than $2D_p$ from the plastic hinge location, the flexural cracks will be small, and the strength can be based on $\mu_\phi = 1.0$.

Different values of k are provided in Figure 3-30 for new design and for assessment. It is appropriate to be more conservative for new design than for assessment, since the economic consequences of extra conservatism are insignificant when new designs are considered, but can be substantial when assessment of existing structures are concerned. Different values are also given depending on whether the pile is likely to be subjected to inelastic action in two orthogonal directions (biaxial ductility) or just in one direction (uniaxial ductility).

Transverse Reinforcement (truss) Mechanism: The strength of the truss mechanism involving transverse spirals or hoops is given by:

Circular spirals or hoops:

$$V_s = \frac{\pi}{2}.A_{sp} f_{yh}(D_p - c - c_o) \cot\theta/s \qquad (3\text{-}37)$$

where A_{sp}= spiral or hoop cross section area

Figure 3-30. Concrete shear mechanism.

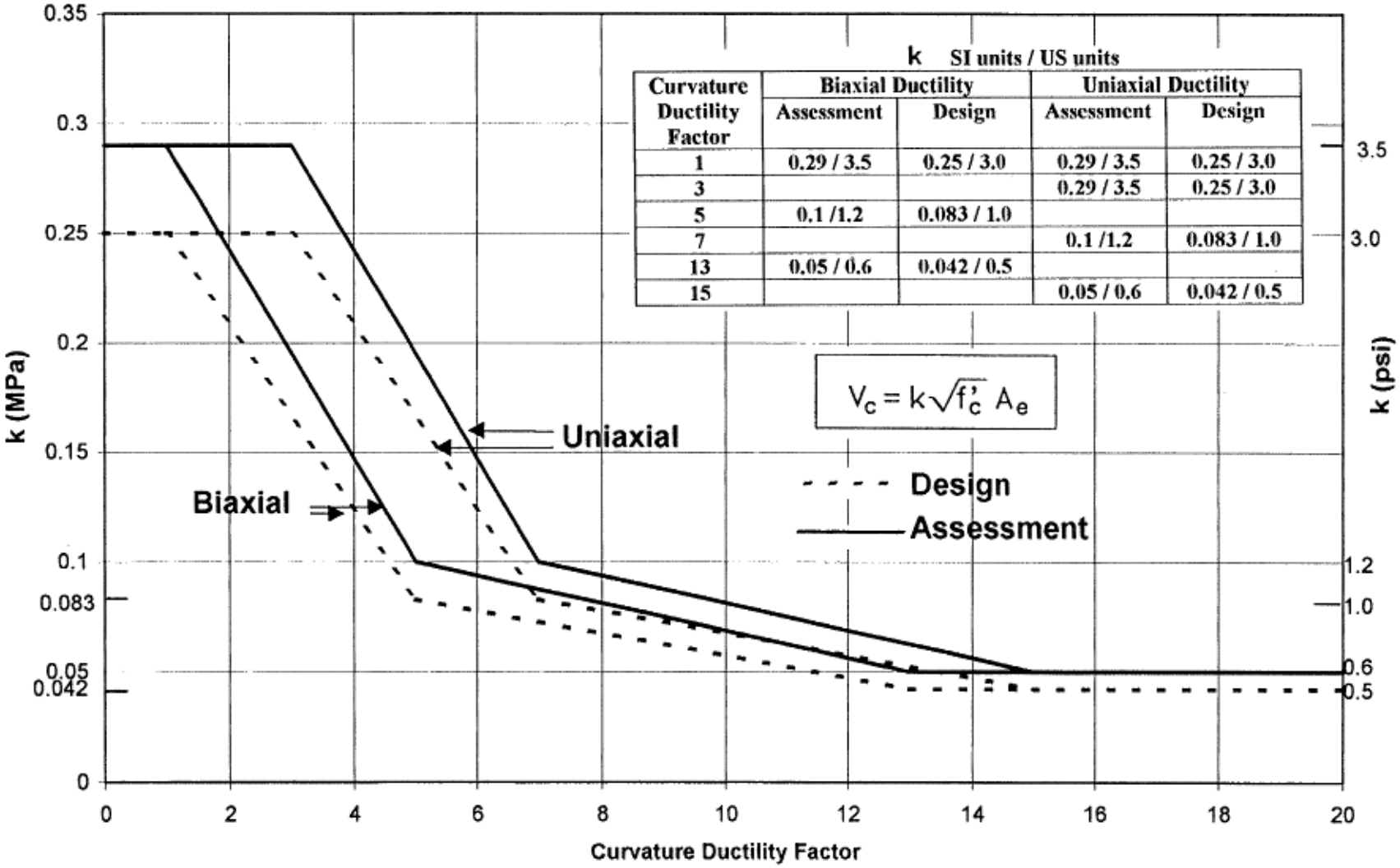

f_{yh}= yield strength of transverse spiral or hoop reinforcement
D_p= pile diameter or gross depth (in the case of a rectangular pile with Spiral confinement)
c = depth from extreme compression fiber to neutral axis at flexural strength (see Figure 3-31)
c_o= concrete cover to center of hoop or spiral (see Figure 3-31)
θ = angle of critical crack to the pile axis (see Figure 3-31) taken as 30^0 for assessment, and 35^0 for new design.
s = spacing of hoops or spiral along the pile axis.

Rectangular hoops or spirals:

$$V_s = A_{h.}f_{yh}(D_p - c - c_o)\cot\theta/s \qquad (3\text{-}38)$$

Where A_h= total area of transverse reinforcement, parallel to direction of applied shear cut by an inclined shear crack.

Axial Load Mechanism: The presence of axial compression enhances the shear strength by development of an internal compression strut in the pile between the compression zones of plastic hinges, whose horizontal component V_p opposes the applied shear force. Axial prestress also acts in similar fashion to enhance shear strength. Thus, with reference to Figure 3-32, the shear strength provided by axial compression is

$$V_p = \Phi\,(N_u + F_p)\tan\alpha \qquad (3\text{-}39)$$

Where N_u = external axial compression on pile including load due to earthquake Action,
F_p = prestress compression force in pile,
α = angle between line joining the centers of flexural compression in the deck/pile and in-ground hinges, and the pile axis (see Figure 3-32)
Φ = 1.0 for assessment, and 0.85 for new design.

Shear Strength of Concrete-filled Steel Shell Piles:

The flexural and shear strength of concrete-filled steel shell piles can be determined assuming normal reinforced concrete theory, and full composite action between the shell and the infill concrete. Although some slip between the shell and concrete may occur, it does not appear to significantly influence flexural strength or displacement capacity.

Shear strength can be determined using the equations above, and considering the steel shell as additional transverse hoop reinforcement, with area equal to the shell thickness, and spacing along the pile axis of s=1.0. The contribution of the shell to the shear strength is thus

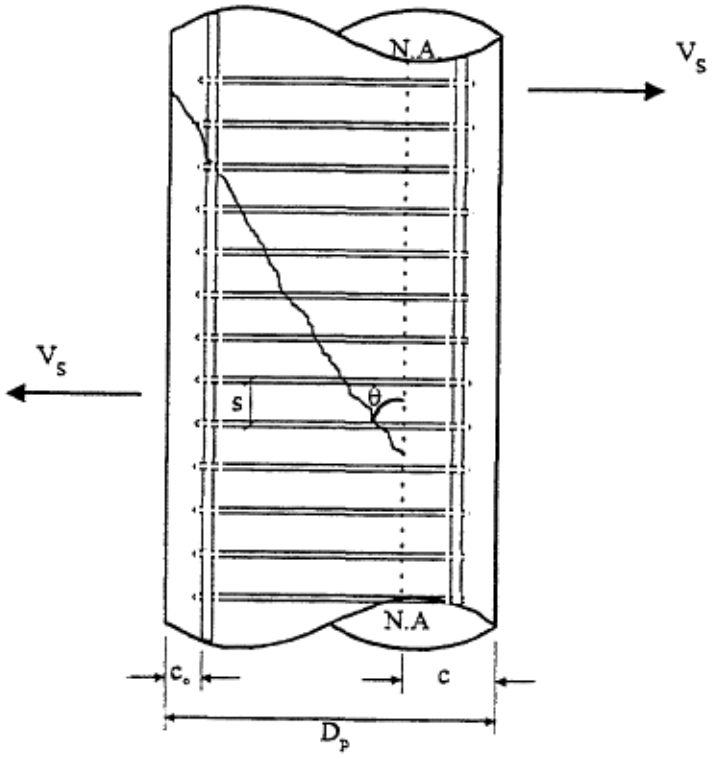

Figure 3-31. Transverse shear mechanism.

$$V_{shell} = (\pi /2)\, t.f_{yh}(D_p - c - c_o) \cot \theta \qquad (3\text{-}40)$$

Design Strength for Deck Members

The required strength for deck members should be determined by adding the actions resulting from the "upper bound" pushover response, at the displacement levels corresponding to the level 2 earthquake, to those resulting from gravity action. Particularly in assessment of existing structures some redistribution of design actions is appropriate, provided overall equilibrium between internal actions and external forces is maintained.

Dependable strength for flexure and shear actions can be determined in accordance with ACI 318 principles.

Assessment of Wharves and Piers with Batter Piles

Batter piles primarily respond to earthquakes by developing large axial compression or tension forces. Bending moments are generally of secondary importance. The strength in compression may be dictated by material compression failure, by buckling, or, more commonly by failure of the deck/pile connection, or by excessive local shear in deck members adjacent to the batter pile. Strength in tension may be dictated by connection strength or by pile pull out. In assessing the seismic performance of wharves and piers with batter piles the following additional items should be considered.

Pile pull-out is ductile and has the potential to dissipate a considerable amount of energy. Displacement capacity is essentially unlimited.

In compression, displacement capacity should consider the effect of reduction in pile modulus of elasticity at high axial load levels, and the increase in effective length for friction piles, resulting from local slip between pile and soil. Typical calculations indicate that displacement ductilities of 2 or more are possible.

Where the prime concern is the prevention of oil spillage, t should be recognized that failure of the batter piles does not necessarily constitute failure of the wharf or pier, nor the initiation of oil spillage. It is possible that after failure of the batter piles, the wharf or pier may be capable of sustaining higher levels of seismic attack. Although the strength will be diminished as a consequence of the batter pile failure, the displacement capacity of the wharf or pier will generally be greatly increased before the secondary failure stage, involving the vertical piles, develops. Consequently this system, involving only the vertical piles should be checked independently of the batter pile system.

Assessment of Wharves and Piers with Timber Piles

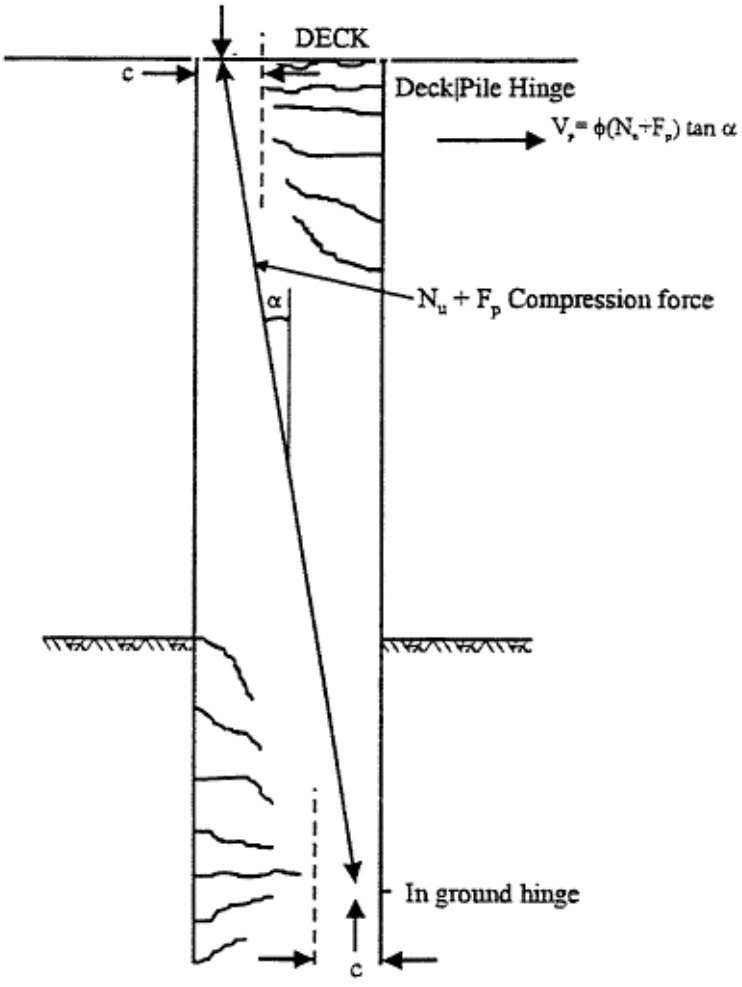

Figure 3-32. Axial force shear mechanism.

There is little reported evidence of damage to timber piles in earthquakes, despite their wide spread usage for wharf and Pier supports for the past 150 years on the West Coast of the USA. This is due to their large displacement capacity, and the typically low mass of the supported wharf, if also constructed of timber, though there are cases of timber piles supporting concrete decks.

Extensive testing of timber piles, both new and used, in both dry and saturated conditions has been carried out by British Columbia Hydro (B.C.Hydro, 1992). No significant difference between results of new and old, wet and dry piles was found. The tests were carried out on nominal 12-inch (300mm) diameter. Peeled Douglas fir piles, though actual dimensions were as large as 14 inches (350mm) at the butt end, and as small as 9 inches (225mm) at the tip end. Three types of tests were carried out:

1. A simple bending test using a non-central lateral load on a pile simply supported over a length of 27.2 feet (8.28m).

2. Cantilever bending tests on piles embedded in concrete pile caps, with a free length of about 4 feet (1.2m)

3. In-situ testing of piles embedded in a firm silty-sand foundation, with a free length of about 16.4 feet (5m).

In all cases the piles were subjected to cyclic loading, though in only the first series of tests were the displacements equal in the opposite loading directions. All piles were subjected to axial loads of about 20 kips (89kn) throughout the testing.

The results indicated that the piles typically exhibited ductile behavior. Failure generally initiated by compression wrinkling at the critical section, followed by a period of essentially plastic deformation at approximately constant lateral load, terminated in a tension fracture. The first series of tests gave the lowest results in terms of displacement capacity. This may have been due to the steel loading collar, which applied lateral force to the pile at the location of maximum moment, causing local distress because of the sharp edges of the collar. In fact, failure was not achieved in the other two test series before actuator travel capacity was reached, despite displacement of 1.00m (40 in) for the in-situ pile tests.

Back-analyses from the more conservative, (and more extensive) first series (simply supported beams) indicated that the following data may conservatively be used for checking the capacity of existing Douglas fir piles:

Modulus of Elasticity:	10 GPa ($1.5x10^6$ psi)
Modulus of Rupture:	35 GPa (5000 psi)
Serviceabilty limit strain:	0.004
Ultimate limit strain:	0.008
Damping at ultimate limit:	12 %

The fracture strain has been back-calculated from the maximum displacements assuming a linear curvature distribution along the pile. This is because there is insufficient data to define a true ultimate strain, and an effective plastic hinge length. Thus displacement capacity should be based on the same assumptions. Note that this will result in the ultimate displacement capacity of a 12-inch (300 mm) pile with an effective length of 25 feet being about 40 inches (1000 mm).

Since the effectiveness of lateral bracing in timber wharves will generally be at best suspect, it is recommended that, as a first approximation, it conservatively be ignored when assessing seismic performance. This assumes that the bracing connections, or members, will fail or soften to the extent that they will be ineffective after the initial stages of lateral response. Similarly, it may be sufficient to assume that the connections between batter piles and the wharf fail, and to check the "worst case" condition without the batter piles. Generally, calculations based on these conservative assumptions will still produce displacement demands that are significantly less than displacement capacity.

Deck/Pile Connection Details

Connection details between the pile and the deck depend on the type of pile used to support the wharf or pier. Although connection details for buildings and bridges are often detailed to act as pinned connections, piles for wharves and piers are almost always designed for moment resistance at the pile/deck connection. Consequently only moment-resisting connections will be considered in this document.

Steel-Shell Piles

Steel shell piles will normally be connected to the deck via reinforcing bars and a concrete plug, even when the concrete infill is not continuous down the height of the pile. If the concrete plug is only placed in the vicinity of the connection, care is needed to ensure that shear transfer exists between the concrete and the steel shell. Although this may often be adequately provided by natural roughness of the inside surface of the steel shell, some more positive method of transfer should be considered. One possibility is the use of weld-metal laid on the inside surface of the steel shell in a continuous spiral in the connection region, prior to placing the concrete plug. Park et al (1983), investigating concrete filled steel-shell piles showed that dependable flexural strength and extremely large ductility capacity could be achieved when the steel shell was discontinuous 50mm inside the deck concrete, and the connection was made by dowel reinforcement properly anchored in the deck. An example of the force-displacement hysteresis response is shown in Figure 3-33. It will be observed that the flexural strength considerably exceeds the nominal strength, denoted H_{ACI} when P-Δ effects are included. This is partly a result of the enhanced concrete strength resulting from very effective concrete confinement by the steel shell, and partly due to the steel shell acting as compression reinforcement, by bearing against the deck concrete. The remarkable ductility capacity of the pile apparent

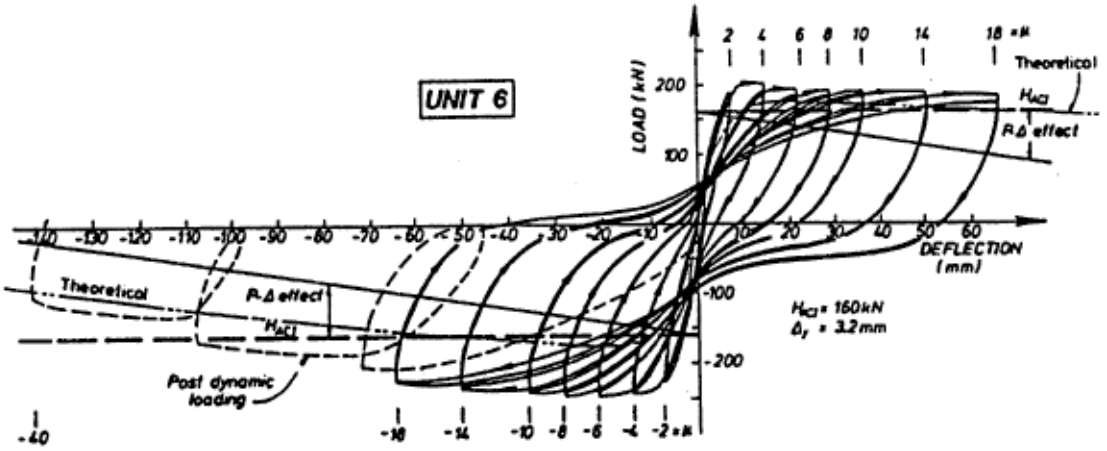

Figure 3-33. Force displacement response of concrete-filled steel shell pile connected to deck by dowels.

in Figure 3-33 has been duplicated in other tests with discontinuous casings at the interface. This pile, subsequent to two cycles at a displacement ductility of $\mu_\Delta = 18$ was subjected to 81 dynamic cycles at $\mu\Delta = 20$, and then a static half cycle to $\mu\Delta = 40$ without significant strength degradation.

Prestressed Piles

In the USA, prestressed piles are normally connected to the deck with mild-steel dowel reinforcement, as discussed in the next section. However, other details are possible, and have been successfully tested under simulated seismic conditions.

Pam et al. (1988), tested a number of connection details appropriate for prestressed solid piles. The details were based on 400mm octagonal piles with 10-12.5mm tendons, but the results can be safely extrapolated to the 600mm piles more commonly used in wharf structures. Two units were tested with the solid end of the pile embedded 800mm into the deck, with a 10mm diameter spiral at 150mm pitch placed around the embedded length of the pile. Two further piles were tested with the strand exposed, enclosed in a 12mm spiral at 47mm pitch, and embedded straight in the deck for a distance of 600mm. In each of the pairs of piles one pile contained only strand while the other included 10-20mm diameter mild steel dowels, thus increasing the flexural strength of the piles. All pile units were subjected to an axial load ratio of $N_u/f'_cA_{gross} = 0.2$, in addition to the axial compression resulting from prestress.

Results for the force-displacement response of these four units are shown in Figure 3-34. In each case the piles were capable of developing the theoretical moment capacity of the connection, and to maintain it to high ductility levels. The apparent strength degradation in Figure 3-34 is a result of P-Δ effects from the moderately high axial load.

First sign of crushing of the concrete in the plastic hinge region was noted at displacement ductility factors of about 2.0 for the embedded pile and about 2.5 for the embedded strand. The difference was due to the higher total compression force at the critical section (due to the pile prestress force) when the full pile section was embedded in the pile cap. Since the piles were very slender, with an aspect ratio of 7, these values might be considered as lower bound estimates for a serviceability criterion for the piles. However, this would be compensated by increased yield displacements if the flexibility of the deck had been included in the tests.

In all cases, the strand was fully developed, despite the rather short development length of $48d_b$ in the exposed strand tests. These results indicate that strand is sufficient to develop moment capacity at the deck/pile interface, and that mild steel dowels are not necessary.

The test units by Pam et al had rather light joint reinforcement surrounding the pile reinforcement in the joint region. However, it must be realized that the deck in these

tests was rigidly connected to a reaction frame, which reduced stress levels in the joint region. Practical details should thus not be based on the joint rebar in Pam's tests.

Practical Connection Considerations.

The most common connection detail consists of dowel reinforcing bars, typically of size # 8, # 9, or # 10, inserted in ducts in the top of the pile after the pile has been driven to the required level, and the top cut to the correct final elevation. Typically the dowel bars in the past have been bent outwards, with the top of the bend below the level of the top mat of the deck reinforcement, as suggested in Figure 3-35(a). In the past the top of the bend has often been much lower than shown in this figure.

If hooks are provided on dowels, they must have the tails bent inwards, rather than outwards. The reason for this is that if significant tension force is transferred up to the hook, which is bent outwards, it adds tension stress within the joint region which is already subjected to high tension stress as a result of joint shear forces. There is then a tendency for the diagonal joint shear crack to propagate and bend horizontally outside the hook, particularly if the hooks are below the top layer of deck reinforcement, as illustrated in Figure 3-35(a). The problem is compounded if the top of the dowel hooks is lower in the deck than shown in Figure 3-35(a). Proper force transfer between the pile and deck becomes increasingly doubtful, and spalling of the soffit concrete may occur, as has been observed in response to moderate earthquakes in Southern California.

If the hooks are high, and are bent inwards as shown in Figure 3-35(b), the bend results in anchorage forces directed back towards the compression corner of the deck/pile connection, resulting in a stable force-transfer mechanism.

Although satisfactory force transfer is expected with the detail of Figure 3-35(b), it can be difficult to construct. This is because tolerances in the final position in plan of a driven pile may be as high as +/- 150mm. In such cases interference between the bent dowels and the deck reinforcement can cause excessive placing difficulties, which may result in one or dowel bars being omitted. Design details need to be developed that are simple and insensitive to pile position. This means that bent dowels should not generally be used.

Two alternative details, developed for the Port of Los Angeles, Priestley (1998) are shown for typical 600mm prestressed piles in Figure 3-36. The first uses straight bar development up as high as possible into the deck, but with bars not terminating more than 100mm below the top surface. This is combined with spiral reinforcement to control the potential joint shear cracking. The second uses reduced embedment length of the dowels, with partial anchorage provided by enlarged end upstands (end bulbs), with bars lapped with headed vertical bond bars. The lap and joint are again confined by a spiral.

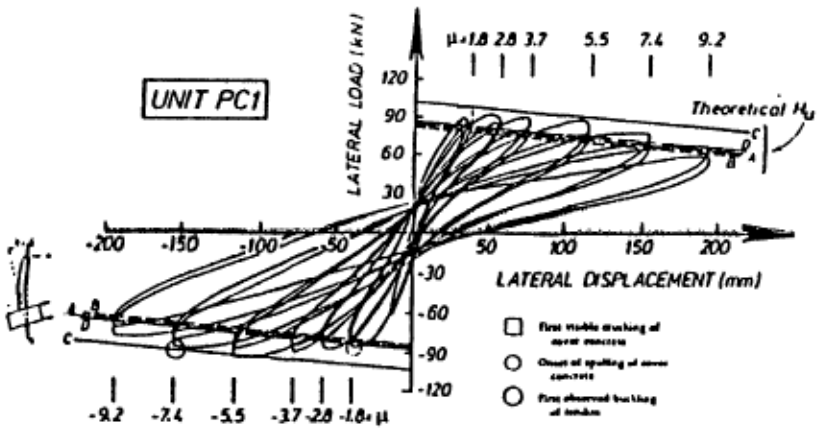

a) Solid pile embedded 800 mm, no dowels

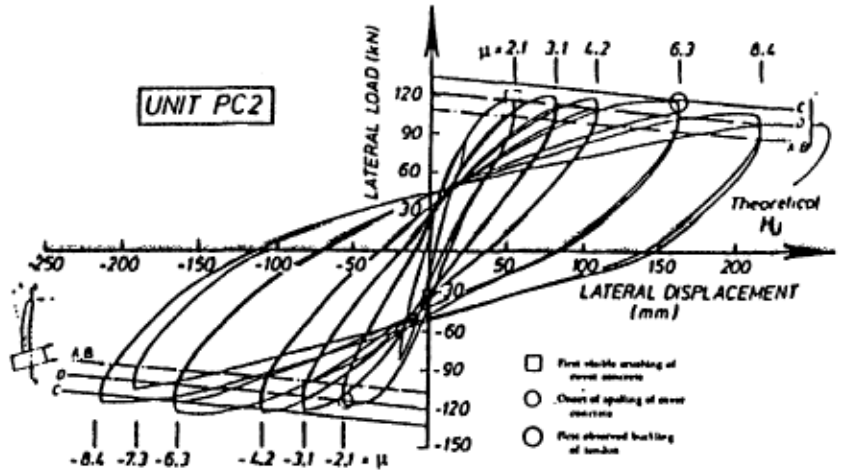

b) Solid pile with standard dowels embedded 800 mm

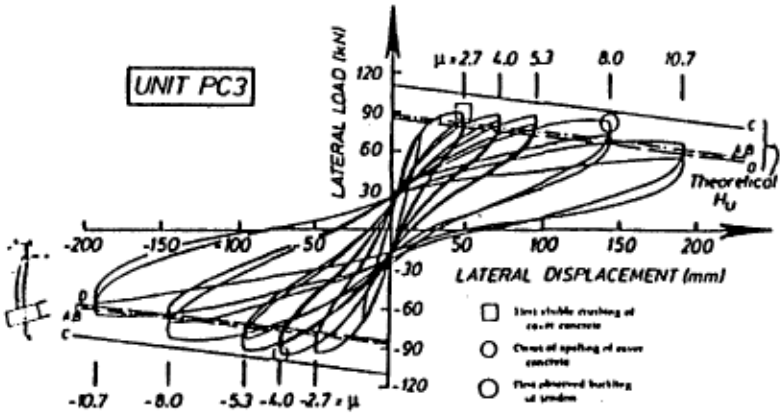

c) Exposed strand embedded 600 mm, no dowels

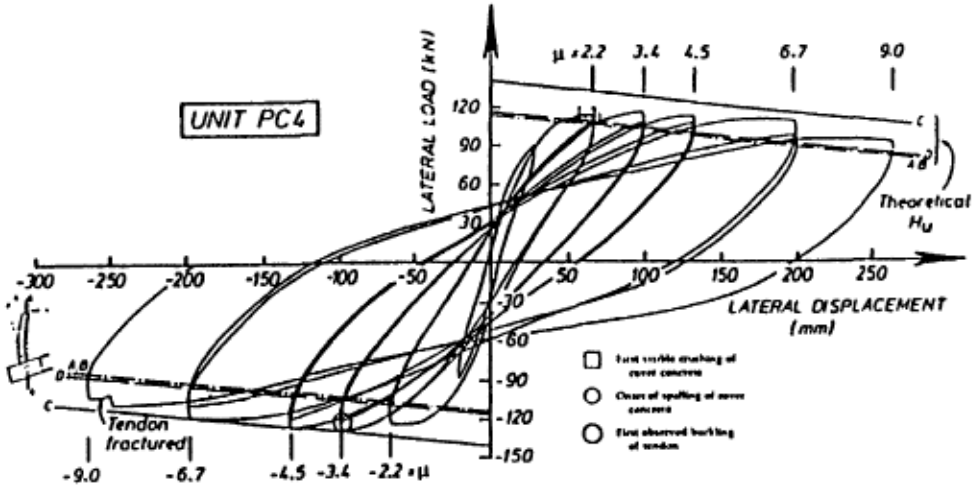

d) Exposed strand and dowels embedded 600 mm

Figure 3-34. Lateral force-displacement response for four pile-pile cap connection details (D=400mm) tested by Pam et al.

Straight-bar Embedment Detail: The straight bar embedment detail of Figure 3-36(a) is directly analogous to details used for moment-resisting column/cap-beam connections for seismic response of bridges, Priestley et al. (1996). The required embedment length is thus given by

SI units $$l_e = 0.3 d_b \frac{f_{ye}}{\sqrt{f'_c}}$$ (Mpa, mm) (3-41a)

US units $$l_e = 0.025 d_b \frac{f_{ye}}{\sqrt{f'_c}}$$ (psi, in.) (3-41b)

where the dowel bar diameter l_e is in mm, and the material strengths are in MPa.

For typical concrete strengths of about f'_c = 30MPa and dowel strength of f_{ye} = 450MPa, Equation 3-41 indicates that it is feasible to anchor # 8 to # 10 dowels by straight embedment in a 900mm deep deck beam, allowing 100mm from the top of the dowel to the deck surface. Anchorage of a # 11 bar in a 900mm deck would require a somewhat higher deck compression strength. Note that the use of the specified 28 day concrete compression strength in Equation 3-41 is very conservative, given expected conservatism in concrete batch design, and expected strength gain before occurrence of the design earthquake, and it would be more realistic, particularly for assessment of existing structures to use a more characteristic strength, say $1.2f'_c$. This would still be considerably less than the probable strength at the age of the concrete when subjected to seismic loading.

Priestley (1998) requires that, if additional external joint reinforcement is not provided, the anchored bars must be enclosed in spiral or hoop confinement in accordance with

$$\rho_s = \frac{0.46 A_{sc}}{D' l_a}\left[\frac{f^o_{yc}}{f_s}\right] \qquad (3\text{-}42)$$

where f^o_{yc} =1.4f_y is the dowel overstrength bar capacity,
f_s = 0.0015E_s,
l_a =actual embedment length provided,
A_{sc}= total area of dowel bars in the connection
E_s = dowel modulus of elasticity
D'= diameter of the connection core, measured to the centerline of the spiral confinement.

The detail shown in Figure 3-36(a) is adequate for embedment of 8 # 11 dowels in a 900mm deck beam.

Headed Rebar Detail: This detail, shown in Figure 3-36(b), is designed to allow the dowels to terminate below the top layer of beam reinforcement. Anchorage is improved

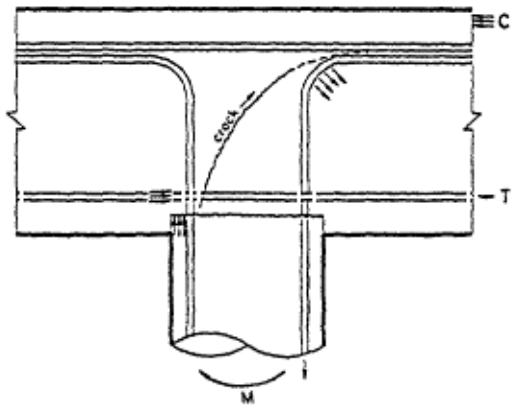

(a) hooks, low, bent out

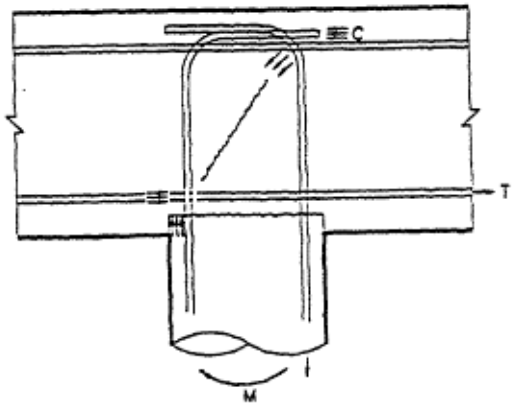

(b) hooks high, bent in

Figure 3-35. Anchorage with hooked dowels.

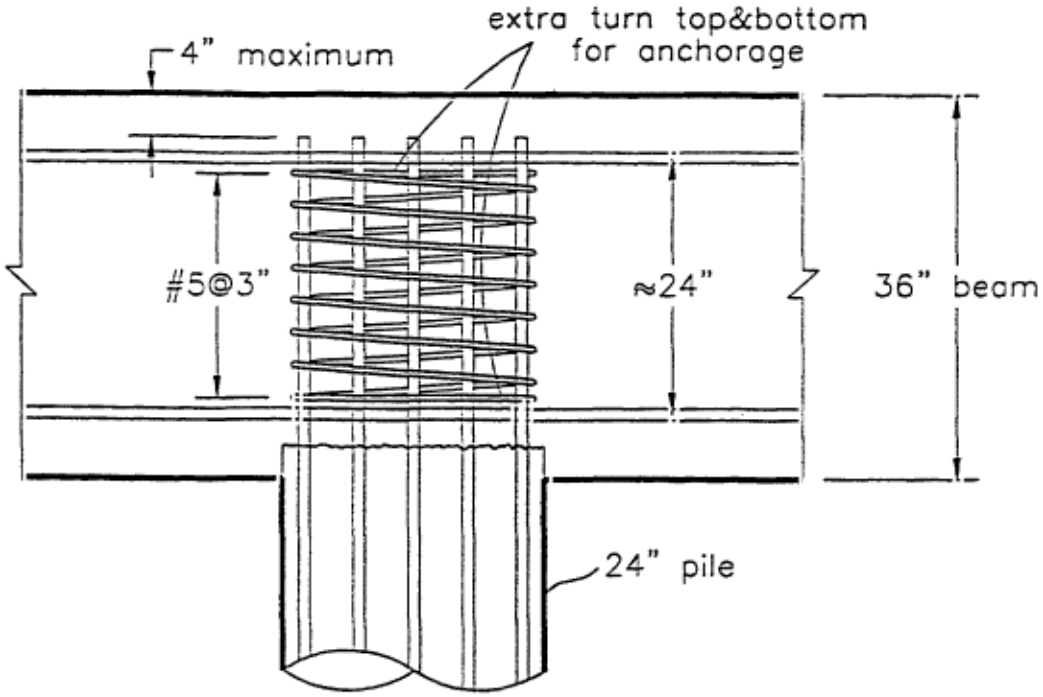

(a) Anchorage detail for dowels in 36-inch beam

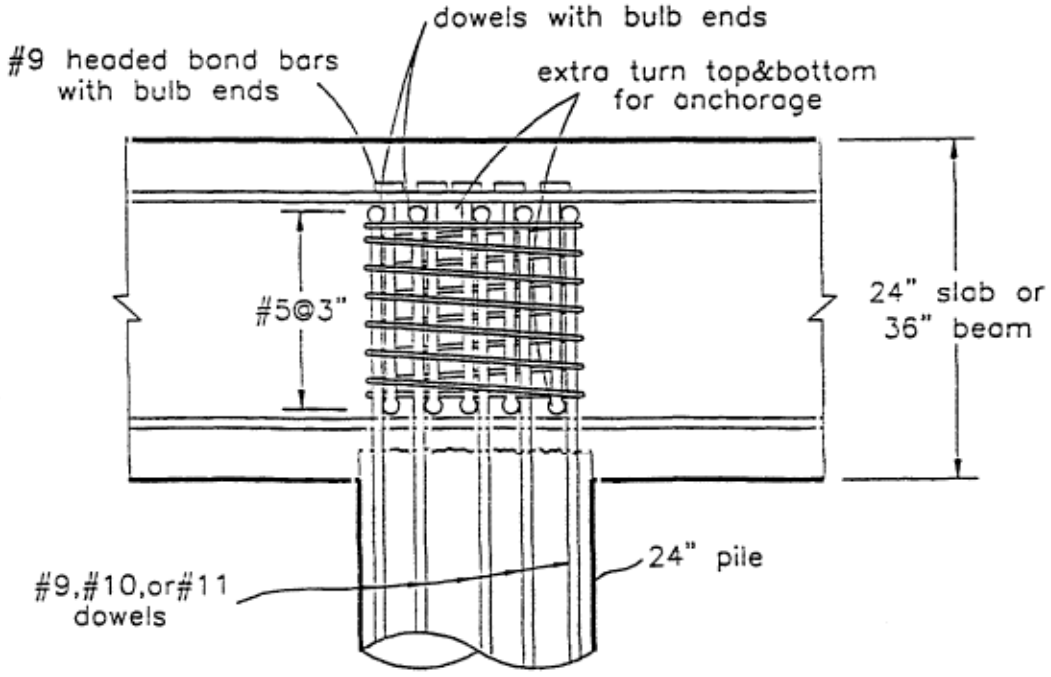

(b) Anchorage detail for dowels with upstands.

(Note: Take dowels up to as high as possible: 3 in. from C.G. top or bottom mat okay)
#9 headed bond bars: 30 in. long for 36 in. beam 18 in. long for 24 in. beam

Figure 3-36. Anchorage details for dowels.

by using an upstand on the end of the dowel. In this design, 50% of the dowel anchorage force is transferred by the upstand, and 50% by bond, using special headed reinforcement bond bars. This allows the minimum embedment length to be reduced to 50% of that given by Equation 3-41. The top of the dowel should be as high as practicable, but in this case may be below the top mat of reinforcement. With this detail, all bar sized up to # 11 can safely be anchored in a 900mm deck beam, and all sizes up to # 10 can be anchored in a 600mm deep deck beam.

The total required area of the headed bond bars is $A_t = 0.65A_{sc}$. Spiral confinement around the connection must be provided in accordance with Equation 3-42.

Details similar to those shown in Figure 3-36(a) have been tested for bridge designs, Sritharan and Priestley (1998) and found to perform well, with displacement ductilities typically exceeding $\mu_\Delta = 6$. The detail of Figure 3-36(b) was recently tested for the Port of Los Angeles, and found to have excellent response (see Figure 3-37), with failure finally occurring outside the connection at high displacement ductility. Only minor cracking developed in the joint region.

Steel H-Section Piles. Connection of steel H-Piles to pile caps or decks is normally by partial embedment in the deck. Full moment-resisting connections are rarely attempted with this detail. If moment-resistance is required of the connection, sufficient transverse reinforcement must be placed around the pile head to enable the pile moment to be transferred by bearing in opposite directions at the upper and lower regions of the pile embedment.

Capacity of Existing Substandard Connection Details

Many existing piers and wharves will have connection details similar to that shown in Figure 3-35a, where the dowels bend outwards from the pile centerline, and the top of the 90 degree bend, h_d above the soffit, is well below the deck surface. Typically, the dowels will not be enclosed in a spiral within the joint region, and there is thus a probability of joint shear failure.

There are no known test data related to the detail of Figure 3-35, but poor performance of such details in the recent moderate Northridge earthquake, and similarity to bridge T joints, which have been extensively tested, leads to a need for conservative assessment.

A relevant procedure is available in Priestley et al. (1996), and is adapted in the following for wharves and piers with reinforced concrete decks.

1. Determine the nominal shear stress in the joint region corresponding to the pile plastic moment capacity.

$$v_j = \frac{M^o}{\sqrt{2}\ h_d D_p^2} \tag{3-43}$$

where M_o is determined as described in "Capacity Protection of Elastic Actions and Members" above and h_d is defined above and in Figure 3-35a.

2. Determine the nominal principal tension stress in the joint region:

$$p_t = \frac{-f_a}{2} + \sqrt{\left(\frac{f_a}{2}\right)^2 + v_j^2} \tag{3-44}$$

where

$$f_a = \frac{P}{(D_p + h_d)^2} \tag{3-45}$$

is the average compression stress at the joint center, caused by the pile axial compression force P. Note, if the pile is subjected to axial tension under the seismic load case considered, then the value of P, and f_a will be negative.

3. If p_t calculated from Equation 3-44 exceeds 0.42 $\sqrt{f_c'}$ Mpa, joint failure will occur at a lower moment than the column plastic moment capacity M^o. in this case, the maximum moment that can be developed at the pile/deck interface will be limited by the joint principal tension stress capacity, which will continue to degrade as the joint rotation increases, in accordance with Figure 3-38. The moment capacity of the connection at a given joint rotation can be found from the following steps.

4. From Figure 3-38, determine the principal tension ratio $p_t / \sqrt{f_c'}$ corresponding to the given joint rotation, referring to the T-joint curve.

5. Determine the corresponding joint shear stress force from:

$$v_j = \sqrt{p_t(p_t - f_a)} \tag{3-46}$$

where f_a is determined from equation 3-45.

6. The moment at the pile/deck interface can be approximated by:

$$M_c = \sqrt{2}\ v_j h_d D_p^2 \leq M^o \tag{3-47}$$

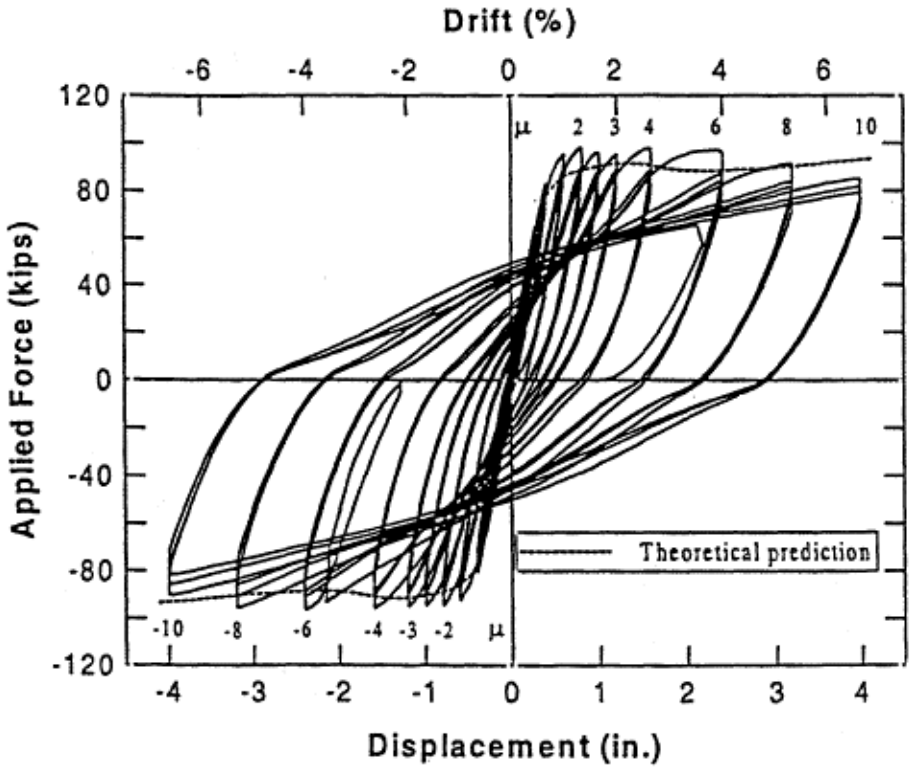

Figure 3-37. Force - displacement response of pile connected to deck with headed rebar (detail of Figure 3-36b.)

This will result in a reduced strength and effective stiffness for the pile in a push-over analysis. The maximum displacement capacity of the pile should be based on a drift angle of 0.04.

Discussion Of Criteria

The criteria presented above are developed from a compilation of current practice by many agencies combined with state-of-the-art technology for estimation of seismic damage potential. It is not a revolutionary step forward but rather an evolution of design. This specification has developed a cohesive integrated criteria specifying:

1. The required pier performance under expected loads
2. Specification of the expected loads
3. Specification of strain limits to ensure structural response limits to achieve performance requirements.

The overall effect on the design, selection of pile sizes and cost of the pier is not expected to be great; however, the assurance in meeting performance goals is thought to be substantially enhanced.

In the application of these criteria to existing construction, it is thought that the objective of a uniform set of performance goals should be maintained across the waterfront. Where adequate capacity is lacking in the existing system, it is thought better to strive for the performance goal, develop several candidate upgrade alternatives, and then perform an economic/risk analysis to determine what is the most cost effective solution considering the potential for a damaging earthquake and the existing lateral force system. This approach is preferred over any system which arbitrarily establishes some percentage reduction of a new-construction criteria. Any single reduction coefficient is probably not optimal over a range of structures and is at best arbitrary.

Strengthening of an Existing Structure

Various methods of strengthening existing structures are possible:

Plating. Where the top of flange is not accessible for adding cover plates, reinforcement can be added to the web plate. The beam shall be relieved of load before the reinforcement is added. When cover plates are added, the flange to web connection and the web plate stresses at the toe of the flange shall be investigated.

Composite Action. Beam section properties can be materially increased by causing the concrete slab to act as a composite with the beam. The slab serves as a top cover plate.

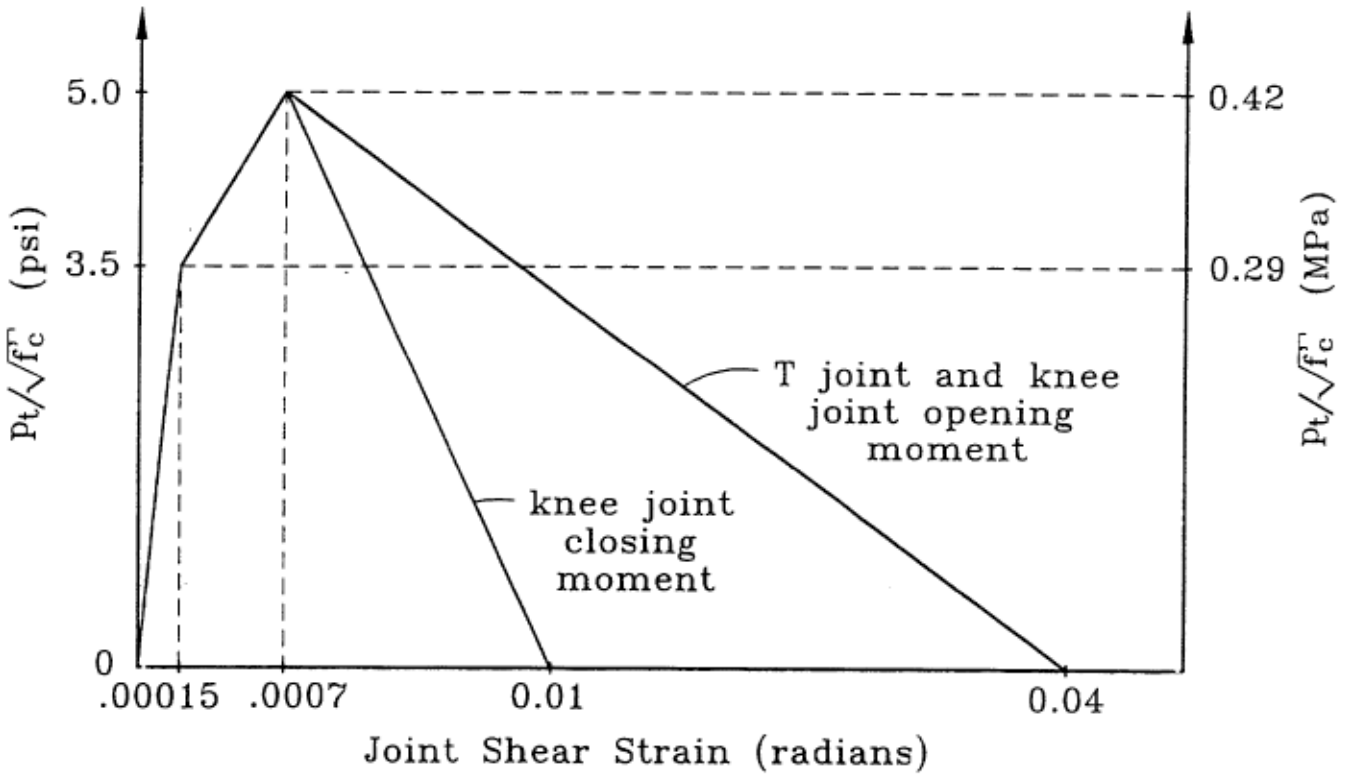

Figure 3-38. Degradation of effective principal tension strength with joint shear strain. (After Priestley, Seible, and Calvi, 1996)

Prestressing Jacks can be used effectively to reduce stresses in existing flanges. Cover plates are welded before removing jacks.

Shear Reinforcement. Vertical stirrups serve as hangers that support the beam from the uncracked portion of concrete near the column.

Flexural Reinforcement. Longitudinal reinforcement can be added effectively if positive means for preventing separation and for transferring horizontal shear are used. Composite materials can be glued to the underside of pier decks to increase section capacity. Composite rods can be inserted and epoxied in groves cut in the topside of pier decks to add reinforcement.

Pile/Column Reinforcement. Pile/Column sections may be strengthened by adding concrete with longitudinal and lateral reinforcement or by adding unreinforced concrete restrained by hoop bars. Wrapping by composite materials has been used very effectively for bridge columns. Mandrels have been applied to piles and filled with concrete.

Compatibility The design details shall encompass any inherent incompatibility of old and new materials. Provision shall be made to resist separation forces. flew concrete shall have a different modulus of elasticity, coefficient of thermal expansion, and shrinkage than old concrete. Consider differing expansion effects due to differing absorption of moisture. Provide resistance against "curling" due to thermal gradients.

Compatibility of connectors must be considered. For example, rivets or bolts are not compatible with welds. Friction bolts are not compatible with rivets. Creep is an important factor.

Dead Load Versus Live Load Stresses. Unless the load on a structure is relieved (for example, by removal or by jacking), the existing framing will continue to carry:

a) the full dead load of the construction,

b) any part of the live load which is in place when the new framing is connected, and

c) a proportionate share of the live load subsequently added.

The new framing will carry only a part of the live load. As a result, under the final loading condition, the stresses in the new and existing material of the same or similar members will be different, often radically so. For example, assuming a 1:1 ratio of dead to live load and of new to existing material in the cross section of a given member and disregarding plastic deformation, the stress in the existing material would be three times the stress in the new. As a result, the new material cannot be stressed up to allowable

values without simultaneously overstressing the existing sections. It is necessary either to provide an excess of new material or to relieve the load on the structure before strengthening. This may not apply if plastic deformation of the structure (and its associated, increased deflection) can be permitted.

Deterioration Of Waterfront Structures

The more common causes of deterioration associated with steel, concrete, and timber waterfront structures are as follows.

Steel Structures. For steel structures deterioration is caused by:

a) corrosion
b) abrasion
c) impact.

Concrete Structures. In concrete structures deterioration is caused

a) corrosion of reinforcement,
b) chemical reactions
c) weathering
d) swelling of concrete, and
e) impact

Timber Structures. In timber structures deterioration is caused by:

a) corrosion and abrasion of hardware
b) borer attack,
c) decay, and
d) impact.

Preventive Measures in Design and Construction

Steel Structures All parts that will be subject to corrosion should be accessible for inspection and repair. If not accessible, encase with concrete or provide some other long-life, high-resistance type of coating. Shapes shall be selected that have a minimum of exposed surface. Detailing shall be designed so that accumulations of dirt and debris will be avoided. Avoid narrow crevices that cannot be painted or sealed. Draw faying surfaces into tight contact by use of closely spaced stitch rivets, bolts, or welds. Prime faying surfaces before assembly. In general, detailing framing to shed water is the single most important factor in inhibiting corrosion and deterioration of coatings. If the potential for ponding is unavoidable, provide drain holes. Drain holes shall be a minimum of 4-inch (101.6 mm) in diameter to inhibit clogging. The use of sacrificial metal shall be avoided in favor of using protective coatings.

The thickness of metal and section properties shall be determined from consideration of loss of section as established in MIL-HDBK-1003/3, Steel Structures, unless corrosion protection is provided. Typical average corrosion rates for bare carbon steel are as follows:

Zone	Average Corrosion Rate (mills per year)
Imbedded Zone 0 to 15 ft	2
Erosion Zone 15 to 21 ft	10
Immersed Zone 21 to 29 ft	8
Atmospheric Zone 29 to 35 ft	12

The minimum thickness shall not be less than 0.40 inches (10.55mm). When the required minimum thickness is excessive, corrosion protection using approved products or cathodic protection shall be used. When coatings are used care must be exercised in driving the piles to preclude damage to the coatings. Additionally consideration must be given to abrasion of the piles by contact with fendering. Tips of all steel H piles having a thickness of metal less than 0.5 inches (12.7mm) and driven to end-bearing on sound rock by an impact hammer shall be reinforced.

Concrete Structures Good quality is the important factor in obtaining a dense concrete. This, in turn, is the most important factor in preventing penetration of moisture, which is the primary cause of deterioration of concrete. Do not use poorly graded aggregate, or a water-cement ratio greater than 6 gal (22.71 1)/sack of cement, reduced to 5 gal (18.92 1)/sack of cement for thinner sections such as slabs and wherever clear cover over reinforcement is 2 in. (50.8 mm) or less. Watertight concrete can be obtained by using air entrainment (maximum 6 percent by volume) and a water-cement ratio not greater than 5 gal/sack of cement. Type III (high early strength) cement is excessively susceptible to sulfate attack, and shall not be used. In general, avoid the use of Type I cement in a saltwater environment. Type IX (sulfate-resistant) cement shall be used. The use of Type V (high sulfate-resistant) cement is seldom required. Provision shall be made for an adequate number of expansion joints. Use types of expansion joints such as double bents with movement taken up by bending of the piles or elastomeric pads with some form of joint sealer. In tropical climates and in areas subject to salt spray, consider the use of galvanized or plastic coated reinforcing bars. If plastic coated bars are used, attention should be given to bond stresses. Excessively rich mixes, over 6 bags per yd^3 (0.764 m^3), shall be avoided, as excess cement tends to enhance the potential chemical reaction with seawater. For most aggregates, alkali-aggregate reaction can be prevented by specifying maximum alkali content of the cement (percent Na_20, plus 0.658 times percent K_20) not to exceed 0.60 percent. In a surf zone, the concrete cover and streamline

sections shall be increased to prevent abrasion. Calcium chloride (as an accelerator) shall not be used in prestressed concrete and concrete exposed to seawater. The use of calcium nitrite or other chemicals as a deterrent to corrosion of embedded reinforcing steel is not an adequate substitute for good quality concrete and adequate cover. This is not to say that these additives do not have merit; however, use of coated reinforcing bars may be required. Timber jackets for concrete piles and stone facing for concrete seawalls work extremely well to prevent deterioration due to corrosion of reinforcement, weathering, and chemical attack. They tend to isolate the concrete from chemical constituents in the environment, insulate against freezing, and keep free oxygen from the reinforcing bars.

Reinforced concrete has been used as one of the major construction materials at the waterfront. Since concrete is much weaker in tension, cracking would be expected to occur when the tensile stresses in the concrete were exceeded, typically at numerical level equal to about 10 percent of the maximum compressive stress. Cracking is a normal occurrence in concrete members under flexural load. When the concrete cracks the section moment of inertia is reduced; generally the cracked moment of inertia is about 30 to 60 percent of the gross moment of inertia depending on the axial load level and reinforcement content. In a marine environment it is desirous to control the cracking to prevent corrosion of the reinforcing steel. Confining steel is used to increase concrete strength, ductility and shear strength. An initial prestress force is used in piles as a mechanism for improving concrete performance by keeping the cracks closed. It has been noted that crack widths of 0.007 to 0.009 inches are sufficiently small to preclude deterioration of the reinforcement so an allowable crack width may be approximated at about 0.01 inches. It is not possible to directly equate the crack width to an allowable tensile strain since crack spacing is not known; however, corrosion has not been a problem when reinforcing stress has been restricted to a tension of 17 ksi or less under service loads. At concrete compressive strains below 0.0021 in/in the compression concrete does not evidence damage and crack widths under cyclic load should be acceptable. Occasional larger loads may be sustained without deterioration as long as a permanent offset does not occur and the prestress forces can close the cracks. Reinforcement deterioration is most pronounced in the presence of oxygen such as in a pier pile where the pile is freestanding out of water or in the splash zone. At deep-water depths or in soil, the oxygen content is reduced such that pile reinforcement deterioration is less. Large loads causing loss of the concrete cover result in loss of pile capacity and facilitate deterioration; such conditions can be repaired if accessible by jackets around the pile. Loss of concrete cover may begin at displacement ductilities of about 1.5 to 2.0.

Timber Structures. Timber structures shall conform to the following criteria:

a) Design detail shall minimize cutting, especially that which must be done after treatment.

b) Design detail shall provide for ventilation around timbers. Avoid multiple layers of timbers as decay is enhanced by moist conditions at facing surfaces. Curb logs shall be set up on blocks. Walers shall be blocked out from face of pier. Thin spacers between chocks and wales, and gaps between deck and tread planks shall be provided.

References

API (1994) Recommended Practice 2A-LRFD (RP2A-LRFD) "Recommended Practice for Planning, Design and Constructing Fixed Offshore Platforms - Load and resistance Factor Design" July 1993 Approved April 1994

B.C.Hydro, 1992 "Seismic Withstand of Timber Piles. Volume 2 of 2: Appendices-Detailed Test Procedures and Test Results. B.C.Hydro, Hydroelectric Engineering Division, Geotechnical Department, August, 1992.

Bogard, D. and H. Matlock, (1980) "Simplified calculation of P-y Curves for Laterally Loaded Piles in Sand" Unpublished report Ertec, April 1980

Budek, A.M., Benzoni, G, and Priestley, M.J.N (1997) "Experimental Investigation of Ductility of In-Ground Hinges in Solid and Hollow Prestressed Piles". Div. Of Structural Engineering Report SSRP 97-xx, University of California, San Diego, 1997

Duan Lian and Thomas Cooper (1995) "Displacement Ductility Capacity of Reinforced Concrete Columns" Concrete International Nov. 1995

Erickson B and G Fortinos (1995) "Code Recommendations for Waterfront Structures" ASCE Ports 95 Proceedings, Tampa FL

Falconer and Park "Pile Tests"

Ferritto, J, (1997) NFESC Technical Report TR-2069SHR, "Seismic Criteria for Piers and Wharves", March 1997

Gazetas, G and P. Dakoulas, (1991) " Seismic Design Chart For Anchored Bulkheads", Proceedings from the Third Japan-US Workshop on Earthquake Resistant Design Of Lifeline Facilities and Countermeasures For Soil Liquefaction, State University Buffalo, New York Feb. 1991

Gulkan, P. and Sozen, M. (1974) "Inelastic Response of Reinforced Concrete Structures to Earthquake Motion" ACI Journal, Dec 1974.

Harn R and B. Malick (1995) "Proposed Seismic Design Method for Piers and Wharves", ASCE Ports 92 Proceedings, Seattle Wa

Hayashi, S (1974) " A New Method of Evaluating Seismic Stability of Steel Pile Structures", Proceedings of the Fifth World Conference on Earthquake Engineering, Rome

Kowalski, M.J. and Priestley, M.J.N. (1998) "Shear Strength of Ductile Bridge Columns" Proc. 5th Caltrans Seismic Design Workshop, Sacramento, June 1998

Kubo, K. (1969) “Vibration Test of a Structure Supported by Pole Foundation” Proceedings of the Fourth World Conference on Earthquake Engineering, Chile

Liftech (1995) “Earthquake Damage Kobe Container Terminals”, Liftech Consultants, Oakland CA

Mander J. B., M. J. N. Priestley and R. Park (1988) “Theoretical Stress-strain Model for Confined Concrete” Journal of Structural Engineering, American Society of civil Engineers, Vol. 114, No 8 August 1988 pp. 1805-1826

Martin G. R. and I. Po Lam (1995) “State of the Art Paper Seismic Design of Pile Foundations: Structural and Geotechnical Issues” Proceedings Third International Conference on Recent Advances in Geotechnical Earthquake Engineering and Soil Dynamics” April 1995 St. Louis, Missouri

Matso, K. (1995) “Lessons From Kobe”, ASCE Civil Engineering April 1995

Meyerson W, T. O’Rourke, and F. Miura (1992) Lateral Spread Effects On reinforced Concrete Pile Foundations”, US Japan Workshop On Earthquake Disaster Prevention For Lifeline Systems, Public Works Research Institute, Tsukuba Science City, Japan

NCEL Handbook for Marine Geotechnical Engineering (1985) Port Hueneme CA

Novak M (1991) “Piles Under Dynamic Loading”, Proceedings Second International Conference on Geotechnical Earthquake Engineering and Soil Dynamics, St. Louis, March 1991

O’Niell, M. W. and J. M. Murtcheson (1983) “ An Evaluation Of P-y Relationships in Sands”, PRAC 82-41-1, University of Houston, Research Report GT DF02-83

Pam, H.J. Park,R., and Priestley, M.J.N. (1988) “Seismic Performance of Prestressed Concrete Piles and Pile/Pile Cap Connections”. Research Report 88-3, Dept. of Civil Engineering, University of Canterbury, 1988,319pp.

Pam, Hoat Joen and Robert Park (1990a) “Flexural Strength and Ductility Analysis of Spiral Reinforced Prestressed Concrete Piles” PCI Journal, Vol. 35 No 4, July/August 1990

Pam Hoat Joen and Robert Park (1990b) “Simulated Seismic Load Test on Prestressed Concrete Piles and Pile-Pile Cap Connections” PCI Journal, Vol. 35 No 6, November/December 1990

Park, R.J.T, Priestley, M.J.N., and Walpole, W.R. (1983) “The Seismic Performance of Steel Encased Reinforced Concrete Piles” Bulletin, NZNSEE Vol 16 No.2, June 1983, p123-140

Parker, F and L. C. Reese (1970) “Experimental and Analytical Study of the Behavior of Single Piles in Sand Under Lateral and Axial Loading”, Research report No. 117-2, Center for Highway Research, The University of Texas, Austin, Texas, Nov, 1970

Priestley, M.J.N. (1997) “Comments on the ATC32 Seismic Design Recommendations for New Bridges” Proc. 4th Caltrans Seismic Design Workshop, Sacramento, June 1997

Priestley, M.J.N. (1998) “Berth 144 Container Terminal” Seqad Consulting Engineers, Solana Beach, Report 98/xx

Priestley, M.J.N. (1999) “POLA Berth 400. Dynamic Analyses of Linked Wharf Segments” Seqad Consulting Engineers, Solana Beach, Report 99/01, April 1999

Priestley, M.J.N., Seible,F., and Calvi, G-M (1996) “Seismic Design and Retrofit of Bridges” John Wiley and Sons, NY, 1996, 686pp

Priestley, M.J.N., and Seible,F. (1997) “Bridge Foundations under Seismic Loads – Capacity and Design Issues” Seqad Consulting Engineers, Solana Beach, Report 97/10, Oct. 1997

Priestley, M. J. N., F. Seible, and Y. H. Chai (1992) Design Guidelines For Assessment Retrofit And Repair Of Bridges For Seismic Performance, University of California, San Diego August 1992

Reese, L.C. W. R. Cox and F.D. Koop (1974) “ Analysis of laterally Loaded Piles in Sand”, Sixth Annual Offshore Technology Conference, Vol. 2 Paper No 2080, Houston, Texas, May 1974.

Seed R. B. S. E. Dickenson et al. (1990) EERC-90/05 “Preliminary Report On The Principal Geotechnical Aspects Of The October 17, 1989 Loma Prieta Earthquake”, University of California, Berkeley CA, April 1990

Sritharan,S, and Priestley, M.J.N. (1998) “Cyclic Load Tests on a Pile/Deck Haded Reinforcement Connection Detail.” Div. Of Str. Eng., Test Report TR98/xx, University of California, San Diego, 1998

Swanson B. (1996) “Observations From Kobe Earthquake and Lessons Learned For Reducing The Seismic Vulnerability Of US Ports” PIANC Bulletin No. 92 Sept. 1966

Takeda (Degrading Stiffness Hysteresis Rule)

Tudor/PMP (1976) Seismic Design of Piers, Consulting Report to NAVFAC, August 1976

Werner, S. D. and S. J. Hung (1982) “Seismic Response Of Port And Harbor Facilities”, Agbabian Associates, El Segundo CA Oct. 1982

Wison, E.L., Der Kiureghian, A, and Bayp, E.P.” (1981)A Replacement of the SRSS Methos in Seismic Analysis” Earthquake Engineering and Structural Dynamics Vol.9, 1981, pp187-194

Wolf, J. P. and B. Weber (1986) “ Approximate dynamic stiffness of Embedded Foundation Based On Independent Thin layers With Separation Of Soil” Proceedings 8th European Conference on Earthquake Engineering, Lisbon 1986

Yoshida, N and M. Hamada (1991), Damage to Foundation Piles and Deformation Pattern of Ground Due to Liquefaction-Induced Permanent Ground Deformation”, Proceedings 3rd Japan-US Workshop on Earthquake Resistant Design Of Lifeline Facilities and Countermeasures for Soil Liquefaction, National Center for Earthquake Engineering Research, State University of New York, Buffalo, Feb. 1991